AMPK in the control of hepatic glucagon signalling and protein synthesis

PhD thesis

Manuel JOHANNS

Table of content

INTRODUCTION

1. Metabolic regulation and energy homeostasis

All living organisms are made up of cells, which are defined as the smallest functional biological entities capable of reproducing themselves. It is estimated that the human body is composed of around a hundred trillion (10^{14}) of its own cells, without considering the at least evenly high number of colonizing microbiota[1]. Whatever taxonomical classification they belong to, from the simplest unicellular prokaryotes to the most complex multicellular eukaryotes such as humans, all living organisms require a regular supply of physical or chemical energy. The principle that most of the food we ingest is transformed into energy allowing us to power all our body functions, goes back to the work of Santorio Santorio as early as the beginning of the 15^{th} century[2]. It is metabolism, defined as all chemical reactions occurring in the body, that creates the link between food intake and maintenance of life. The main purposes of metabolism are, first, energy generation for cellular and physiological processes, creation of building blocks for macromolecules such as proteins, lipids and nucleic acids and, second, waste elimination such as ammonia and carbon dioxide. In the 19^{th} century, it became clear that the metabolism of the 6-carbon sugar (hexose) glucose plays a central role in energy metabolism of most species, witnessed by the fact that the sequence of reactions converting glucose into pyruvate –

glycolysis – occurs in a similar way in almost any living cell. In order to maintain the energy level of a living organism (energy homeostasis), the whole set of these biochemical reactions needs to be coordinated and continuously controlled in a tight manner: the concept of metabolic regulation.

1.1. Enzymes

1.1.1. **Definitions**

Enzymes are proteins with catalytic activity, i.e. they can render biochemical reactions possible or accelerate them under physiological conditions. Like all catalysts, enzymes increase the reaction rate by lowering the activation energy (the energy required to start a chemical reaction) and do not alter the equilibrium of a reaction. The catalytic properties of an enzyme can be described by kinetic parameters: V_{max} is the maximal velocity of the enzyme or the maximal amount of substrate converted into product over time. The turnover number k_{cat} (V_{max}/[enzyme]) measures the number of substrate molecules converted to product per enzyme molecule per second and gives an indication of the performance of an enzyme. K_M inversely reflects the affinity of the enzyme for its substrate.

1.1.2. **Protein kinases**

Protein kinases are a class of enzymes of major interest for protein regulation by posttranslational modification. They can transfer phosphate (-PO_4) groups to available amino acid residues carrying a free hydroxyl group

(-OH) on their side chains (Ser, Thr, Tyr). The presence of negatively charged phosphate groups can strongly affect protein function via electrostatic effects and conformational changes, provide docking sites for protein-protein interactions or affect protein localization and stability. As a consequence, protein phosphorylation represents a major mechanism for the regulation of protein (enzyme) function in cells. Of note, many protein phosphorylations are probably silent i.e. without consequences on enzyme activity.

1.1.3. **Regulation**

The activity of an enzyme can be regulated positively or negatively by covalent posttranslational modifications such as phosphorylation, acetylation, methylation, glycosylation, lipidation, … that are catalyzed by specialized enzymes. In most cases, these modifications are reversible by enzymes catalyzing the opposite reaction. For example, in the case of protein phosphorylation, a specific protein kinase adds the phosphate while a protein phosphatase can remove it. This provides dynamic regulation of the target protein, when both the kinase and the phosphatase are active to some extent at the same time, thereby increasing the sensitivity and flexibility of the system.

Besides covalent modifications, enzymes can be regulated allosterically by small molecules that bind to sites distinct from the active site. Binding of allosteric effectors causes conformational changes in the enzyme, affecting kinetic properties (K_M and/or V_{max}). Like covalent modifications, allosteric effectors can cause activation or inhibition of the target enzyme. Very often, allosteric effectors are metabolites upstream or downstream of the reaction

catalyzed by the enzyme within a metabolic pathway. This allows control of metabolic pathways via feedback or feedforward mechanisms.

1.2. Metabolites and metabolic pathways

1.2.1. **Definitions**

Metabolites are defined as the biochemical substrates, intermediates and products of metabolism. The term is usually restricted to relatively small molecules such as carbohydrates, amino acids, nucleotides, etc. in contrast to macromolecules such as proteins and DNA. Metabolites can be used for energy production, signalling, enzyme regulation and have many other functions.

A metabolic pathway is a series of enzyme-catalyzed chemical reactions that are linked one to each other, i.e. the product of a reaction serves as a substrate for the next one. The end product of a pathway can be used immediately to serve another metabolic pathway, or be stored for later use. Two types of metabolic pathways can be distinguished according to whether they are biosynthetic requiring energy consumption (anabolic pathways) or whether they break down molecules to release energy (catabolic pathways). For the correct function of cell metabolism, the metabolic pathways are often compartmentalized, taking place in different parts of the cell. For example, fatty acid synthesis occurs in the cytosol whereas β-oxidation takes place in mitochondria, in order to avoid energy (ATP) waste by "futile cycling". Our cells follow the principle of intrinsic metabolic homeostasis to

keep metabolite concentrations relatively constant while changing the flux through a pathway. This is important for maintaining intracellular osmolarity to avoid changes in osmotic pressure and concomitantly, in cell volume.

1.2.2. **Glycolysis**

Glycolysis is a catabolic pathway converting the 6-carbon sugar glucose into two molecules of the 3-carbon α-keto acid pyruvate. It consists of 10 sequential enzymatic reactions **(Scheme 1)** producing 2 ATP molecules (energy) and 2 NADH molecules (reducing equivalents) per molecule of glucose. In fact, two ATP molecules have to be "invested" in the first and third reactions but a total of 4 ATP molecules are "paid off" in the lower part of the pathway. Out of the ten reactions, seven are close to thermodynamic equilibrium in the cell, meaning that they are easily reversible and rate is the same in both directions, whereas three are far from equilibrium (quasi-irreversible) reactions. As a consequence, they represent control steps of the whole pathway and checkpoints for the regulation of glycolytic flux. Metabolic control analysis (MCA) provides a more quantitative study of metabolic pathways, showing how control is shared amongst its enzymes and how this is modulated in response to a change in flux[3]. Of note, glycolytic intermediates in between control points can be funneled into other metabolic pathways, e.g. glucose-6-phosphate (G6P) towards glycogen or dihydroxyacetone phosphate (DHAP) towards triglycerides.

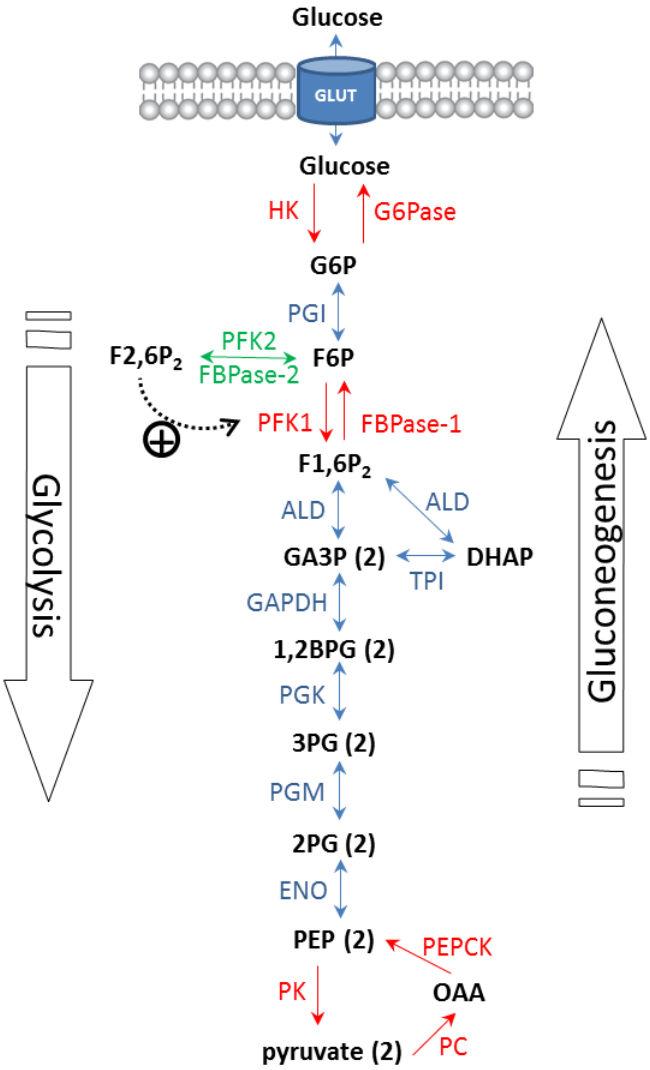

Scheme 1: Glycolysis and gluconeogenesis.
Glycolysis converts one glucose molecule into two molecules of pyruvate under the production of ATP. Gluconeogenesis is the *de novo* synthesis of glucose from substrates such as pyruvate and requires ATP consumption. The enzyme reactions of the two opposite pathways are shown (blue = reversible reaction; red = irreversible reaction; green = side-reaction). Abbreviations: hexokinase (HK); glucokinase (GK); glucose 6-phosphatase (G6Pase); glucose 6-phosphate (G6P); fructose 6-phosphate (F6P); phosphoglucose isomerase (PGI); fructose 1,6-

bisphosphate ($F1,6P_2$); fructose 2,6-bisphosphate ($F2,6P_2$); phosphofructokinase-2/fructose-2,6-bisphos-phatase (PFK-2/FBPase-2) phosphofructo-kinase-1 (PFK-1); fructose-1,6-bisphosphatase (FBPase-1); glyceraldehyde 3-phosphate (GA3P); dihydroxyacetone phosphate (DHAP); aldolase (ALD); triose phosphate isomerase (TPI); 1,3-bisphosphoglycerate (1,3BPG); glyceraldehyde phosphate dehydrogenase (GAPDH); 3-phosphoglycerate (3PG); phosphoglycerate kinase (PGK); 2-phosphoglycerate (2PG); phosphoglycerate mutase (PGM); phosphoenolpyruvate (PEP); enolase (ENO); pyruvate kinase (PK); pyruvate carboxylase (PC); PEP carboxykinase (PEPCK). The coenzymes (ATP, ADP, Pi and NAD/H) are not shown.

1.2.3. **Gluconeogenesis**

Gluconeogenesis (GNG) is the metabolic pathway that allows *de novo* glucose production from alternative (non-carbohydrate) sources. It is a ubiquitous process, occurring even in microorganisms, to avoid shortage of glucose as a fuel in conditions such as fasting, exercise and stress. In humans, GNG occurs in the liver and to a lesser extent in the renal cortex[4]. The transformation of two pyruvate molecules into one glucose molecule requires 6 equivalents of ATP and is thus energy-consuming. In humans, the main GNG precursors are lactate (from exercising muscles), glycerol (from lipolysis) and certain "glucogenic" amino acids (from proteolysis), mainly alanine and to a lesser extent glutamine. Intermediates of the TCA cycle can also be used as substrates for GNG, via conversion of oxaloacetate (OAA) into phosphoenolpyruvate (PEP) by phosphoenolpyruvate carboxykinase (PEPCK), linking the two-carbon TCA cycle to the three-carbon GNG pathway. In higher mammals, fatty acids (yielding acetyl-CoA via β-oxidation) cannot be converted into glucose. Unlike plants and some animals, enzymes of the glyoxylate cycle (malate synthase and isocitrate lyase), are not expressed for the conversion of acetyl-CoA to succinate for

glucose synthesis rather than oxidation to CO_2 by TCA cycle enzymes[5]. GNG essentially takes places in the cytosol but the formation of OAA only occurs in mitochondria via pyruvate carboxylase (PC) and TCA cycle enzymes. The link between these two parts of GNG is provided by PEPCK which converts OAA into PEP. The location of this enzyme depends on the species and in humans it is present both in the cytosol and mitochondria[6]. PEP can cross the mitochondrial membrane via an anion transporter protein or via the malate-aspartate shuttle with the help of malate dehydrogenase (MDH). GNG can thus start in the cytosol or in mitochondria, depending on the substrate. The steps from PEP to glucose-6-phosphate mainly use those of glycolysis in the reverse direction. The equilibrium reactions are catalyzed by the same enzymes in reverse, whereas the three irreversible reactions require specific enzymes: PC/PEPCK, fructose-1,6-bisphosphatase (FBPase-1) and glucose-6-phosphatase (G6Pase). MCA indicates that GNG flux control in hepatocytes is mainly exerted by PC[7], an effect that is reinforced when PK-L is inhibited by PKA-mediated phosphorylation under the effect of glucagon. At the end, G6P can be used by other pathways such as the pentose phosphate pathway or is hydrolyzed to glucose by G6Pase. This last reaction of GNG occurs in the lumen of the endoplasmic reticulum (ER). Glucose can then be exported back to the cytosol and diffuses into the blood via the low-affinity glucose transporter GLUT-2.

1.2.4. **Short-term regulation**

The coordinated regulation of glycolysis and gluconeogenesis has been reviewed elsewhere[8-10]. Along with allosteric mechanisms, the phosphorylation state of key enzymes of glycolysis, fatty acid synthesis,

cholesterol synthesis, gluconeogenesis, and glycogenolysis participate in flux control. Generally, glucagon (as well as catecholamines) leads to the phosphorylation of key enzymes, whereas insulin has the opposite effect, leading to their dephosphorylation. The glycolytic enzymes that are regulated are hexokinase (glucokinase), phosphofructokinase and pyruvate kinase.

- HK/GK: Hexokinase (HK) is expressed ubiquitously and favors glucose entry, as its product G6P cannot exit the cell. However, HK is controlled through product-inhibition by G6P and cellular glucose uptake is thus limited by the rate of utilization of G6P by glycolysis, glycogen synthesis and the pentose phosphate pathway. Hepatocytes and pancreatic β- and α-cells express an isoenzyme called glucokinase (GK), which is not directly inhibited by G6P and has a much lower affinity (higher K_M) for glucose, thus acting as a glucose sensor because its activity varies according to blood glucose levels[11]. When blood glucose rises, GK therefore favours glycolysis rather than GNG in the liver. Of note, even though GK is not product-inhibited by G6P, it is inhibited by a regulatory protein (GRP) and inhibition is reinforced by F6P (which is in equilibrium with G6P)[12]. Insulin in the long-term increases GK expression, thereby stimulating hepatic glucose uptake.

- PFK1: Phosphofructokinase-1 is an important checkpoint of glycolysis, since it catalyzes one of the irreversible reactions and is stimulated by the key allosteric effectors AMP and fructose-2,6-bisphosphate (F2,6BP). The latter is produced from F6P by phosphofructokinase-2 (PFK2)[13], in a side-reaction of glycolysis (**Scheme 1**). PFK2 is phosphorylated by PKA in liver when glucagon increases cAMP signalling, switching the activity of this

bifunctional enzyme from kinase to phosphatase, thereby lowering $F2,6P_2$ levels[14-16]. This provides a switch from glycolysis to GNG in the liver, because $F2,6P_2$ is both a stimulator of PFK1 and an inhibitor of FBPase-1[17]. When cAMP signalling ceases, PFK2 is rapidly dephosphorylated, favoring glycolysis. A rise in AMP is a sign of a decreased energy charge (ATP levels) in the cell. It is thus logical that AMP is a positive allosteric regulator of PFK1. Also, PFK1 is inhibited allosterically by ATP, PEP and citrate.

- PK: The liver isoenzyme of pyruvate kinase (PK-L), but not the muscle isoenzyme (PK-M), is regulated by glucagon through phosphorylation-induced inactivation by PKA[18-20]. Thus glycolysis is inhibited by glucagon in liver, but not in muscle, to prevent it from being active in parallel with PC and PEPCK (GNG enzymes) which would create a futile cycle. Also, PK is allosterically stimulated by $F1,6P_2$, providing feedforward control of the last step by the upper part of glycolysis.

In GNG, the regulated (irreversible) reactions are those catalyzed by PC, PEPCK, FBPase-1 and G6Pase. Acetyl-CoA (AcCoA) allosterically stimulates PC, whereas FBPase-1 is allosterically inhibited by AMP and $F2,6P_2$. In the long-term, PKA signalling increases the expression of the GNG key enzymes PEPCK and G6Pase at the transcriptional level.

1.3. Systemic regulation by hormones

During embryonic development, cells acquire specific capacities in order to fulfil various biological functions, in other words they differentiate. Cells

with the same physiological function assemble to form organs. With regard to the body's energy concerns, the organs of main interest are the gastro-intestinal tract (digestion and absorption), the liver (homeostasis, conversion and storage), fat tissue (fuel storage and mobilization), heart and skeletal muscle (storage and expenditure by contraction for locomotion and heat generation). The main focus of this thesis is on the body's central and essential metabolic power plant, the liver, and more precisely the hepatic control of glucose metabolism.

The hormonal control of normal glycaemia is summarized in **Scheme 2**. After a meal, blood glucose levels in healthy individuals rise from fasted state levels of 4-6 mM (70-100 mg/dl) to up to 8 mM (140 mg/dl) in the post prandial state, whereas in diabetics glycaemia never goes lower than at least 7 mM (hyperglycaemia) even in fasting conditions[21]. The increase in glycaemia is sensed by pancreatic β-cells which react by rapidly secreting insulin, which is pre-synthetized and stored in intracellular vesicles. Human insulin is a 51 amino acid (5.8 kDa) polypeptide composed of disulfide-bond-linked α and β chains. Normal human plasma insulin levels oscillate between below 0.2 to almost 2 nmol/L (25-300 mIU/L)[22]. The insulin receptor is ubiquitously expressed on the cell surface but to a different extent, with the highest expression in liver, fat and skeletal muscle[23]. Upon insulin binding, the receptor triggers a signalling cascade (see section 1.3.1.) which impacts on sugar, fat and protein metabolism. Generally, insulin signalling promotes glucose uptake in adipose and muscle tissue, mainly by promoting the translocation to the plasma membrane of the high-affinity transmembrane transporter for glucose, GLUT4.

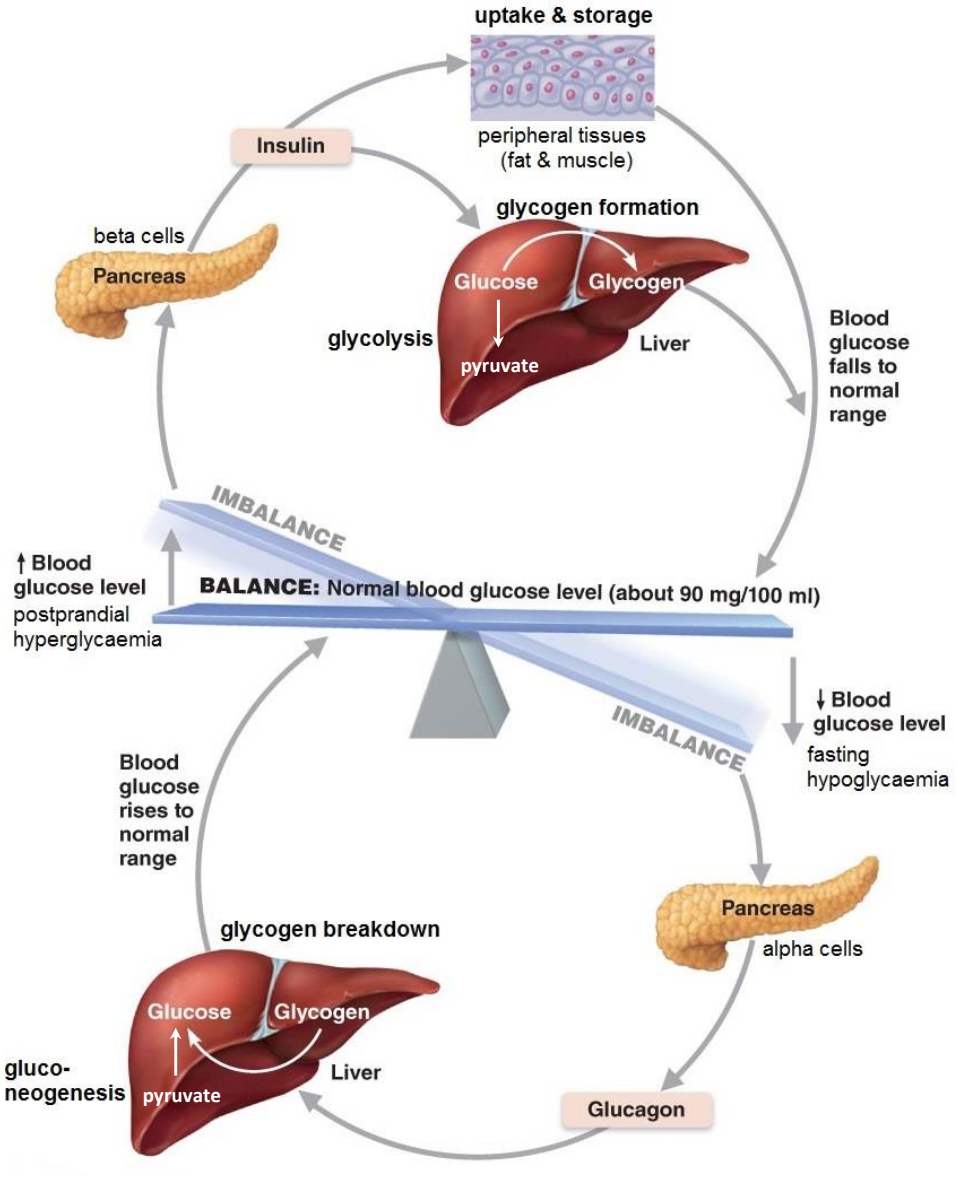

Scheme 2: Homeostasis of glycaemia by insulin and glucagon.
Glycaemia is sensed by specialized cells in the pancreas that react to a rise or drop in blood glucose by secreting insulin or glucagon, respectively. Insulin favours glucose uptake and storage by tissues and antagonizes the effect of glucagon, whose main effect is to stimulate glucose production by the liver. Together, these two hormones keep glycaemia balanced in a physiologically optimal range. (Source: adapted from 2013 Pearson Education, Inc.)

After entry into these tissues, under the effect of insulin, glucose is either utilized for ATP production via glycolysis or transformed into glycogen, triglycerides, or both for storage. Insulin action in the liver, at least in the short-term, is controversial. It is generally accepted that insulin opposes glucagon action and that hepatic GNG is inhibited by insulin[24]. The underlying mechanism involves activation of a cAMP phosphodiesterase[25], probably PDE3B by (PKB-mediated) phosphorylation[26], since a similar mechanism applies in adipocytes[27] to decrease lipolysis and therefore circulating free fatty acids. Besides favouring lipogenesis and glycogen synthesis (only in presence of glucose), in the long-term insulin also promotes protein synthesis in many tissues including skeletal muscle and liver[28] and can be considered as an anabolic hormone. Following insulin action, the hormone-receptor complex can be internalized by endocytosis for proteolytic cleavage involving the insulin-degrading enzyme. It is estimated that an insulin molecule is degraded or cleared from the circulation within minutes after its initial release (4-6 min estimated half-life)[29]. The primary sites for insulin clearance are liver and the kidney. When blood glucose levels have dropped back to normal levels, the pancreatic β-cells stop secreting insulin. Neighboring α-cells react to low glycaemia by releasing another peptide hormone, glucagon, into the bloodstream. High plasma concentrations of insulin inhibit the secretion of glucagon, thus allowing a switch from one hormone to the other according to the state of glycaemia. Glucagon is a single-chain 29 amino acid polypeptide of 3.5 kDa and its receptor is expressed mainly in liver and kidney[30]. Even in the fasted state, normal human plasma glucagon levels only rise to about 20 pmol/L[22]. Binding of glucagon to its receptor triggers

an intracellular signalling cascade (see section 1.3.2.) but which is quite distinct from the insulin pathway. Glucagon stimulates hepatic glucose output, firstly by glycogenolysis (conversion of stored glycogen into glucose) in the short-term within minutes after glucagon release and secondly by gluconeogenesis (*de novo* synthesis of glucose from various substrates such as amino acids and glycerol) in the long-term after several hours or days of starvation[31]. In the short-term, glucagon shuts down liver glycolysis and in the same time stimulates GNG, shifting glucose metabolism towards its production rather than utilization. The net result is an increase in blood glucose levels back to normal values. The fate of glucagon is similar to that of insulin, i.e. endocytosis of the hormone-receptor complex followed by degradation or clearance from the circulation within minutes after release. It is mainly the balance between insulin and glucagon that maintains blood glucose levels within a narrow and physiologically optimal range, in the fed and absorptive states as well as after exercise and in fasting periods.

1.3.1. **Insulin signalling**

For a review on this topic, see De Meyts, 2000[32].

Binding of insulin to its plasma membrane receptor activates the intrinsic receptor tyrosine kinase activity. The receptor subunits cross-phosphorylate, providing docking sites for the adaptor protein insulin receptor substrate 1 (IRS1), which on turn becomes phosphorylated by the insulin receptor tyrosine kinase. The resulting protein complex then recruits the membrane-bound lipid phosphoinositol-3-kinase (PI3K) that produces phosphatidylinositol 3,4,5-triphosphate (PIP3) from phosphatidylinositol

4,5-bisphosphate (PIP2). Phosphoinositide-dependent protein kinase-1 (PDK1) and protein kinase B (PKB, also called AKT) are then sequestered to PIP3 at the plasma membrane, where PKB becomes phosphorylated and activated by PDK1. PKB has many downstream targets in response to growth factor/cytokine signalling and participates in the regulation of key cellular processes[33] such as growth, survival, proliferation, protein synthesis and, of course, metabolism. The main effect of insulin is to decrease blood glucose levels by promoting its uptake and utilization in skeletal muscle (and adipose tissue) while shutting down its production by the liver. Insulin increases glucose uptake by promoting GLUT4 translocation from storage vesicles to the plasma membrane[34]. This involves phosphorylation of AS160 (AKT substrate of 160 kDa) by PKB, which inhibits its GTPase-activating protein (GAP) activity[35]. As such, monomeric G proteins RAB and RAC involved in vesicle trafficking, stay in their active, GTP-bound form. Secondly, PKB phosphorylates and inactivates glycogen synthase kinase 3 (GSK3)[36] and as a consequence, glycogen synthase (GS) converts to its active (dephosphorylated) form which catalyzes the rate limiting step in glycogen synthesis. Simultaneously, glycogen breakdown by glycogen phosphorylase (GP) is prevented via activation of protein phosphatase-1 (PP1), maintaining GP in its dephosphorylated (inactive) state. In adipose tissue, insulin has an anti-lipolytic effect via PKB-induced phosphodiesterase 3B (PDE3B) activation[27], decreasing cyclic AMP (cAMP) levels and consequently, the activities of cAMP-dependent protein kinase (PKA) and its substrate hormone-sensitive lipase (HSL). Lastly, in liver, PKB signalling suppresses the expression of key gluconeogenic enzymes at the transcriptional level

through regulation of transcription factors and coactivators such as the FOXO family[37] and PGC1α[38], while promoting the expression of GK and PK-L for glycolysis.

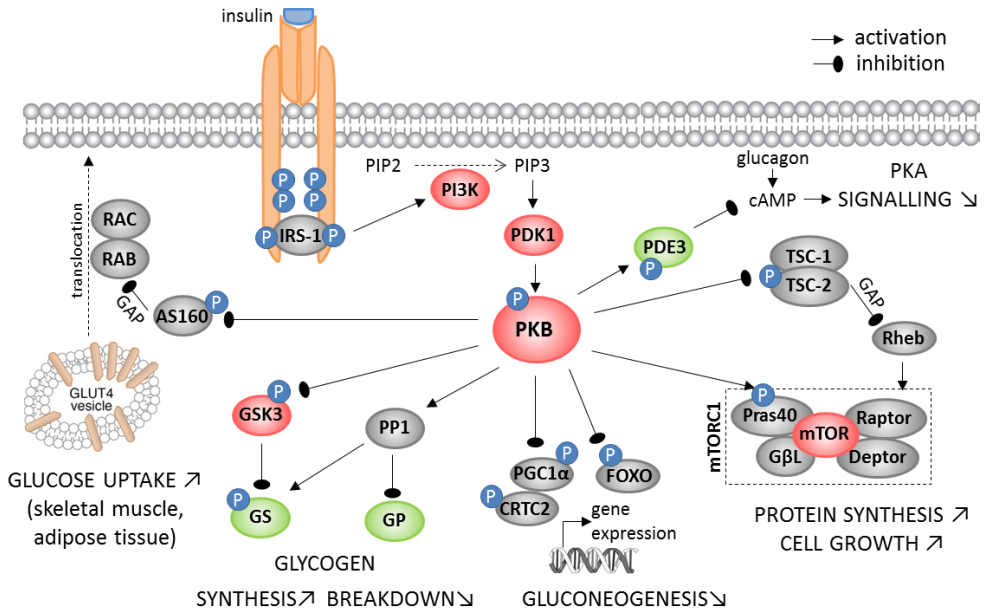

Scheme 3: Insulin signalling and main functions with focus on liver metabolism. Binding of insulin to its plasma membrane receptor triggers an intracellular signalling cascade involving phosphorylation of multiple proteins. The main effector is protein kinase B (PKB or AKT) which phosphorylates various downstream targets to mediate the effects of insulin such as glucose uptake and glycogen synthesis to restore normal blood glucose levels in the postprandial state.

1.3.2. **Glucagon signalling**

Glucagon secretion from pancreatic α-cells (as well as stress hormones such as (nor)adrenaline from the adrenal glands) increases blood glucose levels by promoting glycogenolysis and gluconeogenesis in the liver, while turning off glycolysis[31]. The glucagon receptor is a 7-transmembrane G protein-coupled receptor (GPCR) expressed primarily on hepatocytes. Membrane-bound G proteins are heterotrimeric complexes composed of α, β and γ subunits, and the α-subunit is bound to a GDP molecule in its inactive state. Upon binding of glucagon, the receptor and the associated G protein undergo conformational changes, resulting in exchange of the GDP by GTP and detachment of the active α-subunit from the complex. The free α-subunit can then activate adenylate cyclase (AC), a membrane-bound enzyme which converts ATP into cyclic adenosine-3',5'-monophosphate (cAMP), which then activates cAMP-dependent protein kinase (PKA). PKA in its inactive state is a homodimeric complex consisting of two catalytic (C) subunits sequestered by two regulatory (R) subunits. Upon binding of two cAMP molecules to each R subunit, the two active PKA C subunits are released to phosphorylate downstream targets. In the context of glucose metabolism, PKA phosphorylates and activates phosphorylase kinase (PhK)[39], which then phosphorylates glycogen phosphorylase, GP*b*, converting it to active GP*a*. GP*a* catalyzes phosphorolysis of stored glycogen to glucose-1-phosphate (G1P, further converted to G6P by phosphoglucomutase) and is the rate-limiting step of glycogenolysis. In parallel, PKA phosphorylates and inactivates glycogen synthase (GS)[40], preventing the formation of new glycogen.

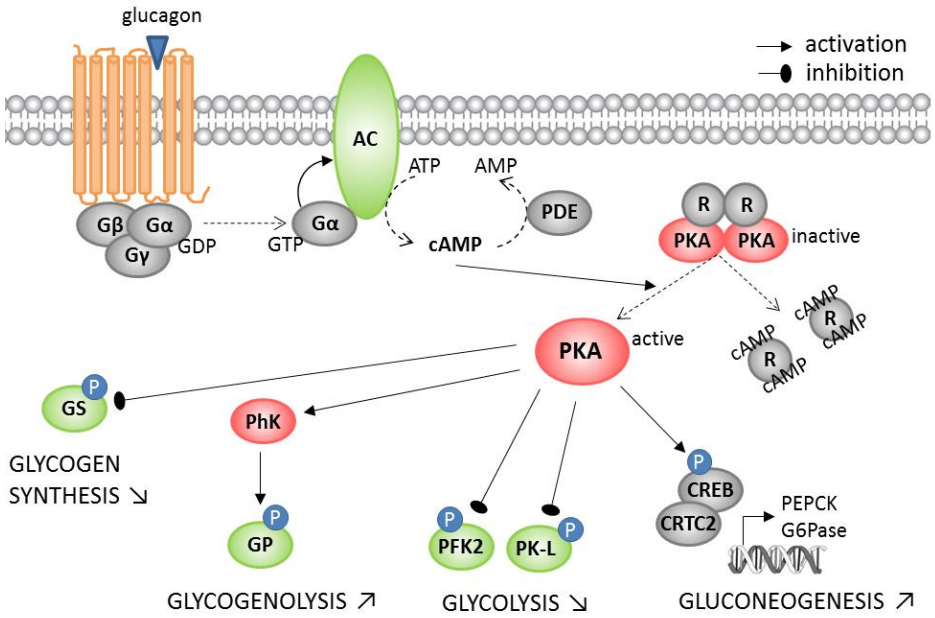

Scheme 4: Glucagon signalling and main functions in liver.
Glucagon mainly acts on the liver, where the expression of its receptor is highest. Glucagon signalling activates adenylate cyclase (AC) to produce cyclic AMP (cAMP) which in turn activates protein kinase A (PKA). PKA is the main effector of cAMP signalling by phosphorylating downstream targets and mediates the effects of glucagon such as glycogen breakdown and gluconeogenesis to maintain blood glucose levels in the fasted state.

In addition, PKA phosphorylates the liver isoform (PFKFB1) of the bifunctional PFK-2/FBPase-2[14], inactivating PFK-2 and activating FBPase-2, resulting in a decrease of intracellular F2,6P_2, the most potent positive allosteric effector of the key glycolytic enzyme PFK-1. This leads thus to an inhibition of glycolysis and favours gluconeogenesis. Lastly, phosphorylation-induced inactivation of liver pyruvate kinase (PK-L)[18] imposes a dual lock on glycolysis by glucagon. The cAMP-PKA pathway also leads to increased expression at the transcription level of key gluconeogenic enzymes such as phosphoenolpyruvate carboxykinase

(PEPCK) and glucose-6-phosphatase (G6Pase), through phosphorylation-induced activation of the transcription factor CREB (cAMP-responsive element binding protein)[41]. During long-term starvation, glucagon indirectly influences glucose production by the liver by stimulating lipolysis in adipocytes via PKA-induced activation of hormone-sensitive lipase (HSL)[42], thereby increasing blood glycerol, which can be used by the liver as a substrate for GNG.

1.4. Metabolic disorders – type 2 diabetes

Diabetes mellitus type 2 or type 2 diabetes (T2D), also known as non-insulin-dependent diabetes mellitus (NIDDM) or adult-onset diabetes, is a long-term metabolic disorder characterized by hyperglycemia and insulin resistance. T2D accounts for about 90% of all diabetes cases, the others cases being primarily type 1 diabetes and gestational diabetes[43]. Major complications include cardiovascular disease and hypertension, eventually promoting heart failure. Among the main causes are overweight and obesity, often linked to a sedentary lifestyle (lack of exercise), as well as poor nutrition including excessive food intake. Many genetic predispositions have been identified in T2D. More than 40 genes, most of them involved in pancreatic β-cell function, appear to be linked to T2D but together are thought to account for only around 10 % of the heritable component of the disease[44]. Incidence of T2D, in parallel with obesity, has increased dramatically over the last 50 years especially in developed countries. In 2013 there were an estimated 387 million diagnosed cases worldwide with a typical onset at mid or old age (>40 years)[45]. T2D is estimated to be

responsible for 3-4 million deaths every year and this number is anticipated to double by 2030, already classifying the conditions as pandemic[43]. The socio-economic impact of T2D is enormous. In the USA alone, T2D is estimated to cost up to 300 billion USD per year. Therefore, prevention and treatment of T2D will be a primary health objective of future generations. Diet control combined with regular exercise is recommended for the individual management of T2D. The most commonly prescribed anti-diabetic, blood glucose-lowering medication used world-wide is the biguanide derivative metformin, which is believed to act mainly by decreasing hepatic glucose production[46]. GNG in the liver is elevated in patients with T2D, probably due to higher levels of circulating glucagon (and stress hormones)[47-49] and increased hepatic glucose production is the main contributor to hyperglycaemia in T2D[50].

T2D is due to insufficient insulin production and release from pancreatic β-cells, as a consequence of chronic insulin resistance, i.e. the inability of cells (mainly muscle, liver and fat) to respond to the hormone. It appears that not all insulin-resistant individuals are diabetic, as long as there is no impairment of compensating increased insulin secretion[51]. Decreased sensitivity of cells to insulin is a long-term, multi-factoral and complicated metabolic dysregulation (for review, see Boucher *et al*, 2014[52]). The causes and precise molecular mechanisms of insulin resistance remain poorly understood. At the cellular and molecular level, some elements linked to the onset of insulin resistance have been proposed:

- Inflammatory signalling seems to play an important role, as mice deficient for JNK1-signalling do not develop obesity/high fat diet-induced insulin resistance[53,54]. Indeed, members of the JNK (c-Jun N-terminal kinases)

family can phosphorylate insulin receptor substrates (IRSs), inhibiting their involvement in insulin signalling[55]. Furthermore, secretion of pro-inflammatory cytokines such as TNFα, IL1 and IL6 are believed to reduce insulin signalling via NF-κB pathway signalling[56]. Also, Toll-like receptor (TLR) signalling has been linked to the establishment of insulin resistance[57].

- The chronic presence of insulin down-regulates the expression of GLUT4, as a part of a negative feed-back mechanism for normal glucose homeostasis, which results in decreased glucose uptake by fat and muscle[58]. This effect may be opposed or reversed by regular exercise in skeletal muscle[59].

- As a consequence of excessive nutrition, reactive oxygen species (ROS) such as superoxide ($O_2^{\cdot -}$) accumulate in mitochondria[60]. This could occur through inhibition or saturation of superoxide dismutase (SOD), the antioxidant enzyme converting it to H_2O_2 (which in turn can be eliminated by catalase). In murine fat and muscle, insulin resistance was shown to be reversible by overexpression of SOD[61] or by treatment of cells with SOD mimetics[62] as well as inhibitors of the electron transport chain and mitochondrial uncoupling agents.

- High circulating free fatty acids (FFA) due to high-fat diet and increased lipolysis in adipocytes can cause an accumulation of triglycerides and derivatives such as ceramide and diacyglycerol in other cells, e.g. skeletal myocytes. The resulting activation of protein kinase C (PKC) isoforms can lead to reduced glucose uptake[63]. Another link has been made with poor content of dietary polyunsaturated phospholipids in myocyte membranes, which at optimal levels increase membrane fluidity and the number of

insulin receptors present on the cell surface, thereby enhancing insulin sensitivity[64]. It is believed that skeletal muscle is the primary site of early insulin resistance[65].

As a consequence of insulin resistance, glucose uptake into fat and muscle cells is decreased, as well as glucose storage as triglycerides and glycogen, respectively. In liver cells, glycogen synthesis is reduced and insulin fails to suppress glucose production and secretion. Besides effects on glucose metabolism, insulin resistance also affects other functions. Adipocytes take up less fatty acids and increase lipolysis of stored triglycerides. This further increases circulating free fatty acids and ultimately leads to accumulation of fat in the liver (NAFLD – non-alcoholic fatty liver disease).

In the natural history of T2D, once insulin resistance is established, the pancreas reacts by increasing the production and release of insulin to keep glycaemia balanced. Eventually this compensatory effect ceases by exhaustion of the pancreas, blood glucose levels rise and T2D establishes[66]. First, postprandial hyperglycemia develops because the body fails to react to high blood glucose after a meal and in a second phase, even fasting glucose levels become elevated, probably at least in part due to elevated glucagon levels whose secretion and action are normally antagonized by insulin. Not surprisingly, nowadays treatments against late-stage T2D successfully include injections of high doses of insulin, best in combination with metformin which has insulin-sensitizing effects[67]. Of note, insulin resistance has been proposed as a protective mechanism of the body against lipo- and glucotoxicity due to fuel overload, protecting organs such as the heart against protein glycation/acetylation and oxidative damage by ROS production[68].

2. AMPK, a master regulator of metabolism

2.1. Generalities

A common feature of eukaryotes is the presence of mitochondria, which are the main source of ATP production via oxidative phosphorylation. The cellular ATP pool needs to be monitored and metabolism to be adapted accordingly to guarantee energy homeostasis – the main role of the AMP-activated protein kinase (AMPK). Virtually all eukaryotes express homologues of AMPK that are essential for cell survival under nutrient starvation[69]. Since ATP is the universal energy currency and upon its utilization, is converted into ADP, one obvious way to monitor cellular energy status would be to sense changes in ADP, which is the case of AMPK. However, the adenylate kinase (AK) equilibrium reaction (2ADP ↔ AMP + ATP) converts ADP into AMP plus ATP and causes a substantial increase in AMP when ATP is consumed[70]. As such, when energy demand increases, cellular ATP concentrations rarely drop by more than 10 %, but this is sufficient to cause AMP levels to increase by at least 10-fold, thus amplifying the sensitivity of the system when sensing AMP rather than ATP (or ADP). Though, free AMP concentrations in basal conditions (<10 µM) are more than 10-fold lower than ADP and 100-fold lower than ATP concentrations (in the millimolar range)[71], although only "free" i.e. non-Mg^{2+}-bound ATP might compete with AMP for regulation of AMPK. The sensor therefore needs to have a much greater affinity for AMP than for the other nucleotides, which again is the case of AMPK and a 6-fold increase AMP was shown to be sufficient to almost maximally activate the kinase[72]. Once activated, AMPK switches on catabolic (energy-producing) pathways

while simultaneously switching off anabolic (energy-consuming) pathways to restore energy balance. In the long term, AMPK also stimulates the formation of new functional mitochondria in order to increase the cellular energy capacity[73].

2.1.1. **History**

Twenty years before its purification and sequencing in 1994, a protein kinase was characterized in liver capable of phosphorylating and inactivating the two rate-limiting enzymes of lipogenesis and cholesterol synthesis, acetyl-CoA carboxylase (ACC) and HMG-CoA reductase (HMGR), respectively[74]. Soon it became clear that this protein kinase was stimulated by nucleotides and most potently by AMP and was therefore named AMP-activated kinase[75]. In the late 1960's, Daniel Atkinson had proposed the "adenylate energy charge" hypothesis for allosteric enzyme regulation by the [ATP]/[ADP][AMP] ratio to couple anabolic and catabolic metabolic pathways[76]. It became clear that AMPK was a central player in this type of metabolic control.

2.1.2. **Genetics**

AMPK is a highly conserved Ser/Thr protein kinase with homologs present in virtually all eukaryotes down to unicellular organisms such as yeast SNF1. Phylogenetically, the AMPK catalytic subunit belongs to the CAMK (Ca^{2+}/calmodulin-dependent protein kinase) branch of the human kinome. There are 12 so-called AMPK-related kinases (NUAK1-2, MARK1-4, SIK1-3, BRSK1-2, MELK) within the same family that share common features such as activation by the upstream kinase LKB1 (except for MELK)[77].

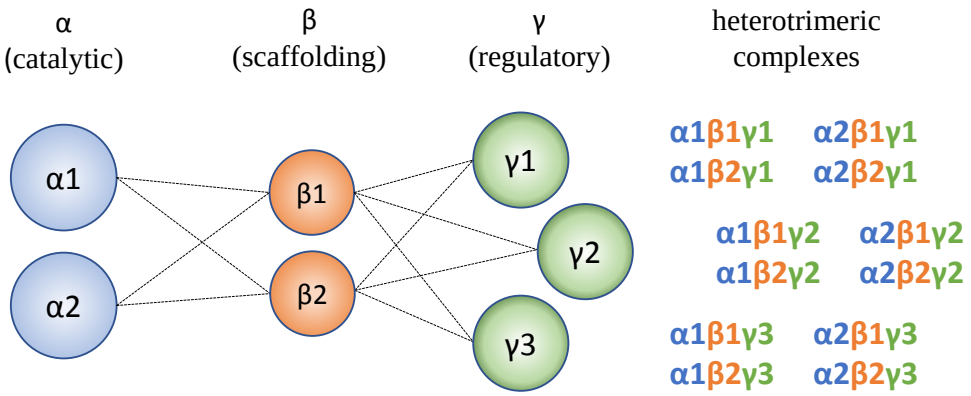

Scheme 5: Possible association of 12 AMPK heterotrimeric complexes.
The three subunits of AMPK associate as heterotrimers to form functional kinase complexes. The catalytic α-subunit and the scaffolding β-subunit are coded each by two distinct genes and the regulatory γ-subunit by three genes. Permutational substitution allows thus formation of 12 different heterotrimeric complexes, even though some of them appear to be rarely expressed.

In mammals, AMPK is a heterotrimer composed of a catalytic α, a scaffolding beta β and a regulatory γ subunit. Each subunit exists in multiple isoforms that are coded by 7 different genes: *PRKA1/2, PRKAB1/2, PRKAG1/2/3*. Thus in theory, 12 different AMPKαβγ complexes can be generated (**Scheme 5**). In addition, alternative initiation codons and splice variants have been identified for certain subunits (α1, γ2, γ3) resulting in minor forms that differ in length. Also, single nucleotide polymorphisms (SNPs) resulting in residue changes occur in all isoforms, some of which can affect AMPK activity and have been linked to metabolic disorders[74]. Together, they increase the potential complexity of AMPK heterogeneity.

2.1.3. **Expression**

In rats and mice, the α1 mRNA is equally expressed in liver, kidney, lung, heart, brain and skeletal muscle whereas α2 mRNA is found mostly in heart and skeletal muscle, followed by liver and kidney **(Table 1)**. The expression profile of β1 seems to be comparable to that of α1, whereas β2 expression is highest in heart and skeletal muscle. Among the gamma subunits, γ1 has the most ubiquitous expression and γ2 is also broadly expressed but highest in heart. Expression of γ3 is the most restricted and seems to be confined to skeletal muscle[74]. Most of the mRNA expression data can be confirmed by measuring AMPK activity following selective immunoprecipitation from tissues, since subunit-specific antibodies are now available. However, these activity measurements mainly reflect the (basal) T172 phosphorylation state of the kinase. Therefore, a complete expression profile at the protein level, especially for human tissues, remains to be established. Our laboratory is currently developing a semi-quantitative MS-based method to address this issue. Interestingly, recent genome-wide analysis of various human tumor biopsies revealed that the *PRKAA1* gene (coding AMPKα1) is frequently amplified whereas *PRKAA2* (coding AMPKα2) often presents inactivating mutations[78]. It is thus tempting to hypothesize that AMPKα1 would have tumor-promoting functions whereas AMPKα2 would be tumor- suppressive. However, the role of AMPK in cancer appears to be much dependent on context (tissue, type, stage, size of the tumor) and might even vary among cells belonging to the same tumor due to cellular and metabolic heterogeneity.

A

subunit	function	gene	isoform	expression
α	catalytic (protein kinase)	*PRKAA1*	α1	ubiquitous
		PRKAA2	α2	heart, skeletal muscle, (liver)
β	scaffolding (localization?)	*PRKAB1*	β1	ubiquitous
		PRKAB2	β2	heart, skeletal muscle, (liver)
γ	regulatory (nucleotide binding)	*PRKAG1*	γ1	ubiquitous
		PRKAG2	γ2	heart, (skeletal muscle, liver)
		PRKAG3	γ3	skeletal muscle

B

metabolic tissue	AMPK catalytic subunit expression
liver	α1 ≈ α2
skeletal muscle	α1 < α2
heart	α1 <<< α2
adipose	α1 >>> α2
pancreatic β-cells	α1 >>> α2

Table 1: Expression profile of AMPK subunits in rodent tissues (A) and AMPKα catalytic subunit expression in key metabolic tissues (B). The different AMPK subunits follow distinct tissue expression profiles and specific heterotrimers are predominant in certain tissues. The catalytic α-subunit in particular is preferentially expressed e.g. isoform 1 in adipose tissue or isoform 2 in heart.

2.1.4. **Localization**

In basal conditions, AMPK is mainly cytosolic showing a particulate extranuclear distribution[79]. However, AMPKα2 has been shown to partially delocalize to the nucleus in skeletal muscle under contraction[80], where it might alter gene expression by phosphorylating translation factors and coactivators. Further investigation is needed to clarify the detailed subcellular localization of different AMPK trimers in tissues under different physiological conditions. Even though the different subunit isoforms display some tissue-specific expression, their subcellular localization might be a major factor determining their function.

2.1.5. **Structure (see Scheme 6)**

AMPKα in its N-terminal half contains the catalytic kinase domain (KD) regulated by the so-called activation loop via the critical phosphorylation site Thr172. This is followed by an auto-inhibitory domain (AID) that limits maximal kinase activity by preventing allosteric activation by AMP. The C-terminal part of AMPKα contains a β-subunit-interacting domain (CTD or βSID) essential for complex formation. Between the AID and the SID is a mostly unstructured region called the α-linker, which contains two motifs that interact with the regulatory γ-subunit (RIM1/2). The AMPKβ subunit contains a central carbohydrate binding module (CBM) that allows AMPK binding to glycogen and a C-terminal subunit binding domain (CTD or αγSBD) providing a scaffold for trimer formation by binding to AMPKα/γ. AMPKγ subunits differ in length by N-terminal extensions (NTE) of unknown function. The most important structural feature of AMPKγ is the four tandem repeats termed cystathionine β-synthase (CBS) motifs that form surface pockets and are responsible for adenine nucleotide binding. It appears that of these four binding sites, CBS2 always remains unoccupied whereas CBS4 contains a permanently bound AMP molecule. CBS domains 1 and 3 reversibly bind ATP, ADP and AMP in a competitive manner, but probably with higher affinity for AMP as suggested by the use of nucleotide analogs[71]. Conserved Asp residues in the binding pockets are essential for adenine nucleotide binding to hydroxyl groups of the ribose moiety while the phosphate groups are coordinated by positively charged basic residues. Certain mutations located close to the nucleotide binding sites in the AMPKγ subunits cause constitutive activation of the kinase, resulting in glycogen storage disease, probably due to excessive glucose uptake[74].

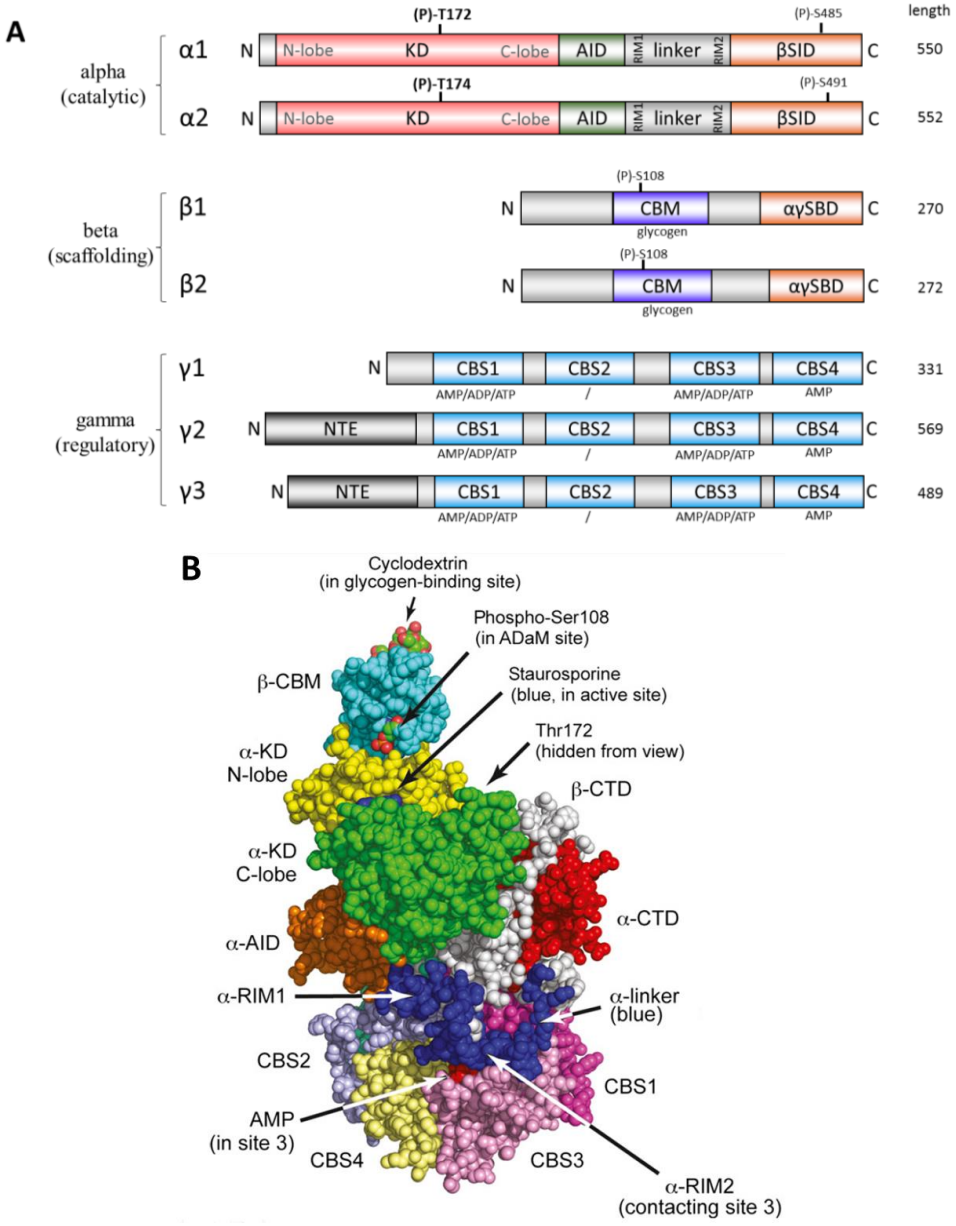

Scheme 6: Main features of AMPK subunit domain structures (A) and 3D crystal structure of the AMPKα1β2γ1 complex (B). Abbreviations: KD = kinase domain; AID = autoinhibitory domain; RIM = regulatory subunit interacting motif; SID = subunit interacting domain; CBM = carbohydrate binding module; SBD = subunit binding domain; CBS = cysthionine beta synthase-like repeats; NTE = amino-terminal extension. Source: Adapted from Ross *et al*, 2016[81].

2.2. Regulation

2.2.1. **Autoinhibition**

AMPK has an absolute requirement for phosphorylation of AMPK α1 T172 or AMPK α2 T174 (rat sequences) located in the activation loop for full activation[82]. Indeed, phosphorylation of this residue prevents the autoinhibitory domain from blocking access to the catalytic site, which maintains AMPK in its inactive form in absence of activating stimuli[83]. Further autoregulatory mechanisms seem to imply the binding of portions from the AMPKβ and AMPKγ subunits to the catalytic domain but are less well established.

2.2.2. **Nucleotide binding**

Adenine nucleotides compete for two of the four binding sites on the AMPKγ subunit[71]. Upon energy depletion, intracellular ATP levels drop and are accompanied by a rise in ADP and AMP. Since AMP displays the greatest affinity and in the same time the biggest relative increase, it is the main positive effector. AMPK activation via a rise in AMP binding to the AMPKγ subunit occurs via three mechanisms: firstly, protection against T172 dephosphorylation by protein phosphatases (also to some extent by ADP binding to AMPKγ); secondly by promoting T172 phosphorylation by upstream kinases; thirdly by allosteric stimulation of AMPK activity. All these effects are antagonized by free ATP and therefore, AMPK activation is actually sensitive to increases in the AMP:ATP (and ADP:ATP) ratio. Of note, AMPK heterotrimers containing different AMPKγ subunits were shown to react with different sensitivities to a rise in cellular AMP[84].

2.2.3. **Myristoylation**

After removal of the initiator Met residue, the N-terminal Gly of the AMPKβ subunit can be myristoylated[85]. In general, this post-translational modification provides an anchor for protein binding to cellular membranes but it can also participate in the regulation of enzyme activity. Myristoylation of AMPKβ seems to participate in autoregulation but also to affect its subcellular localization[79]. Recent evidence suggests that AMPKβ myristoylation is required for AMPKα activation upon metabolic stress[86,87].

2.2.4. **Glycogen binding**

AMPKβ has been shown to interact *in vitro* with glycogen (and other long oligosaccharides containing 1-6 linkages) via its CBM[88], inhibiting AMPK activity and activation by upstream kinases[89]. In intact cells, AMPK can colocalize with glycogen[88]. However, in which tissues and under what physiological conditions AMPK associates with glycogen remains to be determined. In hepatocytes, AMPK was shown to localize around glycogen α-particles[90]**.** In skeletal muscle, binding to glycogen seems to be inhibitory both for AMPK activation by exercise and AICAR[91]. Therefore, AMPK could act as a glycogen sensor and it seems logical that AMPK would be inhibited when fuel reserves are filled and activated when glycogen is depleted such as in exercising muscle or fasting liver.

2.2.5. **Substrate recognition**

As discussed above, the tissue and subcellular localization of both AMPK and its targets could be a critical determinant of AMPK function. Also, it is possible that certain subunit isoforms (not only AMPKα but also AMPKβ and AMPKγ) preferentially interact with certain substrates. AMPK subunits could differ in their affinity for certain substrates and the heterotrimer subunit composition could thus dictate the function. So far, there is no physiological evidence for preferential target phosphorylation by specific heterotrimers. However, AMPKα1- or AMPKα2-containing heterotrimers displayed differences in kinetic properties towards peptide substrates *in vitro*[92]. In addition, mice deficient for either AMPKα1 or AMPKα2 in tissues that normally express both isoforms, showed that certain AMPK functions seem to be mediated mainly by AMPKα2, such as AICAR-stimulated glucose uptake in skeletal muscle[93] (together with AMPKβ2 and AMPKγ3) or control of hepatic glucose production[94].

A consensus motif has been established for AMPK targets[95], by using sequence alignments of validated substrates, site-directed mutagenesis of protein substrates and peptide substrate screening. The general consensus motif is as follows: ΦxβxxS/TxxxΦ, where Φ is a hydrophobic residue, preferentially Leu in the -5 (or -4) position, and β is a basic residue, preferentially Arg in the -3 (or -4) position **(Scheme 7)**. Interestingly, a commercially available monoclonal antibody mixture has been raised against a part of this consensus (LxRxxS) and has been used to identify new AMPK substrates in hepatocytes[96]. However, it is obvious that this sequence motif can only be used for prediction and the sequence must be structurally accessible within the target protein. Also, the fact that several

AMPK substrates poorly match the consensus suggests a certain degree of flexibility or that there are other determinants for AMPK substrate recognition. Two minimal substrate peptides commonly used as tools for measuring AMPK activity *in vitro* are the "SAMS" peptide (HMRSAMSGLHLVK) based on the sequence surrounding Ser79 in the rat sequence of ACC1, the best physiological AMPK substrate, and the optimized "AMARA" peptide (AMARAASAAALARRR).

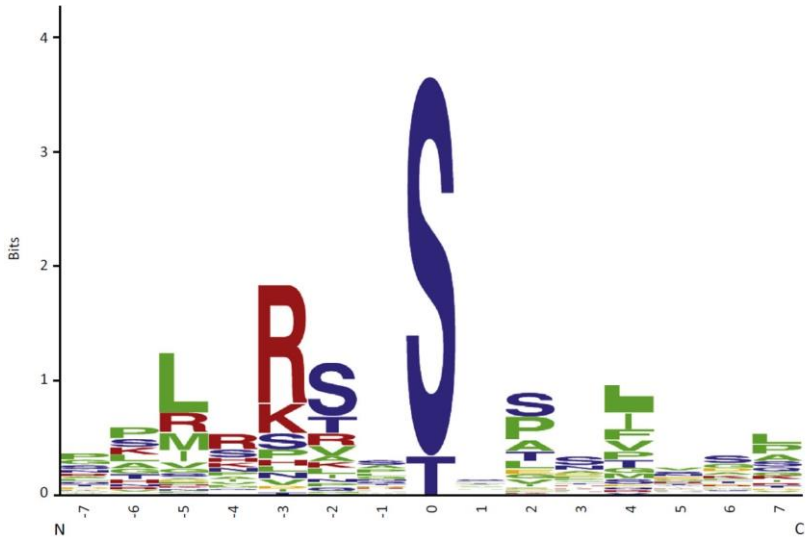

Scheme 7: AMPK consensus target motif. The sequences surrounding AMPK phosphorylation sites (7 residues on either side) from 64 validated human targets were used to establish a residue preference chart for AMPK substrates. Amino acid color scheme: green = hydrophobic; red = basic; yellow = acidic; blue = Ser/Thr, (Source: Hardie *et al*, 2016[97]).

2.2.6. **Phosphorylation**

As mentioned above, maximal AMPK activity strictly depends on AMPKα T172 phosphorylation **(Scheme 8).** Three upstream kinases have been identified: liver kinase B1 (LKB1), Ca^{2+}/calmodulin-dependent kinase kinase-β (CaMKKβ, now known as CaMKK2) and TGFβ-activated kinase 1 (TAK1). The constitutively active LKB1-STRAD-MO25 complex is ubiquitously expressed and is the major AMPK-activating kinase in most cell types and in response to most stimuli[98]. However, the second kinase, CaMKKβ, was shown to activate AMPK when LKB1-deficient cells were treated with Ca^{2+}-ionophores such as A23187, without affecting the AMP:ATP ratio[99]. This could be physiologically relevant in situations where Ca^{2+} is elevated and where CaMKKβ is expressed, such as in contracting smooth muscle, neurons during signal transmission or pancreatic β-cells upon stimulation by glucose. There could be subunit preference for activation by upstream kinases, as indicated by reduced AMPKα2 but not AMPKα1 phosphorylation in contracting skeletal muscle[100] or ischaemic heart[101] from LKB1-deficient mice. Using genetic deletion models, a third kinase, TAK1 was shown to participate in AMPK activation[102]. However, whether TAK1 is a physiologically relevant upstream kinase for AMPK is questionable.

In addition to the AMPKα T172activation site, the AMPKα and AMPKβ subunits contain other (auto)phosphorylation sites, many of which are of unknown function. Importantly, AMPKα1 S485 phosphorylation antagonizes pT172-mediated AMPK activation. Indeed, this site is phosphorylated by PKB[103], PKCs[104], PKD[105] and PKA[106], providing crosstalks from other signalling pathways.

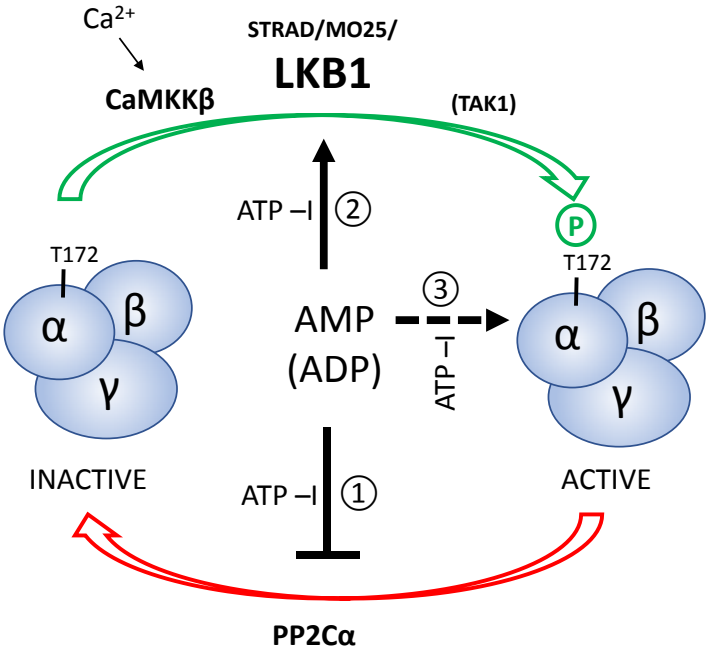

Scheme 8: AMPK activation by upstream kinases and nucleotides.
AMPK is mainly activated by the upstream kinase complex LKB1-STRAD-MO25, through phosphorylation of Thr172 located on the activation loop of the α-subunit. This is favoured by binding of AMP to the γ-subunit, which also protects against dephosphorylation by protein phosphatases and also activates AMPK allosterically. These effects are antagonized by high concentrations of ATP.

2.3. Physiological functions and substrates

Only some of the roles of AMPK are summarized in this section and have been reviewed in more detail elsewhere[74,81,97,107]. An overview of AMPK substrates implicated in metabolism is given in **Scheme 9** and a more integrative picture of the role of AMPK in the control of whole-body metabolism is shown in **Scheme 10**.

2.3.1. **Carbohydrate metabolism**

- Glucose uptake: A rate-limiting step for glucose uptake in response to AMPK activation by skeletal muscle contraction is the translocation of the glucose transporter GLUT4 from cytosolic storage vesicles to the plasma membrane. During exercise, AMPK phosphorylates key residues of AS160/TBC1D4 (S588) and TBC1D1 (S237), causing inactivation of these GTPase-activating proteins[108,109]. As a consequence, RAB proteins involved in exocytosis switch to their active GTP-bound states. Another target of AMPK in the GLUT4 translocation machinery is the lipid kinase PIKfyve (FYVE domain-containing phosphatidylinositol kinase) producing PIP_2[110]. The mechanism by which AMPK activation stimulates muscle glucose transport is independent of the proximal part of insulin signalling and therefore a potential therapeutic target for bypassing insulin resistance to treat T2D-linked hyperglycaemia[111]. In addition, exercise-induced AMPK activation might increase insulin-sensitivity by directly phosphorylating insulin-receptor substrate 1 (IRS) at S789[112] and indirectly by decreasing S6K-mediated inhibitory IRS1 phosphorylation at S307 via reduced mTOR signalling[113]. However, at least in heart, affecting this negative feedback loop of insulin signalling alone is not sufficient for a change in glucose uptake[114]. Finally, AMPK activation by exercise or AICAR treatment was shown to increase the transcription of hexokinase and GLUT4[115], probably through direct activation of the transcriptional coactivator PGC1α[116].
- Glycogen metabolism: AMPK inhibits glycogen synthesis by phosphorylating glycogen synthase (GS) at S7, an inhibitory site[117]. However, this effect can be overcome by increased glucose uptake and

subsequent allosteric stimulation of GS by increased G6P[118]. Therefore, chronic AMPK activation in muscle results in glycogen accumulation. AMPK activation by AICAR could increase glycogenolysis but via allosteric stimulation of glycogen phosphorylase (GP) by ZMP[119].

- Glycolysis: AMPK can increase the glycolytic flux by phosphorylation-induced activation of heart PFKFB2 at S466[120] and of the ubiquitous inducible PFKFB3 at S461[121] (at least in leukocytes), thereby increasing $F2,6P_2$ production, to stimulate PFK1 and glycolysis.
- Hepatic glucose production: Mice deficient for AMPKα2[94] or LKB1[122] have hyperglycaemia and increased hepatic glucose output, due to higher expression of the GNG enzymes PEPCK and G6Pase. The underlying mechanisms involve AMPK-mediated phosphorylation and inhibition of the transcription factor HNF4α (hepatic nuclear factor-4α)[123] and CRTC2 (CREB-regulated transcription coactivator-2)[124] downstream of glucagon/cAMP signalling. Even though AICAR and metformin both activate AMPK and lead to decreased hepatic GNG, long-term effects of these treatments seem to be independent of AMPK as indicated by genetic deletion[125]. However, our results demonstrate short-term antagonism of hepatic glucagon signalling specifically by AMPK activation[126]. Whether AMPK really inhibits GNG in liver in the short-term and the underlying mechanism(s), particularly in the short term, remains to be determined (see Discussion section).
- Glucose sensing: In specialized neurons of the hypothalamus, AMPK is activated in response to low fasting glucose and regulates the expression of neuropeptides (Agouti-related peptide, neuropeptide Y, proopiomelanocortin) to increase hepatic glucose production and appetite

while decreasing peripheral energy expenditure such as by thermogenesis[74].

2.3.2. **Lipid metabolism**

- Fatty acid uptake: AMPK-activating conditions such as muscle contraction or AICAR treatment increase fatty acid uptake in heart and skeletal muscle. However, it is not clear whether and how AMPK is implicated in these effects[74], even though AMPK might increase the expression/translocation of the plasma membrane fatty acid transporter FAT/CD36[127].
- Fatty acid fate: Cytosolic ACC1 and mitochondrial ACC2 catalyze the formation of malonyl-CoA, a precursor for fatty acid synthesis and inhibitor of fatty acid mitochondrial transport (via CPT1) for β-oxidation. AMPK phosphorylates ACC1 at S79 and ACC2 at S221 causing inactivation[128], thereby increasing the oxidation *vs*. synthesis of cytosolic fatty acids[129]. Interestingly, using double knock-in mice, ACC phosphorylation at these sites by AMPK was shown to be required for the insulin-sensitizing (lipid-lowering) effects of metformin[130]. In addition, AMPK was shown to decrease glucose-stimulated fatty acid synthase (FAS) expression via the transcription factor SREBP1c (sterol regulatory element binding protein 1c)[131].
- Triglyceride (TG) turnover: The tissue TG content is a result of the balance between lipogenesis plus fatty acid esterification and lipolysis (triglyceride hydrolysis). Interestingly, deregulation of this system in obesity results in futile cycling and the formation of reactive lipid intermediates that may participate in insulin resistance[132]. AMPK was

reported to inactivate liver mitochondrial glycerol-3-phosphate acyl-transferase (GPAT), a key lipogenic enzyme, through an unknown mechanism[133]. On the other hand, in white adipose tissue, AMPK has an anti-lipolytic effect by phosphorylating hormone-sensitive lipase (S565), thereby preventing its recruitment to lipid droplets[134]. The role of AMPK would thus be to slow down TG turnover but further investigation is needed to explain the underlying mechanisms.

- Sterol synthesis: AMPK inhibits the production of sterols such as cholesterol by directly phosphorylating and inhibiting the rate-limiting enzyme HMGR[135].

2.3.3. **Protein synthesis**

Protein synthesis is estimated to account for the consumption of up to half of total ATP in growing cells[136]. It is therefore not surprising that upon energy stress, this process is rapidly inhibited to preserve ATP. AMPK activation inhibits translation both at initiation and elongation. On the one hand, AMPK inhibits mTOR signalling by phosphorylating (S1387) and activating TSC2[137], a negative regulator of mTORC1, and by phosphorylating (S722/792) Raptor[138], an essential component of this complex. In turn, mTORC1 positively regulates the activity of several translation factors, directly and via S6K (see Scheme 11 in the Results section). On the other hand, AMPK inhibits peptide chain elongation by phosphorylation-induced activation of elongation factor 2 kinase (eEF2K), which in turn phosphorylates and inhibits eEF2[139]. AMPK also activates eEF2K by inhibition of mTORC1, which negatively regulates eEF2K by multiple inputs[140]. The regulation of eEF2K by AMPK was one of two

main objectives studied during my PhD thesis and is presented in more detail in the Results section.

2.3.4. **Other roles**

Among the additional roles of AMPK in cellular function, mitochondrial biogenesis and mitochondrial respiratory chain genes are upregulated by chronic AMPK activation and exercise, an effect which involves activation of PGC1α among others, resulting in increased energy potential (total ATP content)[74]. Interestingly, impaired mitochondrial function in lipid processing has been linked to the onset of insulin resistance[141]. In pancreatic β-cells, AMPK activation seems to inhibit insulin synthesis/storage/secretion but these effects are controversial[142]. AMPK also participates in the regulation of cell polarity via reorganization of the cytoskeleton[143]. In certain cells, AMPK activation has anti-proliferative effects by causing a cell cycle arrest via phosphorylation at S15 and stabilization of the tumor suppressor p53 and subsequently of the cyclin dependent kinase inhibitors p21 and p27, with potential for anti-cancer treatments[144]. Also, the regulation of cell growth can be affected through AMPK-mediated inhibition of mTOR signalling. Lastly, the balance between autophagy and apoptosis can be modulated by AMPK via activation of the autophagy inducer ULK1[145], either by direct phosphorylation or by reduced mTORC1 signalling which inhibits autophagy.

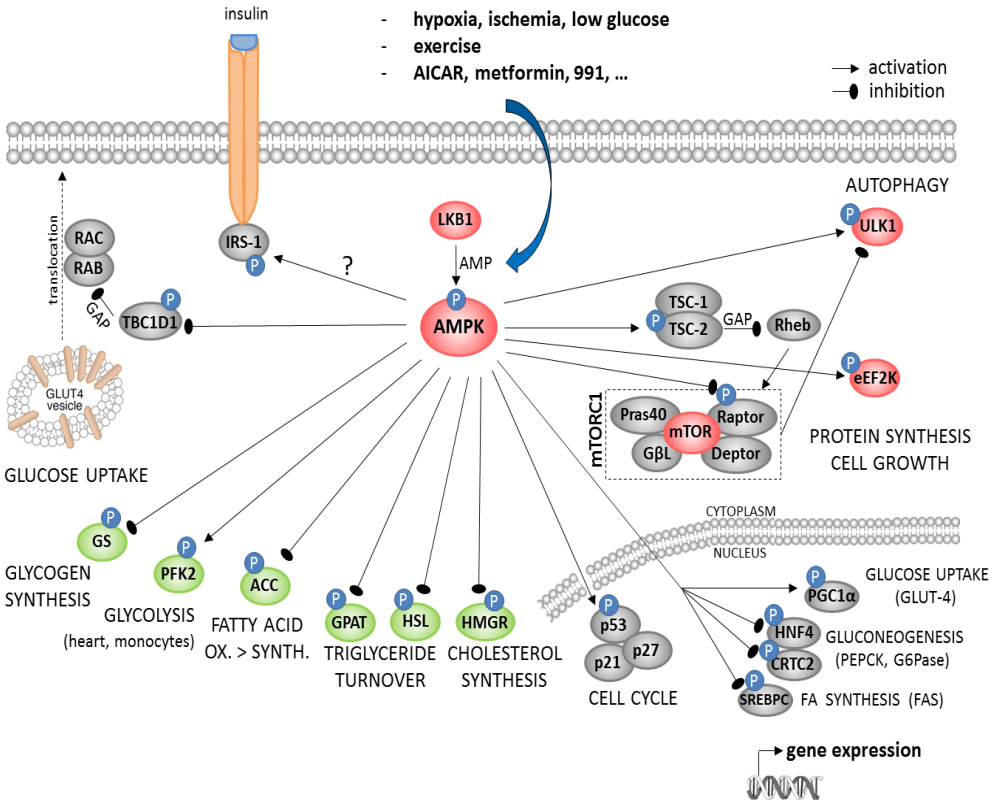

Scheme 9: AMPK signalling, substrates and functions in energy metabolism. AMPK is activated in physiological conditions of energy stress and tends to restore the energy balance by phosphorylation of multiple downstream targets to inhibit ATP-consuming processes such as protein synthesis while simultaneously stimulating ATP-generating processes such as fatty acid oxidation.

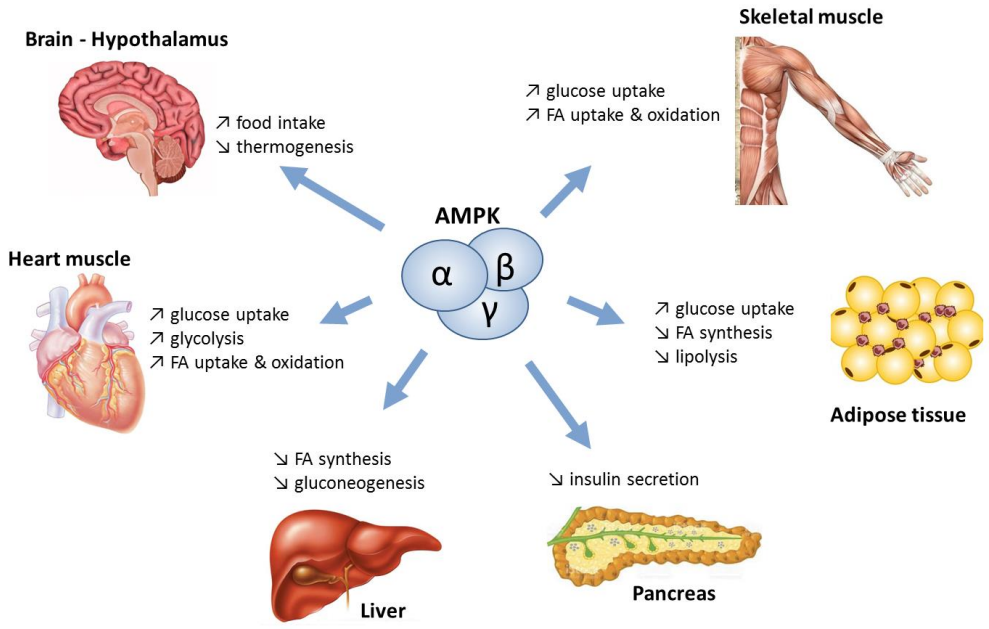

Scheme 10: Roles of AMPK in whole-body energy homeostasis.
AMPK is a central player of energy metabolism with various effects in key metabolic tissues. As such, in heart and skeletal muscle, AMPK favours the uptake and oxidation of fatty acids and glucose from the bloodstream. AMPK also decreases glucose production by the liver.

2.4. Targeting AMPK

2.4.1. **Pharmacological approaches**

The chemical structures of different types of AMPK activators are shown in **Scheme 11**. The different types of AMPK activators have been recently reviewed elsewhere[146-148].

a) Indirect activators

- Inhibitors of glycolysis:

  An easy yet very unspecific way to activate AMPK is to block glycolytic ATP production, resulting in a rise in AMP levels. This can be achieved by using high concentrations of non-metabolizable glucose analogs such as 2-deoxyglucose (2DOG) or 3-O-methyl glucose (3OMG) that cannot be metabolized by PGI or HK, respectively. Interestingly, these compounds have antiproliferative effects on several highly glycolytic cancer cell lines.

- Respiratory chain inhibitors:

  Another indirect way of AMPK activation by increasing AMP levels is to interfere with mitochondrial ATP production, through inhibition of the respiratory electron transport chain or the ATP synthase. A commonly used, rather radical compound is oligomycin, which directly inhibits oxidative phosphorylation of ADP to ATP by inhibiting the proton channel (Fo subunit) of the ATP synthase complex, rapidly causing severe ATP depletion. The most widely used anti-diabetic drug metformin and its more potent yet toxic derivative phenformin also activate AMPK. Although metformin has been reported to directly bind to AMPK[149], it is generally accepted that the drug activates AMPK by inhibiting respiratory chain complex I, thereby increasing the AMP:ATP ratio[150]. Metformin has anti-hyperglycaemic effects mainly by inhibiting glucose production in the liver[46] and by increasing peripheral insulin sensitivity[151], effects that are at least partially mediated by AMPK (see Discussion section). Other polyphenolic compounds known to activate

AMPK by similar mechanisms are resveratrol from red wine and berberine from Chinese medicine.

b) Direct activators

- AMP mimetics:

For many years, the most commonly used AMPK activator was 5-aminoimidazole-4-carboxamide ribonucleoside (AICAR), which is converted to the AMP analog ZMP nucleotide inside cells by adenosine kinase. ZMP binds to the AMPKγ subunit to activate the kinase similarly to AMP. The major drawback of AICAR are off-target effects due to binding to other enzymes allosterically regulated by AMP such as GP, PFK1 or FBPase-1, combined to high concentrations (in the millimolar range) required for maximal AMPK activation. However, AICAR still remains a valuable tool for studying AMPK function as long as the specificity of the effects is validated in genetic deletion models. Interestingly, the hypoglycaemic effect of AICAR was markedly reduced in $\alpha1^{-/-}\alpha2^{liver-/-}$ mice, underlining the role for AMPK in suppressing hepatic glucose production[152]. This supports the notion that the liver rather than skeletal muscle determines glycaemia during starvation and the development of hepatic AMPK activators to combat T2D-linked hyperglycaemia. Another AMP-mimetic compound for AMPK activation is isoxazole “C2”, which can be delivered to cells as a prodrug such as “C13” and which activates AMPK by binding to the gamma subunit in a region located between the AMP-binding sites. The compound appears to have fewer off-target effects than ZMP on AMP-regulated enzymes. Interestingly, C2 seems to selectively activate complexes containing

AMPKα1 and AMPKγ1/2 but not AMPKα2/γ3 and therefore rises hope for isoform-specific AMPK activators to use *in vivo*[153].

- Small molecule activators:

  The first direct non-nucleotide AMPK activator, A-769662, was discovered by Abbott Laboratories in 2006. Interestingly, the compound only activates β1-containing heterotrimers *in vitro* but with a rather poor potency (EC50 ~0.8 µM), which can be increased several-fold though, by using a chlorated form of the compound (Cl-A769662). Also, some off-target effects have been observed at high concentrations. Like metformin, A-769662 decreased hepatic glucose production independently of AMPK in isolated hepatocytes deficient for both α1/α2[125]. A variety of synthetic mid-polar compounds have since been found to activate AMPK *in vitro* and in intact cells. These bind to the recently proposed allosteric drug and metabolite (ADAM) binding site on AMPK, a pocket which is found between the α-subunit kinase domain and the β-subunit CBM[154] (**Scheme 6**). For several of these activators, including A-769662, efficient binding requires autophosphorylation of AMPKβ1 Ser108 located nearby. The most promising class of new molecules are benzimidazole derivatives such 991 (also called ex229), which was first described in 2013[154]. *In vitro*, compound 991 activates both AMPKβ1/2 containing complexes but with a preference for AMPKβ1 and displayed a potency (EC50 ~3 nM; >100-fold compared with A-769662). The activation mechanism seems to involve both protection against AMPKα T172 dephosphorylation and allosteric stimulation. Our laboratory has taken advantage of this novel AMPK activator to demonstrate that it increased glucose uptake in skeletal muscle[155] and antagonized

glucagon/cAMP signalling in hepatocytes[126] (see Results section) through AMPK activation. Interestingly, salicylate from which aspirine is derived (acetylsalicylate), also binds the ADAM pocket to activate AMPK.

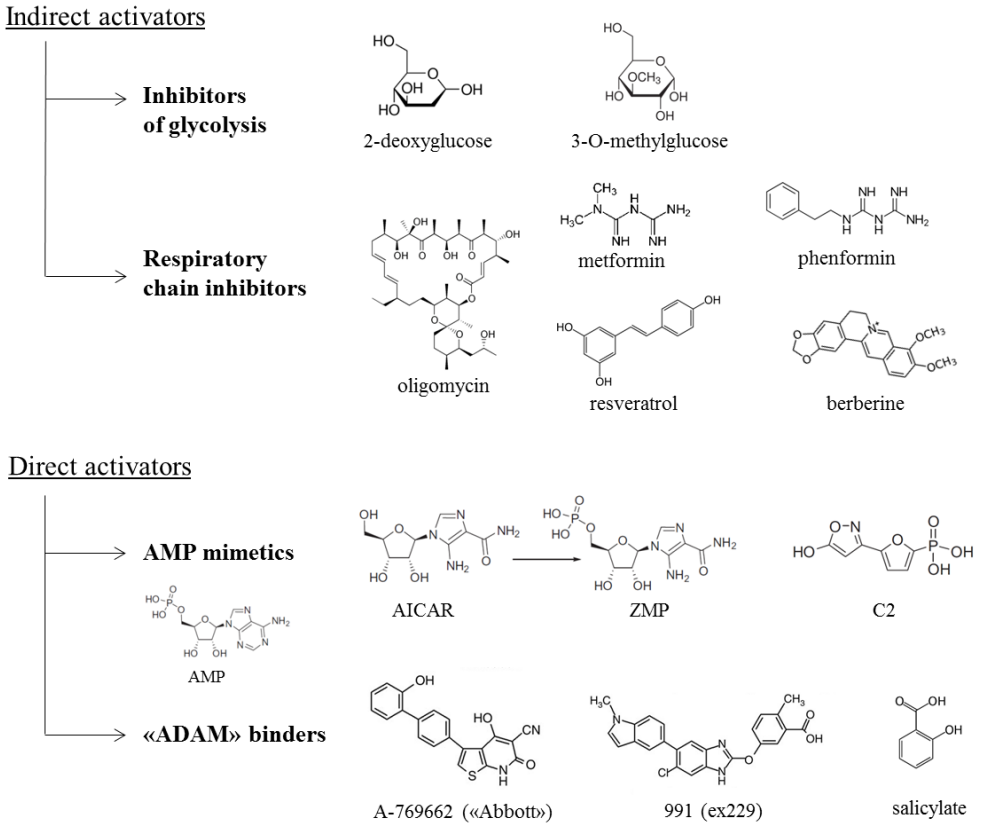

Scheme 11: Classes and chemical structure of pharmacological AMPK activators. AMPK is activated by various chemical compounds that are not structurally related. On the one hand, activation can be achieved indirectly, via inhibition of glycolysis or mitochondrial respiration, both increasing the AMP:ATP ratio. On the other hand, activation can be direct by binding to the γ-subunit (AMP mimetics) or to a pocket ("ADAM") located between the α- and β-subunits.

In conclusion, over the last years there has been enormous progress in the discovery of new direct and therefore more specific AMPK activators. Improvements would include the development of isoform-specific activators for selective targeting of AMPK function in certain tissues, in order to eliminate unwanted side-effects encountered by whole-body AMPK activation. Also, one should be cautious regarding the long-term use of these activators, since chronic AMPK activation in certain tissues can have adverse effects.

2.4.2. **Genetic approaches**

Biomolecular tools

In intact cells, AMPK can be targeted using easily available standard biomolecular tools such as siRNA or shRNA to modulate the expression of the different subunits. In addition, AMPK mutant forms with useful properties have been identified[156] and are widely used tools for assessing the roles of AMPK in cells and whole organisms. An early reagent is the constitutively active truncated catalytic subunit AMPKα1$^{1\text{-}312,T172D}$, which lacks the auto-inhibitory domain and is protected against dephosphorylation by protein phosphatases via the phospho-mimicking mutation into aspartate of the activation loop residue T172. This mutant no longer assembles with AMPKβ and AMPKγ but conserves its kinase activity and ability to phosphorylate (at least certain) AMPK targets. Another tool is the kinase-inactive mutant AMPKα1^{D157A}, which has impaired ATP binding but still

forms heterotrimeric complexes. When highly expressed, this mutant is able to act as a dominant-negative, probably by competing with the endogenous catalytic subunits for AMPKαβγ heterotrimer formation or by competition for substrate binding. Both mutant AMPK forms have been expressed in cells using conventional transfection methods and *in vivo* using adenoviral injection (for example in the tail vein to mainly target the liver).

Mouse models

Most studies on AMPK function have been based on cell incubations with pharmacological activators. However, since no reliable isoform-specific activators exist so far, it has not been possible to assign specific functions to the different isoforms or heterotrimeric complexes. Transgenic and knock-out mouse models (summarized in **Table 2**) have thus been generated to address this question. In particular, the creation of AMPKα1$^{-/-}$ and AMPKα2$^{-/-}$ mice has given important insight to understand the roles of AMPK in energy metabolism. Interestingly, these mice display differences in their metabolic phenotype and response to pharmacological AMPK activation with AICAR. Whole-body deletion of AMPKα1 has no detectable metabolic phenotype whereas whole-body AMPKα2 deletion results in a T2D-like phenotype presenting mild insulin-resistance and hyperglycaemia during starvation together with impaired insulin secretion. However, this appeared to be due mainly to changes in hypothalamic control of the autonomous nervous system, particularly catecholamine release, rather than the function of key metabolic tissues such as liver, skeletal muscle and pancreas. In normal rodent liver, the catalytic subunits AMPKα1 and AMPKα2 are expressed equally. Whole-body double knockout of the two

AMPK catalytic subunits is embryonic lethal, as is the whole-body knockout of LKB1. However, crossing AMPKα1$^{-/-}$ mice with liver-specific AMPKα2$^{LS-/-}$ allowed the creation of mice devoid of any AMPK activity in liver. These mice are a precious tool for the study of liver metabolism and hepatocytes from these animals were used in the present work[126] (see Results section). Liver-specific deletion of AMPK resulted in increased plasma triglycerides and mild hyperglycaemia during starvation due to higher hepatic glucose production. Interestingly, mice lacking LKB1 in liver display more severe hyperglycaemia that cannot be corrected by treatment with AICAR or metformin. Indeed, members of the AMPK-related salt-inducible kinase (SIK) family have also been implicated in the control of hepatic glucose metabolism and could thus be responsible for this effect. Another approach was the transgenic expression of dominant-negative AMPKα in selected tissues. Recently, mice deleted for the AMPKβ subunits have been generated and revealed that AMPKβ1/2 cannot compensate for each other. This is in agreement with our findings in hepatocytes from AMPKβ1$^{-/-}$ mice[126] (see Results section). However, the disadvantage of all these models is the danger of adaptation/compensation due to lack of AMPK during development. It is therefore imperative to generate inducible knock-out models in addition to tissue-specific deletion of AMPK isoforms.

Knockout	Tissue specificity	Remarks	References
AMPKα1$^{-/-}$	full body		Jorgensen, 2004[93]
AMPKα2$^{-/-}$	full body		Viollet 2003[157]
AMPKβ1$^{-/-}$	full body		Dzamko, 2010[158]
AMPKβ2$^{-/-}$	full body		Steinberg, 2010[159]
AMPKβ1$^{mck-/-}$ AMPKβ2$^{mck-/-}$	heart & skel. muscle	β1/2$^{lox/lox}$ + *mck*-Cre	O'Neill, 2011[160]
AMPKγ3$^{-/-}$	full body		Barnes, 2004[161]
AMPKα2$^{alb-/-}$	liver	α2$^{lox/lox}$ + *alb*-Cre	Andreelli, 2006[94]
AMPKα1$^{-/-}$ AMPKα2$^{alb-/-}$	full body/liver	α2$^{lox/lox}$ + *alb*-Cre	Guigas, 2006[162]
AMPKα2$^{agrp-/-}$	hypothalamus	α2$^{lox/lox}$ + *agrp*-Cre	Claret, 2007[163]
AMPKα2$^{pomc-/-}$	hypothalamus	α2$^{lox/lox}$ + *pomc*-Cre	Claret, 2007[163]
AMPKα1$^{-/-}$ AMPKα2$^{pomc-/-}$	full body/hypothalamus	α2$^{lox/lox}$ + *pomc*-Cre	Claret, 2007[163]
LKB1$^{mck-/-}$	heart & skeletal muscle	α2$^{lox/lox}$ + *mck*-Cre	Sakamoto, 2005[101,164]
LKB1$^{alb-/-}$	liver	α2$^{lox/lox}$ + *alb*-Cre	Woods, 2011[165]

Table 2: Selection of AMPK knockout mouse models for the study of roles of AMPK in energy metabolism. AMPK subunits have been genetically deleted in mice, either at the level of the whole body or targeted to certain tissues via tissue-specific expression of the Cre recombinase and flanking of AMPK genes with lox sequences. Abbreviations: *mck* = muscle creatin kinase; *alb* = albumin; *agrp* = Agouti-related peptide; *pomc* = pro-opiomelanocortin.

RESULTS

I. Regulation of hepatic glucagon signalling by AMPK-induced activation of a cAMP phosphodiesterase

Preface

In 2013, Miller *et al.* (*Nature*, 494(7436):256–260) made the major discovery that treatment of hepatocytes with metformin inhibited glucagon signalling by decreasing cAMP levels. This was a novel mechanism by which the drug could inhibit glucagon-induced glucose production by the liver. However, they found the effect to be AMPK-independent based on the use of mouse hepatocytes deleted for both AMPKα catalytic subunits. Miller *et al.* proposed a mechanism by which cAMP production by adenylate cyclase was inhibited by a rise in AMP, due to respiratory chain inhibition by metformin. Together with Dr. Yu-Chiang Lai, a post-doctoral fellow in our laboratory, I explored whether we would obtain the same effects using the novel direct AMPK activator compound 991, which activates AMPK without increasing cellular AMP levels. To our surprise, treatment of hepatocytes with 991 dose-dependently decreased glucagon-induced cAMP levels. In collaboration with Dr. Marc Foretz (Paris), we

went on to show that this effect was completely abolished in AMPKα1$^{-/-}$ α2$^{LS-/-}$ hepatocytes, and was thus AMPK-dependent. The underlying mechanism was found to involve direct activation of a phosphodiesterase (PDE4B) by AMPK, thereby accelerating cAMP degradation. Moreover, treatment of hepatocytes with metformin/phenformin also led to PDE activation and phosphorylation of PDE4B.

The study was published in *Nature Communications* in 2016.

cAMP signalling and phosphodiesterases

The topic has been reviewed in detail elsewhere[166,167].

The 3',5'-cyclic nucleotides monophosphates cAMP and cGMP are key second messengers controlling major body functions such as vascular smooth muscle contraction, heart contractility and brain signalling. Levels of cAMP are determined by the balance between their production by adenylate cyclase (AC) from ATP on the one hand and hydrolysis to AMP by phosphodiesterases (PDEs) on the other hand. cAMP production by AC is activated directly by G protein coupled receptors of various hormones such as glucagon and catecholamines (see Introduction section). The main downstream effectors are cAMP-dependent protein kinase (PKA), cAMP-gated ion channels and cAMP-regulated guanine exchange factors (GEFs) regulating G proteins also called exchange proteins activated by cAMP (EPACs). These signalling molecules and the proteins producing or degrading them can be compartmentalized to control specific cell functions. A multitude of different PDE isoforms exists to specifically control particular signal transduction pathways. Mammalian PDEs have a N-

terminal regulatory domain, often comprising regulatory phosphorylation sites, and a C-terminal catalytic domain with high affinity for cAMP, cGMP or both (K_M ~1-10 µM). The catalytic domain is highly conserved among PDE families whereas unique N-terminal parts determine the regulation, localization and thus the function of particular isoforms. In mammals, 21 PDE-coding genes have been identified, which are classified into 11 families (termed PDE1-11). Most of them comprise several (up to four) isoforms coded by distinct genes designated by letters, e.g. PDE4A-D. Alternative splicing, promoters and initiation can generate multiple transcription products from the same gene, to generate additional isoforms differing in length of the regulatory N-terminus. These are indicated by a second number such as in PDE4B3. The overall variety of PDE isoforms is thus incredibly vast. Unique characteristics include the presence of regulatory phosphorylation or lipidation sites, allosteric regulation by cyclic nucleotides, dimerization, subcellular localization, binding of Ca^{2+}/calmodulin, transmembrane or membrane-association domains and other unique regulatory domains.

In conclusion, studying the function of particular PDE isoforms is a delicate task and interpretation of results is complicated, even though an increasing number of specific biomolecular and pharmacological tools is available, such as antibodies and inhibitors. The matter is further discussed in the Discussion section.

nature COMMUNICATIONS

ARTICLE

Received 10 Jul 2015 | Accepted 27 Jan 2016 | Published 8 Mar 2016

DOI: 10.1038/ncomms10856 OPEN

AMPK antagonizes hepatic glucagon-stimulated cyclic AMP signalling via phosphorylation-induced activation of cyclic nucleotide phosphodiesterase 4B

M. Johanns[1,*], Y.-C. Lai[1,*,†], M.-F. Hsu[1,†], R. Jacobs[1], D. Vertommen[1], J. Van Sande[2], J.E. Dumont[2], A. Woods[3], D. Carling[3], L. Hue[1], B. Viollet[4,5,6], M. Foretz[4,5,6] & M.H. Rider[1]

Biguanides such as metformin have previously been shown to antagonize hepatic glucagon-stimulated cyclic AMP (cAMP) signalling independently of AMP-activated protein kinase (AMPK) via direct inhibition of adenylate cyclase by AMP. Here we show that incubation of hepatocytes with the small-molecule AMPK activator 991 decreases glucagon-stimulated cAMP accumulation, cAMP-dependent protein kinase (PKA) activity and downstream PKA target phosphorylation. Moreover, incubation of hepatocytes with 991 increases the V_{max} of cyclic nucleotide phosphodiesterase 4B (PDE4B) without affecting intracellular adenine nucleotide concentrations. The effects of 991 to decrease glucagon-stimulated cAMP concentrations and activate PDE4B are lost in hepatocytes deleted for both catalytic subunits of AMPK. PDE4B is phosphorylated by AMPK at three sites, and by site-directed mutagenesis, Ser304 phosphorylation is important for activation. In conclusion, we provide a new mechanism by which AMPK antagonizes hepatic glucagon signalling via phosphorylation-induced PDE4B activation.

[1] Université catholique de Louvain and de Duve Institute, Avenue Hippocrate, 75, 1200 Brussels, Belgium. [2] Faculté de Médecine, Institut de Recherche Interdisciplinaire en Biologie Humaine et Moléculaire (IRIBHM), Université Libre de Bruxelles (ULB), Route de Lennik, 808, 1070 Brussels, Belgium. [3] Cellular Stress Group, MRC Clinical Sciences Centre, Imperial College London, Hammersmith Hospital, DuCane Road, London W12 0NN, UK. [4] INSERM U1016, Institut Cochin, 75014 Paris, France. [5] CNRS UMR8104, 75014 Paris, France. [6] Université Paris Descartes, Sorbonne Paris Cité, 75014 Paris, France. * These authors contributed equally to this work. † Present addresses: MRC Protein Phosphorylation and Ubiquitylation Unit, College of Life Sciences, University of Dundee, Dundee, UK. (Y.-C.L.); Graduate Institute of Sports Training, University of Taipei, No. 101, Sec. 2, Zhongcheng Road, Shilin Dist., 11153 Taipei City, Taiwan (M.-F.H.). Correspondence and requests for materials should be addressed to M.H.R. (email: mark.rider@uclouvain.be).

One of the short-term effects of glucagon in liver is to increase glycogen breakdown and inhibit glycolysis[1–3]. Glucagon provides the mechanism for switching the metabolism of liver between the well-fed state and the starved state, which comprises several phases. During the first few hours of starvation, glycogen reserves in the liver are mobilized to maintain blood glucose, but during prolonged starvation, hepatic gluconeogenesis prevails[4]. Glucagon action is mediated by increased cyclic AMP (cAMP) via stimulation of adenylate cyclase and subsequent activation of cAMP-dependent protein kinase (PKA)[5,6]. Glycogenolysis is increased via phosphorylase kinase activation downstream of PKA, which also inhibits glycolysis by phosphorylating and inactivating liver 6-phosphofructo-2-kinase/fructose-2,6-bisphosphatase (PFKFB1 isoenzyme), thereby lowering fructose-2,6-bisphosphate concentrations, and by phosphorylation-induced inactivation of L-type pyruvate kinase. In the long-term, glucagon induces the expression of key gluconeogenic enzymes, such as phosphoenolpyruvate carboxykinase and glucose-6-phosphatase[7,8], which together with its short-term effects, accounts for the increase in hepatic gluconeogenesis and glucose output in the fasted state[9]. Type 2 diabetes is characterized by hyperglycaemia and, due to a combination of insulin resistance and impaired β-cell function, the liver excessively releases glucose into the blood. Also, elevated plasma glucagon concentrations play a role in dysregulated hepatic glucose production[10]. Metformin, the front-line drug used worldwide for the treatment of diabetes, decreases hepatic glucose production and activates AMP-activated protein kinase (AMPK)[11–16]. However, whether AMPK and/or its upstream kinase LKB1 is required for the inhibition of hepatic glucose output by biguanides, such as metformin and phenformin, is controversial[17–22]. Biguanides inhibit mitochondrial respiratory chain complex I (ref. 23), resulting in a fall in ATP, and it was proposed that the resulting increase in AMP in hepatocytes would directly inhibit adenylate cyclase to abrogate glucagon-stimulated increases in PKA activity independently of AMPK[21]. Recently, we studied a small-molecule benzimidazole derivative that rapidly and potently activates AMPK[24], thereby stimulating glucose uptake in skeletal muscle without increasing cellular AMP levels[25]. In the present study, we used the same molecule, referred to as 991, in primary mouse hepatocytes. We propose a mechanism by which AMPK activation antagonizes glucagon signalling by phosphorylating and activating the major hepatic cyclic nucleotide phosphodiesterase (PDE) isoform PDE4B, thereby lowering cAMP levels and decreasing PKA activation.

Results

Compound 991 decreases glucagon-stimulated PKA signalling. Compound 991 (previously called ex229) is a potent small-molecule AMPK activator that increases glucose uptake in incubated rat and mouse skeletal muscles[25]. In primary mouse hepatocytes, treatment with 991 before incubation with glucagon dose-dependently decreased the glucagon-stimulated increase in intracellular cAMP concentrations (Fig. 1a). Consistent with effects on cAMP levels, 991 treatment antagonized increased phosphorylation by glucagon of PKA downstream targets glycogen phosphorylase (GP)[26] at Ser14 and cAMP response element-binding protein (CREB)[27] at Ser133 (Fig. 1b–d,g). Moreover, incubation with a single high dose of 991 antagonized the increases in cAMP levels and PKA activity in response to increasing concentrations of glucagon (Fig. 1e,f). The rise in cAMP levels in response to glucagon is transient (Fig. 2c) and only a small increase in cAMP was needed (Fig. 1e) to elicit PKA activation (Fig. 1f). In hepatocytes preincubated with 991, increased GP activity (Fig. 1h) and increased GP Ser14 phosphorylation induced by glucagon (Fig. 1g) were also reduced.

AMPK activation leads to increased PDE activity. Direct inhibition of adenylate cyclase by AMP has been proposed to explain how biguanides reduce glucagon-stimulated cAMP production in hepatocytes[21]. Indeed, in hepatocytes incubated with phenformin, a reduction in intracellular ATP levels with concomitant increases in AMP, ADP, AMP:ATP and ADP:ATP ratios were observed (Fig. 2a). Also, treatment with 991 or phenformin led to AMPK activation, which was unaffected by glucagon (Fig. 2b). However, the effects of 991 to activate AMPK and antagonize glucagon action in hepatocytes observed in our study were not accompanied by changes in intracellular adenine nucleotide concentrations, even at the maximal dose of 10 μM (Fig. 2a). A time-course study indicated that there was no significant difference in the initial rate of cAMP production by glucagon in hepatocytes preincubated with 991 (Fig. 2c), suggesting that adenylate cyclase activity was not affected by compound treatment. After 7 min of incubation, glucagon-stimulated cAMP levels decreased rapidly in cells preincubated with 991, such that after 30 min of incubation with glucagon, cAMP concentrations were reduced by 80% (Fig. 2c). We hypothesized therefore, that AMPK activation could lead to an increase in PDE activity, thus lowering cAMP accumulation seen in the presence of glucagon. Indeed, in extracts prepared from hepatocytes incubated with 991, total PDE activity increased by ~50% in a dose-dependent manner, which correlated with increased AMPK activity (Fig. 2d). Also, PDE activation after treatment with 991 was comparable to that seen in hepatocytes incubated with glucagon (Fig. 2e), which is known to activate PDE as a negative feedback mechanism for cAMP signalling[28]. PDE activation was also observed in hepatocytes incubated with the AMPK activator 5-aminoimidazole-4-carboxamide ribonucleoside (AICAR), but not significantly with A769662, a small-molecule AMPK activator that is not as effective as compound 991, at least in skeletal muscle[25]. Interestingly, treatment of hepatocytes with phenformin increased PDE activity to similar levels to those observed with 991 (Fig. 2e), and incubation with either phenformin or metformin led to dose-dependent PDE activation, which correlated with increased AMPK Thr172 phosphorylation (Supplementary Fig. 1). Moreover, significant increases in PDE activity were obtained with submaximal doses of phenformin (100 μM) and metformin (100–300 μM). To confirm the implication of PDE activity in the effect of 991 to lower cAMP, hepatocytes were incubated with the pan-PDE inhibitor 3-isobutyl-1-methylxanthine (IBMX) with or without 991, before addition of increasing concentrations of glucagon (Fig. 2f). In the presence of IMBX, the effect of 991 to decrease glucagon-induced cAMP accumulation was lost, suggesting PDE dependence. In this experiment, the dose-dependent increase in cAMP levels in response to glucagon was much higher (Fig. 2f versus Fig. 1e), indicating that the PDE inhibitor was effective.

Effects of compound 991 treatment are AMPK-dependent. To test whether the effects of compound 991 treatment were AMPK-dependent, primary hepatocytes were isolated from mice in which the two catalytic subunits of AMPK had been specifically deleted in liver (referred to as AMPK $\alpha_1^{-/-}\alpha_2^{LS-/-}$). In hepatocytes from wild-type mice incubated with increasing concentrations of glucagon, phosphorylation of ACC and AMPK slightly increased, as seen by immunoblotting extracts (Fig. 3a), even though AMPK activation by glucagon was not detected after one hour of incubation (Fig. 2b). However, the effect of glucagon to increase ACC phosphorylation was absent in hepatocytes from AMPK $\alpha_1^{-/-}\alpha_2^{LS-/-}$ mice (Fig. 3a), suggesting that AMPK mediates this effect. Moreover, the effect of incubation with 991

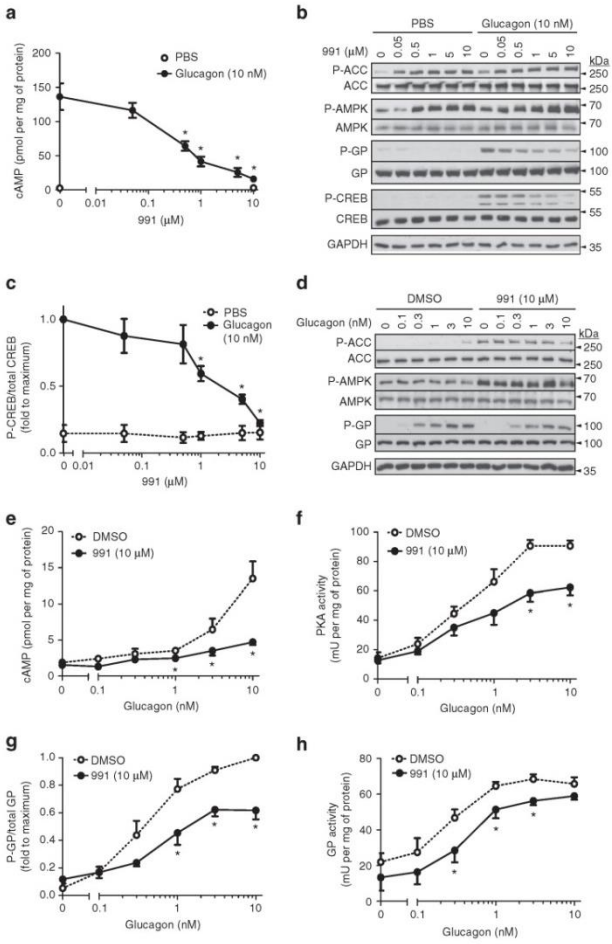

Figure 1 | Compound 991 activates AMPK in hepatocytes and decreases glucagon-stimulated PKA signalling. Primary mouse hepatocytes were serum-starved overnight and incubated for 20 min with the indicated concentrations of 991 or dimethylsulfoxide (DMSO) as vehicle before stimulation with the indicated concentrations of glucagon for 15 min. The cells were collected and lysed for the measurement of intracellular cAMP concentrations by radioimmunoassay (**a**) or enzyme-linked immunosorbent assay (ELISA) (**e**), for immunoblotting phosphorylated and total proteins as indicated (**b**,**d**), for PKA assay (**f**), for GP assay (**h**) and for quantification of CREB and GP phosphorylation by immunoblotting (**c**,**g**). Values are means ± s.e.m. for $n=4$ (**a**,**f**–**h**) or $n=5$ (**c**,**e**) separate experiments, and in **b** and **d** representative blots are shown. Statistical analysis was by a paired Student's *t*-test. *Indicates a significant difference ($P<0.05$) compared with control incubations with DMSO.

to increase ACC phosphorylation in hepatocytes from control mice was almost completely lost in hepatocytes from AMPK $\alpha_1^{-/-}\alpha_2^{LS-/-}$ mice and both total and pThr172-AMPK were undetectable (Fig. 3a). In addition, the effects of 991 to abrogate glucagon-stimulated cAMP accumulation (Fig. 3b) and PKA activation (Fig. 3c) were abolished in incubations of hepatocytes from AMPK $\alpha_1^{-/-}\alpha_2^{LS-/-}$ mice, indicating the requirement of AMPK. Similar results were obtained in incubations of hepatocytes prepared from mice bearing a whole-body deletion of the AMPK β1-subunit, which contributes towards providing a high-affinity binding site for compound 991 (ref. 24). There is almost no AMPK activity in the liver of these mice (Woods and Carling, unpublished data), and residual AMPK activity might have been due to increased expression of the AMPK β2-subunit (Supplementary Fig. 2B). In hepatocytes from AMPK β1-knockout compared with wild-type mice, the effect of 991 to activate AMPK and increase ACC phosphorylation was severely abrogated and the increase in Raptor (regulatory-associated protein of mTOR) phosphorylation, another direct AMPK substrate, was completely lost (Supplementary Fig. 2B). Importantly, in

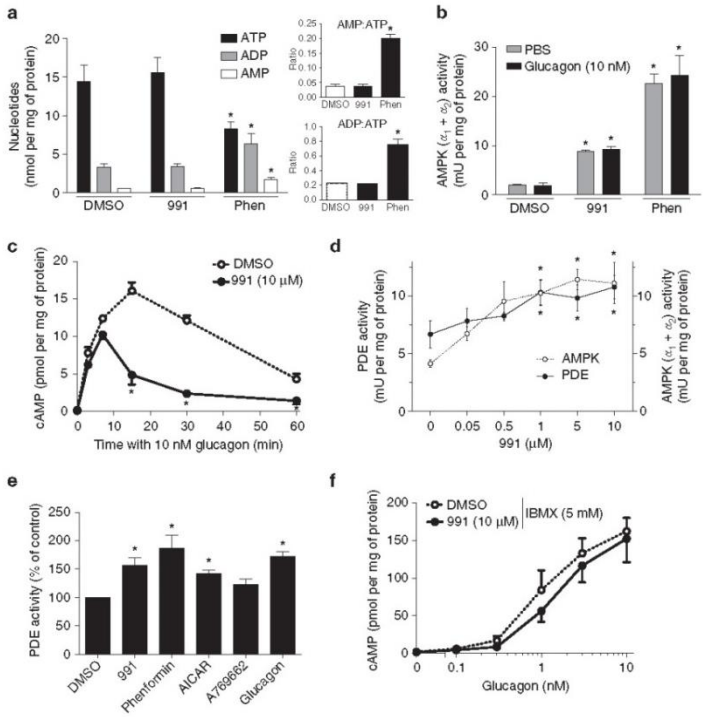

Figure 2 | AMPK activation decreases cAMP levels by activating a PDE. Primary mouse hepatocytes were incubated for 1 h with DMSO as vehicle, 10 μM 991, 500 μM phenformin, 2 mM AICAR, 100 μM A769662, 10 nM glucagon or with concentrations of 991 and glucagon as indicated for measurements of intracellular adenine nucleotide concentrations (**a**), AMPK activity by immunoprecipitation using anti-AMPKα1 and anti-AMPKα2 antibodies (**b**,**d**) and total PDE activity (**d**,**e**). In **e**, the 100% value for PDE activity in the DMSO-treated control condition was 6.4 ± 0.7 μU per mg of protein. In **c**, mouse hepatocytes were incubated for 20 min with 10 μM 991 or DMSO as vehicle before incubation with 10 nM glucagon for ELISA measurements of cAMP concentrations at the indicated times. In **f**, mouse hepatocytes were incubated for 20 min with 10 μM 991 or DMSO as vehicle and 5 mM pan-PDE inhibitor IBMX before incubation with the indicated concentrations of glucagon for 15 min and measurement of cAMP (ELISA method). Values are means ± s.e.m. for $n=3$ (**a**–**d**), $n=5$ (**e**) or $n=4$ (**f**) separate experiments. Statistical analysis was by a paired Student's *t*-test. *Indicates a significant difference ($P<0.05$) compared with control incubations with DMSO.

hepatocytes from AMPK β1-knockout versus wild-type mice, the effect of 991 to lower glucagon-stimulated cAMP accumulation was markedly reduced (Supplementary Fig. 2A). Treatment of hepatocytes from control mice with 991 increased PDE activity in extracts by ~50%, whereas in hepatocytes from AMPK $\alpha_1^{-/-}\alpha_2^{LS-/-}$ mice the effect of 991 was lost, further confirming the requirement of AMPK. By contrast, incubation with glucagon led to PDE activation in hepatocytes from both wild-type and AMPK $\alpha_1^{-/-}\alpha_2^{LS-/-}$ mice (Fig. 3d).

PDE4 is the major isoenzyme activated by 991 in hepatocytes. The expression of PDE isoenzymes in primary mouse hepatocytes was investigated. Earlier studies suggested that the major PDE isoenzymes expressed in liver are members of the PDE3/4 subfamilies[29–31]. Real-time PCR revealed that amongst these, the predominant PDE mRNA in primary mouse hepatocytes was the PDE4B isoenzyme (Fig. 4a). The implication of PDE isoenzymes in cAMP hydrolysis in hepatocytes was assessed by the use of specific inhibitors *in vitro*. When hepatocytes were preincubated with the PDE4-specific inhibitor rolipram and 991 before addition of increasing concentrations of glucagon, the cAMP-lowering effect of 991 was completely abolished (Fig. 4b). Other compounds used were the PDE3-specific inhibitor cilostamide and the pan-PDE inhibitor IBMX, which, along with rolipram, were added to the assays for measuring PDE activity in hepatocyte extracts. PDE activity in control extracts was inhibited by about 70% by rolipram and by over 90% by IBMX, but was not significantly decreased by cilostamide (Fig. 4c), confirming that PDE4 is mainly responsible for cAMP removal in primary mouse hepatocytes. Moreover, PDE activation by 991 was not seen in the presence of rolipram (or IBMX), but was still present when assays were performed in the presence of cilostamide, suggesting that PDE4 was activated in response to 991 treatment. PDE assays routinely contained 1 μM cAMP, but the extent of PDE activation in hepatocytes incubated with 991 was the same when extracts were assayed with a saturating concentration of cAMP (50 μM), indicating an effect of 991 treatment on V_{max} rather than K_M (data not shown).

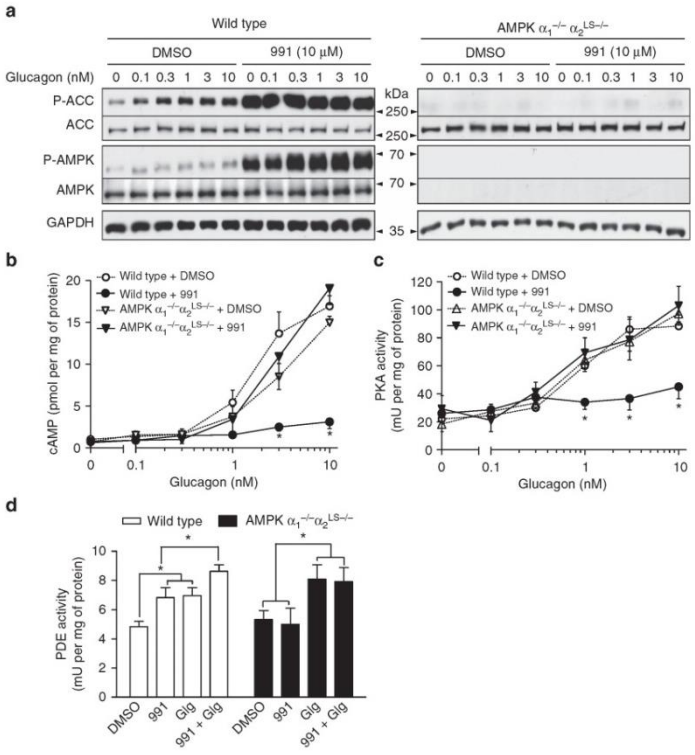

Figure 3 | Compound 991 antagonizes glucagon signalling in an AMPK-dependent manner. Primary hepatocytes from wild-type mice or mice bearing a liver-specific deletion of the two AMPK catalytic subunits (AMPK $\alpha_1^{-/-}$ $\alpha_2^{LS-/-}$) were treated as described in the legends to Figs 1 and 2. The cells were collected and lysed for immunoblotting levels of phosphorylated ACC and AMPK versus total proteins along with GAPDH as a loading control (**a**). Extracts were also prepared for the measurement of cAMP concentrations by ELISA (**b**), for PKA assay (**c**) and for PDE assay (**d**). Values are means ± s.e.m. for $n=3$ (**b**–**d**) separate experiments, and in **a** representative immunoblots are shown. Statistical analysis was by a paired Student's *t*-test. *Indicates a significant difference ($P<0.05$) compared with control incubations with DMSO or between the indicated conditions.

Moreover, analysis of the effects of *in vitro* phosphorylation of purified recombinant PDE4B by AMPK on the kinetic properties of the enzyme revealed that V_{max} increased approximately twofold with no effect on K_M (see below).

AMPK phosphorylates and activates mouse PDE4B *in vitro*. To test whether PDE4B could be a direct AMPK substrate, we cloned the 721-amino-acid-containing PDE4B isoenzyme (GenBank: AF326555.1) from primary mouse hepatocyte total cDNA. The recombinant protein was expressed in *Escherichia coli* as a glutathione S-transferase (GST) fusion protein and purified before removing the tag by specific proteolytic cleavage. Both bacterially expressed recombinant activated AMPK and purified PKA catalytic subunits phosphorylated PDE4B in the presence of [γ-^{32}P] ATP *in vitro* (Fig. 5a), and using AMPK, a stoichiometry of ~1 mol of phosphate incorporated per mol of PDE protein was reached (Fig. 5c). With both AMPK and PKA, phosphorylation of PDE4B in the presence of [γ-^{32}P] ATP was additive, suggesting the presence of distinct phosphorylation sites. After maximal phosphorylation by AMPK and [γ-^{32}P] ATP, followed by trypsin digestion and peptide separation by HPLC, three AMPK phosphorylation sites were identified by liquid chromatography-coupled tandem mass spectrometry (LC–MS/MS) in the major radiolabelled peaks as Ser118, Ser125 and Ser304 (Fig. 5b). Ser118 is located in the upstream conserved regulatory region 1 of PDE4B, and was also phosphorylated by PKA, in agreement with previous reports of phosphorylation at this site leading to activation of long PDE4 isoforms[32,33]. Ser125 is also situated in upstream conserved regulatory region 1, while Ser304 corresponds to Ser245 located in the catalytic domain of PDE4D9 (ref. 34). The sequences surrounding Ser118, Ser125 and Ser304 are well conserved in vertebrate PDE4 orthologues (Supplementary Fig. 3A) and in the different mouse PDE4 isoforms (Supplementary Fig. 3B). When Ala residues were introduced by site-directed mutagenesis to replace each Ser, the stoichiometry of phosphorylation by AMPK decreased by 40–60% for the purified mutant recombinant proteins compared with wild-type PDE4B (Fig. 5c and Supplementary

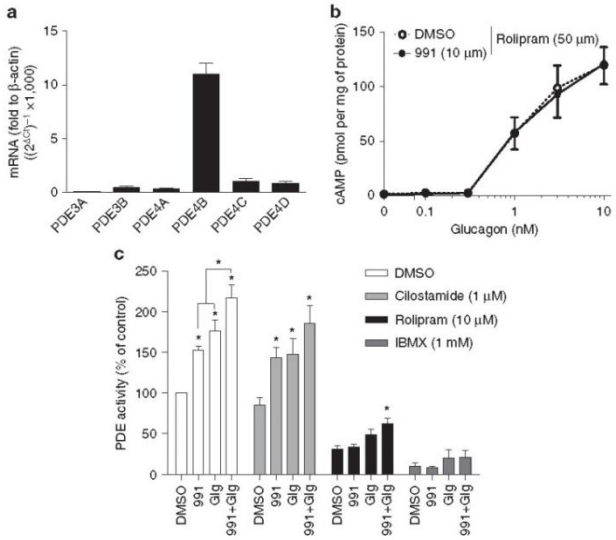

Figure 4 | PDE4 is the major isoenzyme in cultured mouse hepatocytes and is activated by treatment with compound 991. Primary mouse hepatocytes were serum-starved overnight, then total RNA was extracted for cDNA synthesis and real-time PCR using specific primers for the mouse PDE isoenzymes indicated (**a**). In **b**, hepatocytes were incubated for 20 min with 991 or with DMSO as vehicle control in the presence of the PDE4 inhibitor rolipram before stimulation with indicated concentrations of glucagon for 15 min. The cells were collected and lysed for the measurement of cAMP concentrations by ELISA. In **c**, the cells were lysed after 1 h of treatment with 991 (10 μM) and/or glucagon (Glg, 10 nM), and extracts were assayed for total PDE activity in the presence or absence of PDE inhibitors as indicated. The 100% value for PDE activity in extracts from control DMSO-treated cells was 2.7 ± 0.7 μU per mg of protein. Values are means ± s.e.m. for $n=3$ (**a**), $n=6$ (**b**) or $n=5$ (**c**) separate experiments. Statistical analysis was by a paired Student's *t*-test. *Indicates a significant difference ($P<0.05$) compared with control incubations with DMSO or between the indicated conditions.

Fig. 4). *In vitro* phosphorylation of wild-type PDE4B by AMPK increased the V_{max} almost twofold without significantly affecting the K_M for cAMP, which was 3–4 μM (Fig. 5d). When recombinant PDE4B was incubated with ATP and AMPK or PKA, or the two protein kinases in combination, phosphorylation by AMPK or PKA led to a ~50% increase in wild-type PDE4B activity, and an additive effect (twofold activation) was observed when both protein kinases were included together (Fig. 5e). AMPK-induced PDE4B activation was completely abolished in the S304A mutant, suggesting that phosphorylation at this site is crucial for the increase in V_{max}. PKA-induced PDE4B activation was maintained in the S304A mutant, but was abolished in the S118A mutant. Moreover, the additivity of PDE4B activation by PKA and AMPK in combination was lost in the S304A mutant. Interestingly, mutation of S118 or S304 to Ala substantially decreased basal PDE activity of recombinant PDE4B compared with the wild-type protein (Fig. 5e and legend), suggesting that Ser118 and Ser304 could be important for catalysis or play structural roles, as well as being important for phosphorylation-induced PDE activation. Taken together, the findings suggest that Ser304 of mouse PDE4B is probably the major activating phosphorylation site for AMPK *in vitro*.

PDE4B is phosphorylated by AMPK in intact hepatocytes. Finally we looked whether PDE4B could be phosphorylated by AMPK in intact cells. PDE4B was immunoprecipitated from primary mouse hepatocytes incubated with either 991 or phenformin, and extracts were subjected to immunoblotting with phospho-specific antibodies. Commercial antibodies against phosphorylation site peptide motifs for either PKA (to recognize PDE4B phosphorylated at Ser118) or AMPK (to recognize PDE4B phosphorylated at Ser125), as well as an anti-phospho-peptide antibody raised against the sequence surrounding Ser304 that we generated ourselves were used. The specificities of the anti-phospho antibodies were first verified on recombinant PDE4B phosphorylated by AMPK *in vitro* (Fig. 6a). Following immunoprecipitation of endogenous PDE4B from intact hepatocytes incubated with 991 or phenformin and immunoblotting, phosphorylation increased at the three main sites we identified (Fig. 6b), although some basal phosphorylation was seen in control-incubated hepatocytes. In hepatocytes from wild-type mice incubated with increasing concentrations of 991 or phenformin up to maximal doses, phosphorylation of AMPK, ACC and Raptor was increased, and this increase was completely abrogated or reduced in hepatocytes from AMPK $\alpha_1^{-/-}\alpha_2^{1S-/-}$ mice (Fig. 6c). Again, although some basal PDE4B phosphorylation at the activating site Ser304 was seen in untreated hepatocytes, incubation of hepatocytes with the highest doses of 991 and phenformin led to significant increases in PDE4B Ser304 phosphorylation, which were lost in hepatocytes from AMPK $\alpha_1^{-/-}\alpha_2^{1S-/-}$ mice (Fig. 6c). Basal PDE4B Ser304 phosphorylation, which was also apparent in hepatocytes lacking AMPK, suggests that kinase(s) other than AMPK could phosphorylate PDE4B. It is noteworthy that members of the AMPK-related salt-inducible kinase (SIK) family were shown to be involved in the regulation of hepatic gluconeogenesis[35,36], and SIK1 was

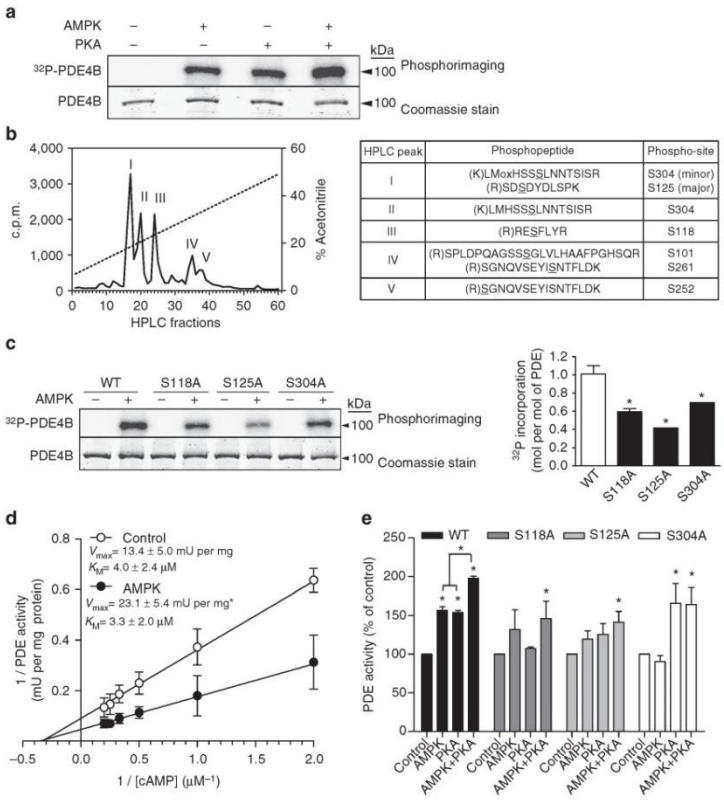

Figure 5 | Phosphorylation-induced activation of mouse liver PDE4B. PDE4B was cloned from mouse hepatocyte cDNA. The recombinant protein was overexpressed *in E. coli* and purified. PDE protein was phosphorylated for 1h with purified recombinant activated AMPK and/or purified PKA catalytic subunits and [γ-^{32}P] ATP, and analysed by SDS-PAGE followed by Coomassie blue staining and phosphorimaging for quantification (**a**,**c**). In **b**, PDE was phosphorylated for 1h with recombinant activated AMPK and [γ-^{32}P]. Phosphorylation sites were identified by LC-MS/MS after trypsin digestion and radioactive peak separation by high-performance liquid chromatography (HPLC). The phosphorylation sites that were identified are underlined in the right hand panel. In **d** and **e**, recombinant PDE was phosphorylated as above but with non-radioactive ATP for PDE assay as indicated. In **d**, separate determinations of V_{max} and K_M were made by linear regression of double reciprocal (Lineweaver Burk) plots. In **e**, the basal PDE activities of the wild-type (WT), S118A, S125A and S304A mutant proteins were 1.97 ± 0.25, 0.14 ± 0.01, 1.59 ± 0.15 and 0.32 ± 0.09 mU per mg of protein, respectively. Values are means ± s.e.m. for $n = 3$ (**c**–**e**) separate experiments. Statistical analysis was by a paired Student's *t*-test. *Indicates a significant difference ($P < 0.05$) compared with control incubations or between the indicated conditions.

recently reported to activate mouse PDE4D in pancreatic β-cells via phosphorylation of Ser136 (ref. 37), the residue corresponding to Ser125 of PDE4B identified here.

Discussion

In the present study, we propose that hepatic AMPK activation leads to phosphorylation-induced PDE4B activation, thereby antagonizing the glucagon-stimulated rise in cAMP and PKA signalling (summarized in Fig. 7). This proposal is based on the following evidence: (1) treatment of hepatocytes with the small-molecule AMPK activator 991 decreased glucagon-induced increases in cAMP (Fig. 1a,e) by accelerating cAMP removal (Fig. 2c) without affecting intracellular adenine nucleotide levels (Fig. 2a); (2) compound 991 treatment led to a stable increase in PDE activity (Fig. 2d,e), and inclusion of the PDE inhibitors IBMX and rolipram in hepatocyte incubations abolished the effect of 991 to reduce increases in cAMP levels in response to glucagon (Figs 2f and 4b); (3) AMPK phosphorylated purified PDE4B *in vitro* (Fig. 5a–c), resulting in an increase in V_{max} (Fig. 5d), and mutation of Ser304 to Ala abolished phosphorylation-induced PDE activation by AMPK (Fig. 5e); and (4) 991 treatment led to increased PDE4B Ser304 phosphorylation in intact hepatocytes (Fig. 6b). Importantly, in hepatocytes from mice bearing a liver-specific deletion of the two AMPK catalytic subunits, the effect of 991 treatment to decrease cAMP levels and subsequent PKA activation in response to glucagon was lost (Fig. 3b,c) along with PDE activation (Fig. 3d) and increased PDE4B Ser304 phosphorylation (Fig. 6c).

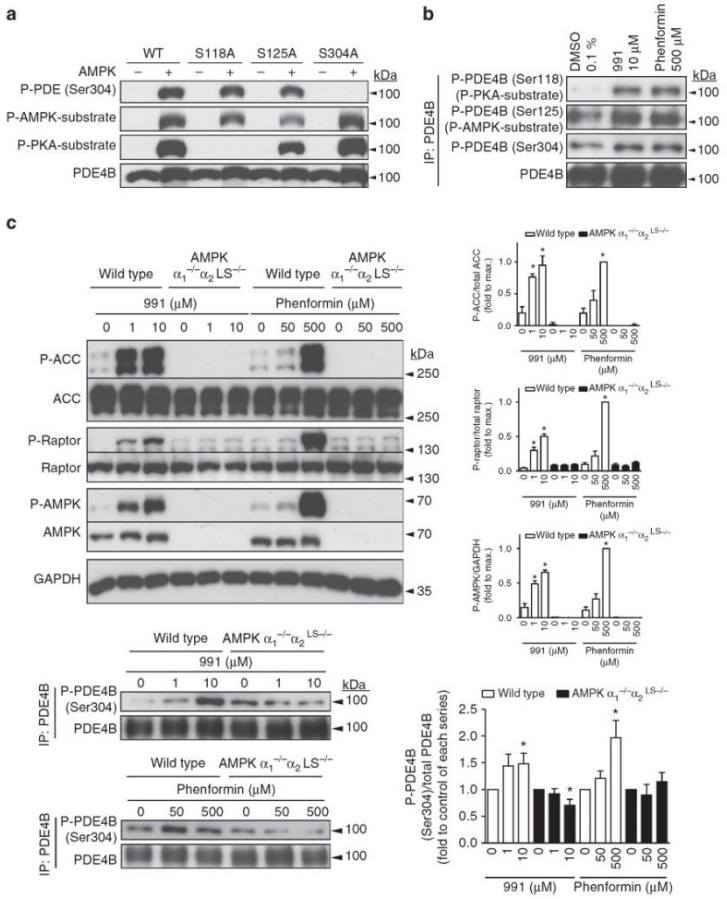

Figure 6 | AMPK activation leads to PDE4B phosphorylation in intact hepatocytes. In **a**, wild-type (WT) or mutant recombinant mouse liver PDE4B was incubated for 1 h with non-radioactive ATP in the presence (+) or absence (−) of recombinant activated AMPK. Proteins (0.1 µg) were seperated by SDS-PAGE for immunoblotting with the indicated antibodies. In **b** and **c**, mouse hepatocytes from either WT (**b**) or both WT and AMPK $\alpha_1^{-/-}\alpha_2^{LS-/-}$ mice (**c**) were serum-starved overnight and incubated for 1 h with the indicated concentrations of 991 or phenformin. The cells were collected and lysed for immunoblotting with the indicated antibodies, except for PDE4B, which was immunoprecipitated as described in the Methods section, before immunoblotting. In **c**, phosphorylation levels of AMPK and its targets ACC, Raptor and PDE4B were quantified by densitometry and expressed relative to the corresponding total protein levels or GAPDH before normalization as indicated. Representative immunoblots are shown and for blot quantification in **c**, the values are means ± s.e.m. for $n=3$ (p-ACC, p-Raptor and p-AMPK) or $n=4$ (p-PDE4B) separate experiments. Statistical analysis was by a paired Student's *t*-test. *Indicates a significant difference ($P<0.05$).

Interestingly, the AMPK phosphorylation sites in PDE4B we identified correspond to recently described phosphorylation sites in PDE4D9, and Ser245 of human PDE4D9 (Ser304 in PDE4B3) was proposed as an activating site phosphorylated by an unknown 'switch kinase' activated by H_2O_2 (ref. 34). Also, in a phosphoproteomics study[38], PDE4C from hepatocytes was found to be an AMPK substrate and the phosphorylation site identified corresponds to Ser125 of PDE4B, present in all long PDE4 isoforms (Supplementary Fig. 3B). Moreover, phosphorylation sites Ser118, Ser125 and Ser304 are well conserved in vertebrate PDE4B orthologues (Supplementary Fig. 3A). Phosphorylation at Ser304 is probably responsible for the increase in V_{max} of PDE4B, since its mutation to Ala abolished AMPK-induced PDE activation (Fig. 5d). However, as reported for PDE4D9 (ref. 34), multi-site phosphorylation of PDE4B might be necessary for full PDE activation, and from our data we cannot rule out the involvement of Ser118 and Ser125 phosphorylation in overall AMPK-induced PDE4B activation. Phosphorylation-induced PDE4 activation by AMPK might be of broad physiological relevance, since PDE4 (especially isoforms B and D) has a wide tissue distribution[39].

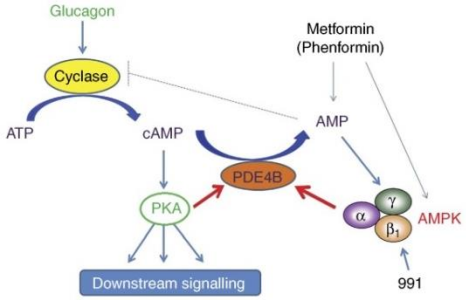

Figure 7 | How biguanides and compound 991 antagonize glucagon signalling. Unlike biguanides, treatment with 991 activates AMPK without increasing cellular AMP levels. Both biguanides and 991 activate the major PDE 4B isoenzyme in hepatocytes in an AMPK-dependent manner. Metformin and phenformin activate hepatic AMPK either directly or via a rise in AMP, which could compete with ATP to inhibit adenylate cyclase. Phosphorylation-induced activation of PDE4B by AMPK reduces glucagon-stimulated cAMP accumulation. As a consequence, PKA activation by glucagon and downstream signalling are decreased in hepatocytes incubated with 991, the effect being AMPK-dependent.

The concentrations of cAMP reached in our study in cultured mouse hepatocytes incubated with glucagon (up to 20 pmol per mg of protein in the absence of PDE inhibitors, Figs 1e,2c and 3b) fit well with values reported in the literature[40–43]. These values were obtained using a commercial ELISA-based assay and were much lower than those measured by radioimmunoassay (~150 pmol per mg of protein, see for example Fig. 1a) or by HPLC (~100 pmol per mg of protein, data not shown) when the three methods were compared on the same sample. Such differences are likely to be due to differences in sample quenching. For radioimmunoassay, hepatocyte incubations were immediately stopped with HCl. For HPLC, the cells were immediately extracted with perchloric acid, whereas for measurements by ELISA, the stopping mixture used for rapid lysis of hepatocytes was a non-deproteinizing buffer containing detergent and EDTA. Radioimmunoassay and HPLC would thus give measurements of total cAMP levels, whereas ELISA would provide measurements of "free" concentrations. However, effects of 991 to decrease glucagon-stimulated increases in cAMP were observed irrespective of the protocol used for cAMP measurement. Increased PDE activity due to AMPK activation would correspond to 5-10 pmol per min per mg of protein (Figs 2d and 3d), which would be sufficient to account for the degradation of cAMP as measured by ELISA in 991-stimulated hepatocytes incubated for 15 min, with glucagon (Fig. 2c).

Whole-body deletions of PDE4B have been made in mice, associated with inhibition of the lipopolysaccharide-stimulated immune response of peripheral leukocytes[44], increased Ca^{2+} transients and contractility of cardiac myocytes[45] and reduced adiposity and high-fat-diet-induced adipose inflammation[46]. PDE4B$^{-/-}$ mice were reported to be normal in terms of body weight and growth rate, showing no obvious abnormalites[44]. Also during starvation, serum glucose/insulin levels as well as glucose/insulin tolerance were not altered in these mice[46]. However, effects on liver metabolism were apparently not investigated in these studies.

The decrease in glucagon-stimulated cAMP accumulation seen in hepatocytes incubated with phenformin was proposed to be due to direct inhibition of adenylate cyclase by AMP, with a half-maximal effect at about 300 μM (ref. 21). In hepatocytes incubated with 500 μM phenformin, AMP concentrations rose to over 1 mM (ref. 21), a value comparable to that of ~2 nmol per mg of protein seen here (Fig. 2a), which would correspond to ~0.5 mM. However, free cytosolic AMP concentrations are much less than total cellular concentrations because AMP is bound by abundant proteins, such as glycogen phosphorylase, adenylate kinase, 6-phosphofructo-1-kinase and fructose-1,6-bisphosphatase[47]. The free AMP concentration in livers of wild-type mice was calculated to be 3.9 nmol per g of wet weight[48], which would correspond to 7 μM AMP based on the intracellular water space of perfused liver[49]. Therefore, even under conditions of ATP depletion induced by phenformin, it is unlikely that free AMP concentrations would rise to levels high enough to inhibit adenylate cyclase. Although we cannot rule out phenformin acting via direct inhibition of adenylate cyclase by AMP, PDE activation could also explain the reduction in glucagon-stimulated cAMP levels by biguanides previously reported[21] (see scheme, Fig. 7). Indeed, we show that submaximal concentrations of 991, phenformin and metformin activated PDE and the increase in PDE activity correlated with AMPK activation due to compound treatment (Supplementary Fig. 1).

In summary, by analogy with insulin signalling[28], activation of AMPK inhibits glucagon-stimulated cAMP accumulation by activating a PDE. Interestingly, effects of metformin to lower blood glucose levels are only seen in diabetic and not in normal subjects[50], consistent with increased circulating glucagon concentrations in diabetic individuals, who presumably would have elevated cAMP levels in liver. Our data suggest that AMPK activation in the liver could be beneficial by opposing short-term glucagon action via PDE activation to reduce cAMP as a new therapeutic strategy for the treatment of metabolic diseases associated with dysregulated cAMP/PKA signalling, such as type 2 diabetes. It is also noteworthy that cAMP signalling is important for the growth of certain cancers and that suppression of negative feedback mechanisms occurs during tumorigenesis[51].

Methods

Reagents and materials. Compound 991 (previously referred to as ex229 (ref. 25) from patent application WO2010036613, Merck Sharp & Dohme Corp., Metabasis Therapeutics, Inc. Novel cyclic benzimidazole derivatives useful anti-diabetic agents, 2010) was kindly provided by AstraZeneca Mölndal, SE. Glucagon (reconstituted GlucaGen) was from Novo Nordisk, phenformin and all other reagents were from Sigma Aldrich. All cell culture reagents were from Life Technologies. Oligonucleotides were from Eurogentec. [γ-^{32}P] ATP and [5′, 8′-^{3}H] cAMP were from Perkin Elmer. Anti-total ACC (Merck Millipore, Catalogue No. 04-322), anti-P-Ser79-ACC (Merck-Millipore, Catalogue No. 07-303), anti-glyceraldehyde-3-phosphate dehydrogenase (GAPDH; Merck-Millipore, Catalogue No. MAB374), anti-total GP (Sigma, Catalogue No. HPA000962), anti-total AMPK β1(R&D Systems, Catalogue No. AF2854) and anti-total AMPK β2 (R&D Systems, Catalogue No. MAB3808), anti-PThr172-AMPK (T172) (Cell Signaling Technologies, Catalogue No. 2535, anti-P-AMPK-substrate (Cell Signaling Technologies, Catalogue No. 5759), anti-P-PKA-substrate (Cell Signaling Technologies, Catalogue No. 9624), anti-total Raptor (Cell Signaling Technologies, Catalogue No. 2280) and anti-P-Ser792-Raptor (Cell Signaling Technologies, Catalogue No. 2083), anti-total CREB (Cell Signaling Technologies, Catalogue No. 9197), anti-phospho-Ser133-CREB (Cell Signaling Technologies, Catalogue No. 9198) and anti-total PDE4B (Origene, Catalogue No. TA503471) antibodies were from the sources cited. Anti-P-Ser14-GP and anti-total AMPK (α1 and α2) antibodies were kindly provided by Grahame Hardie (University of Dundee, UK). A peptide surrounding Ser304 of mouse PDE4B (CKLMHSSSLNNTSI) was synthesized with or without Ser304 phosphorylated and with a Cys (N-term) for coupling to keyhole limpet haemocyanin (KLH) or bovine serum albumin (BSA) (Imject maleimide-activated KLH/BSA kit, Thermo Fisher Scientific). The KLH-coupled phosphopeptide was injected in rabbits (Thermo Fisher Scientific), and the serum was affinity purified on both BSA-coupled phosphopeptide and non-phosphopeptide linked to CH-activated Sepharose 4B (GE Healthcare). Catalytic subunits of PKA were purified from bovine heart as described previously[52]. Recombinant bacterially expressed AMPK ($\alpha_1\beta_1\gamma_1$) was activated with recombinant bacterially expressed LKB1-MO25-STRAD complex[52], both

kindly provided by Dietbert Neumann (Maastricht University, Maastricht, NL). pGEX6p1 vector was generously donated by Christopher Proud (South Australian Health & Medical Research Institute, University of Adelaide, Australia). Synthetic peptides were provided by Vincent Stroobant (LICR, Brussels, BE). Oligonucleotide primers were synthetized by Integrated DNA Technologies.

Animals. Animal experiments were approved by the Université catholique de Louvain Brussels local ethics committee and conducted within the guidelines of the European Convention for the Protection of Vertebrate Animals used for Experimental and Other Scientific Purposes. Male C57BL/6 wild-type mice (3–4 months old) were obtained from the local animal facility and maintained on a 12 h light/12 h dark cycle with free access to food and water. Liver-specific AMPK α_1/α_2 knockout mice were generated[53], and experiments on AMPK α_1/α_2 double knockout and control mice were performed under the approval of the ethics committee from University Paris Descartes (No. CEEA34.BV.157.12) and the French authorization to experiment on vertebrates (No.75-886) in accordance with European guidelines. The AMPKβ1 knockout-mouse strain was generated by the trans-NIH Knock-Out Mouse Project (KOMP) and obtained from the KOMP Repository (www.komp.org). These mice were used in accordance with the United Kingdom Animals (Scientific Procedures) Act (1986).

Primary mouse hepatocyte culture and incubation. Mice were anesthetized (pentobarbital injection, i.p.) and livers were washed (with 50 ml of Krebs-HEPES, pH 7.65, supplemented with 0.5 mM EDTA) and digested (with 50 ml of Krebs-HEPES, pH 7.65, containing 25 mg of collagenase from *Clostridium hystolyticum* and 0.5 mM $CaCl_2$) by perfusion through the inferior vena cava at a rate of 5 ml min^{-1} as described[18]. The liver was removed and hepatocytes were extracted in attachment medium (DMEM supplemented with 1 gl^{-1} glucose, 4 mM glutamine, 1 mM pyruvate, penicillin/streptomycin, 10% (v/v) FBS, 10 nM insulin, 200 nM triiodothyronine (T3) and 500 nM dexamethasone). After filtering through a 100-μm mesh cell strainer (BD Falcon), cells were pelleted (50$g \times 2$ min) and resuspended in attachment medium for counting and seeding. Typically, cells were distributed in six-well plates, 2 ml per well containing 2.5×10^5 cells. After attachment for 4 h, the cells were washed in PBS and incubated for 20 h in overnight medium (DMEM containing 1 gl^{-1} glucose, 4 mM glutamine, 1 mM pyruvate, penicillin/streptomycin and 100 nM dexamethasone). Before treatment, the medium was replaced with fresh overnight medium. Unless otherwise stated, the cells were incubated first with 10 μM 991 (or 0.1% (v/v) DMSO, vehicle controls) for 20 min before treatment with the indicated concentrations of glucagon (or PBS, vehicle controls) for 15 min.

Cell lysis and immunoblotting. Following treatment in six-well plates, the medium was removed and the cells were washed in cold PBS before lysis in buffer containing 50 mM HEPES, pH 7.5, 1 mM EDTA, 1 mM EGTA, 0.5% (v/v) 2-mercaptoethanol, 50 mM NaF, 5 mM $Na_4P_2O_7$, 5 mM sodium β-glycerophosphate, 1 mM Na_3VO_3, 1 mM dithiothreitol, 0.1% (w/v) Triton X-100 and Complete protease inhibitor cocktail (150 μl per well). Extracts were centrifuged (20,000$g \times 5$ min at 4 °C) and protein concentrations were measured. For immunoprecipitation of PDE4B, 1 mg of extract protein was incubated for 2 h at 4 °C with 50 μl of protein G-Sepharose (GE Healthcare) previously coupled to 2 μg of anti-PDE4B antibody. For immunoblotting, 10 μg of sample protein or eluted immunoprecipitated proteins were loaded on 7.5% (w/v) polyacrylamide gels. Following SDS–PAGE, proteins were transferred to polyvinylidene difluoride membranes, which were then blocked in Tris-buffered saline (TBS) containing 0.1% (v/v) Tween and 5% (w/v) BSA. The membranes were incubated overnight at 4 °C with the indicated primary antibodies diluted in blocking buffer, then washed extensively before and after incubation for 1 h with horseradish peroxidase-conjugated secondary antibodies. Anti-total and anti-P-ACC, anti-total GP, anti-total AMPK (β1 and β2), anti-P-AMPK, anti-P-AMPK-substrate, anti-P-PKA-substrate, anti-total and anti-P-Raptor, anti-total and anti-P-CREB antibodies were used at a dilution of 1:1,000. Anti-GAPDH and anti-total PDE4B antibodies were used at dilutions of 1:30,000 and 1:500, respectively. Anti-P-PDE4B (S304), P-GP and anti-total AMPK (α1 and α2) antibodies were used at dilutions of 1:1,000, 1:1,000 and 1:10,000, respectively. For incubation of membranes with the anti-P-PDE4B (S304) antibody, the non-phosphopeptide used for antibody purification was included at a concentration of 10 μg ml^{-1}. Immunodetection was by ECL Classico substrate (Merck Millipore). Immunoblots were quantified by densitometry using ImageJ software. Uncropped scans of the blots used to generate the figures are shown in Supplementary Fig. 5.

cAMP measurement. cAMP was measured using the ELISA-based cAMP XP assay kit (Cell Signaling Technologies) according to the manufacturer's protocol. Following hepatocyte incubations in six-well plates, the cells were lysed in 100 μl of kit buffer (20 mM Tris-HCl, pH 7.5, 150 mM NaCl, 1 mM EDTA, 1 mM EGTA, 1% (w/v) Triton, 2.5 mM $Na_4P_2O_7$, 1 mM sodium β-glycerophosphate, 1 mM Na_3VO_4, 1 μg ml^{-1} leupeptin and 1 mM phenylmethyl sulfonyl fluoride). The samples were diluted in lysis buffer in experiments with PDE inhibitors. After centrifugation (20,000$g \times 5$ min at 4 °C), 50 μl aliquots of supernatant were taken and added to 50 μl of horseradish peroxidase-cAMP kit solution (unknown composition) for cAMP measurement. Quantification was based on a linear concentration curve, established with external cAMP standards. Alternatively, 1 ml of 0.1 M HCl was added to each well for cell lysis, and cAMP was measured in the dried supernatant by radioimmunoassay using a home-made antibody after sample acetylation[54].

Enzyme assays. PKA activity in hepatocyte lysates was measured by phosphorylation of a substrate peptide derived from rat heart 6-phosphofructo-2-kinase (PFK-2, sequence PVRMRRNSFT) in the presence and absence of PKA inhibitor peptide (PKI, sequence TYADFIASGRTGRRNAIHD). Lysates prepared for immunoblotting (corresponding to 30 μg of protein) were assayed at 30 °C in 30 μl of phosphorylation buffer containing 10 mM MOPS, pH 7.0, 0.5 mM EDTA, 10 mM magnesium acetate, 5 mM dithiothreitol, 100 μM substrate peptide and 100 μM [γ-^{32}P] ATP (specific radioactivity 1,000 c.p.m. $pmol^{-1}$) with and without 10 μM PKI. After 5 min, aliquots (20 μl) were spotted on P81 phosphocellulose papers for the determination of ^{32}P-incorporation. AMPK (α1 plus α2) activity immunoprecipitated from hepatocyte lysates was measured as described[55,56]. Purified PKA and recombinant activated AMPK were assayed in phosphorylation buffer by measuring ^{32}P incorporation from 0.1 mM [γ-^{32}P] ATP (specific radioactivity 1,000 c.p.m. $pmol^{-1}$) into 200 μM AMARA peptide (AMARAASAAALRRR) for AMPK and 200 μM the peptide PVRMRRNSFT for PKA[52]. One unit of protein kinase activity corresponds to the amount that catalyses the formation of 1 nmol min^{-1} of product under the assay conditions.

GP activity was determined in the direction of glycogen synthesis as described[57]. Lysates prepared for immunoblotting (corresponding to 100 μg of protein) were assayed in 100 μl of reaction mixture containing 25 mM Tris-HCl, pH 6.1, 50 mM glucose 1-phosphate, 1% (w/v) purified oyster glycogen, 150 mM NaF and 0.5 mM caffeine for 20 min at 30 °C. Blanks for spontaneous glucose 1-phosphate hydrolysis contained lysis buffer. Reactions were stopped by adding 100 μl of ice-cold 1.2 M trichloroacetic acid, and the samples were centrifuged (20,000$g \times 5$ min at 4 °C). Inorganic phosphate in the supernatant was measured spectrophotometrically at 650 nm 30 min after adding 20 mM 8-anilinonaphthalene-1-sulfonic acid and 2 mM ammonium molybdate in a final volume of 1 ml.

PDE in aliquots of lysates prepared for immunoblotting (containing about 50 μg of protein) or 0.5 μg of tag-removed recombinant PDE (see below) was assayed as described[58] for 10 min at 30 °C. The reaction mixture contained 40 mM Tris-HCl, pH 8.1, 0.5% (v/v) 2-mercaptoethanol, 5 mM $MgCl_2$, 0.1% (w/v) BSA and 1 μM [5′, 8′-^{3}H] cAMP (specific radioactivity 400 d.p.m. $pmol^{-1}$) in a final volume of 500 μl. For determination of the effect of phosphorylation by AMPK on the kinetic properties of recombinant PDE, cAMP concentrations were varied between 0.5 and 5 μM with a fixed amount of [5′, 8′-^{3}H] cAMP (1,000 d.p.m. μl^{-1}). Blanks for spontaneous cAMP hydrolysis contained the corresponding buffer. Reactions were stopped by freezing in liquid nitrogen followed by thawing for 1 min in boiling water. The reaction product, radioactive AMP, was further hydrolysed with 0.2 U of snake venom 5′-nucleotidase for 10 min at 30 °C. Residual cAMP and AMP were retained on 1 ml Dowex-formate columns (0.5 × 10 cm, Biorad), and radioactive adenosine in the flow-through was collected after further elution with 2 ml of CH_3OH for liquid scintillation counting. One unit of GP or PDE activity corresponds to the amount that catalyses the formation of 1 μmol min^{-1} of product under the assay conditions.

Nucleotide measurements. Cells in six-well plates were lysed with ice-cold 50 mM perchloric acid (500 μl per well). Following centrifugation (20,000$g \times 10$ min at 4 °C) the supernatants were neutralized with ~60 μl of 1.1 M $NH_4H_2PO_4$. The samples were then vacuum-dried and resuspended in 20 μl of water for HPLC separation and quantification of purine nucleotides as described[59].

Real-time PCR. Total mRNA was extracted from untreated primary mouse hepatocytes in six-well plates using 1 ml per well of Trizol (Life Technologies) reagent, according to the manufacturer's instructions. RNA was quantified by Nanodrop, and 500 ng was used for cDNA synthesis using the M-MLV RT kit (Life Technologies) according to the manufacturer's protocol. Reverse transcription products were diluted 1:3 in nuclease-free water, and 1 μl was used for qPCR with the Kapa Sybr Fast qPCR kit (Kapa Biosystems) in combination with the CFX96 Real Time PCR thermocycler (Biorad). The programme included 40 cycles at 95 °C for 10 s, 66 °C for 10 s, 72 °C for 30 s and a final melting curve. PCR reactions were carried out in a final volume of 10 μl with 1 μM of each of the primers against the different mouse PDE isoforms as described[60].

Expression and purification of mouse recombinant PDE4B. Total mRNA was extracted and retro-transcribed as mentioned above. cDNA product (1 μl) was used as a template for PCR, using Q5 High Fidelity DNA polymerase (New England Biolabs) according to the manufacturer's protocol and with the following oligonucleotide primers: (F) 5′-ggaaggatccATGACAGCAAAAAATTCTCC-3′ and (R) 5′-gctactcgagTTATGTGTCGATCGGAGACT-3′. PCR products were gel-purified with Wizard SV gel and PCR clean-up system (Promega), and verified by sequencing to confirm a 721-amino-acid protein with 95% identity to human PDE4B3. The sequence was cloned into the pGEX6p1 vector using the BamHI

and XhoI restriction sites present in the primers. Site-directed mutagenesis was carried out using the Herculase II Fusion DNA polymerase (Stratagen), with the QuikChange (Agilent) protocol. GST-tagged PDE4B was expressed overnight at 18 °C in BL21 *E. coli* cells induced with 0.5 mM isopropylthiogalactoside. Bacteria were then collected by centrifugation (5,000*g* × 10 min at 4 °C), resuspended in 1/10 of the culture volume of ice-cold lysis buffer (50 mM Tris-HCl, pH 7.5, 150 mM NaCl, 0.1% (v/v) 2-mercaptoethanol, 0.01% (w/v) Brij 35, 0.5 mM phenylmethyl sulfonyl fluoride, 0.5 mM benzamidine Cl, 1 μg ml^{-1} leupeptin and 1 μg ml^{-1} aprotinin) and homogenized using a French press device. The lysate was cleared by centrifugation (17,000*g* × 20 min at 4 °C) and the supernatant was passed through a 45-μm mesh filter (Millex-HA, Merck-Millipore) before loading onto a GSH-Sepharose column (1 × 20 cm, GE Healthcare). After extensive washing, the column was eluted with a 0–10 mM gradient of GSH. Fractions were subjected to SDS–PAGE followed by Coomassie Blue staining. Fractions containing GST-PDE4B protein bands were pooled and concentrated using a 100-kD ultrafiltration unit (Amicon) while changing the buffer to enzyme storage buffer (50 mM Tris-HCl, pH 7.5, 150 mM NaCl, 0.1% (v/v) 2-mercaptoethanol and 10% (v/v) glycerol). The GST tag was removed overnight at 4 °C by incubation of 500 μg of fusion protein with 10 U of HRV 3C protease (Sino Biological) according to the manufacturer's protocol.

***In vitro* phosphorylation**. Recombinant PDE4B (1 μg) was phosphorylated with 0.4 U of purified activated recombinant bacterially expressed AMPK or purified PKA catalytic subunits in 20 μl of kinase assay buffer (see PKA assay) containing 200 μM AMP (for AMPK only) and 100 μM [γ-^{32}P] ATP (specific radioactivity 1,000 c.p.m. pmol^{-1}). For kinetic studies, incubations contained non-radioactive ATP at the same final concentration. After 1 h at 30 °C, the reaction was stopped on ice, and 10 μl of mixture was taken for further analysis. For kinetic studies, samples were diluted fivefold in enzyme storage buffer before PDE assay. For measurements of the stoichiometry of phosphorylation, proteins were separated by SDS–PAGE in 7.5% (w/v) polyacrylamide gels. Gels were stained using PageBlue (Thermo Fisher Scientific) for protein band quantification by Odyssey infrared imaging. Bands were then excised from the gels for measurement of ^{32}P-incorporation by liquid scintillation as described previously[52].

Phosphorylation site identification. Recombinant PDE (3 μg) was phosphorylated as described above with 1 U of activated AMPK in a final volume of 60 μl for 1 h at 30 °C. The reaction was stopped on ice, 20 μg of BSA was added as carrier and proteins were precipitated with a final concentration of 10% (w/v) trichloroacetic acid for 45 min on ice. Precipitated proteins were collected by centrifugation (20,000*g* × 10 min at 4 °C), washed in acetone, vacuum-dried and resuspended in 50 μl of 50 mM NH_4HCO_3, pH 8.0, for overnight digestion at 30 °C with trypsin. Peptides were separated by reverse-phase narrow-bore HPLC and radioactive peaks were analysed by LC–MS/MS as described[61]. Multi-stage activation was enabled for phosphate neutral loss of 98, 49 or 32.66 with respect to the precursor *m/z*. Peak lists were generated and searched using SequestHT and PhosphoRS 3.1 against a home-made protein database containing the human PDE sequences obtained from Uniprot and the different mutants used in this study. Phosphorylation site identification was performed as described[61] and validated manually.

Statistical analysis. The results are expressed as means ± s.e.m. of at least three independent experiments. Unless otherwise stated, all two-group comparisons were tested for statistically significant differences using a paired two-sided Student's *t*-test, and $P<0.05$ was considered significant.

References

1. Exton, J. H., Robison, G. A., Sutherland, E. W. & Park, C. R. Studies on the role of adenosine 3′,5′-monophosphate in the hepatic actions of glucagon and catecholamines. *J. Biol. Chem.* **246,** 6166–6177 (1971).
2. Pilkis, S., Schlumpf, J., Pilkis, J. & Claus, T. H. Regulation of phosphofructokinase activity by glucagon in isolated rat hepatocytes. *Biochem. Biophys. Res. Commun.* **88,** 960–967 (1979).
3. Hue, L., Peliu, J. E. & Hers, H. G. Control of gluconeogenesis and of enzymes of glycogen metabolism in isolated rat hepatocytes. A parallel study of the effect of phenylephrine and of glucagon. *Biochem. J.* **176,** 791–797 (1978).
4. Hanson, R. W. & Mehlman, M. A. *Gluconeogenesis: Its Regulation in Mammalian Species* 515–532 (Wiley, 1976).
5. Sutherland, E. W. Studies on the mechanism of hormone action. *Science* **177,** 401–408 (1972).
6. Walsh, D. A. *et al.* Cyclic AMP-dependent protein kinases from skeletal muscle and liver. *Adv. Cyclic Nucleotide Res.* **1,** 33–45 (1972).
7. Iynedjian, P. B., Auberger, P., Guigoz, Y. & Le Cam, A. Pretranslational regulation of tyrosine aminotransferase and phosphoenolpyruvate carboxykinase (GTP) synthesis by glucagon and dexamethasone in adult rat hepatocytes. *Biochem. J.* **225,** 77–84 (1985).
8. Hornbuckle, L. A. *et al.* Selective stimulation of G-6-Pase catalytic subunit but not G-6-P transporter gene expression by glucagon in vivo and cAMP in situ. *Am. J. Physiol. Endocrinol. Metab.* **286,** E795–E808 (2004).
9. Claus, T. H., Pilkis, S. J. & Park, C. R. Stimulation by glucagon of the incorporation of U-14C-labeled substrates into glucose by isolated hepatocytes from fed rats. *Biochim. Biophys. Acta* **404,** 110–123 (1975).
10. D'Alessio, D. The role of dysregulated glucagon secretion in type 2 diabetes. *Diabetes Obes. Metab.* **13**(Suppl 1): 126–132 (2011).
11. Wollen, N. & Bailey, C. J. Inhibition of hepatic gluconeogenesis by metformin. Synergism with insulin. *Biochem. Pharmacol.* **37,** 4353–4358 (1988).
12. Zhou, G. *et al.* Role of AMP-activated protein kinase in mechanism of metformin action. *J. Clin. Invest.* **108,** 1167–1174 (2001).
13. Hawley, S. A., Gadalla, A. E., Olsen, G. S. & Hardie, D. G. The antidiabetic drug metformin activates the AMP-activated protein kinase cascade via an adenine nucleotide-independent mechanism. *Diabetes* **51,** 2420–2425 (2002).
14. Meng, S. *et al.* Metformin activates AMP-activated protein kinase by promoting formation of the alphabetagamma heterotrimeric complex. *J. Biol. Chem.* **290,** 3793–3802 (2015).
15. Yu, B., Pugazhenthi, S. & Khandelwal, R. L. Effects of metformin on glucose and glucagon regulated gluconeogenesis in cultured normal and diabetic hepatocytes. *Biochem. Pharmacol.* **48,** 949–954 (1994).
16. Duca, F. A. *et al.* Metformin activates a duodenal Ampk-dependent pathway to lower hepatic glucose production in rats. *Nat. Med.* **21,** 506–511 (2015).
17. Shaw, R. J. *et al.* The kinase LKB1 mediates glucose homeostasis in liver and therapeutic effects of metformin. *Science* **310,** 1642–1646 (2005).
18. Foretz, M. *et al.* Metformin inhibits hepatic gluconeogenesis in mice independently of the LKB1/AMPK pathway via a decrease in hepatic energy state. *J. Clin. Invest.* **120,** 2355–2369 (2010).
19. Cao, J. *et al.* Low concentrations of metformin suppress glucose production in hepatocytes through AMP-activated protein kinase (AMPK). *J. Biol. Chem.* **289,** 20435–20446 (2014).
20. He, L. *et al.* Metformin and insulin suppress hepatic gluconeogenesis through phosphorylation of CREB binding protein. *Cell* **137,** 635–646 (2009).
21. Miller, R. A. *et al.* Biguanides suppress hepatic glucagon signalling by decreasing production of cyclic AMP. *Nature* **494,** 256–260 (2013).
22. Madiraju, A. K. *et al.* Metformin suppresses gluconeogenesis by inhibiting mitochondrial glycerophosphate dehydrogenase. *Nature* **510,** 542–546 (2014).
23. Owen, M. R., Doran, E. & Halestrap, A. P. Evidence that metformin exerts its anti-diabetic effects through inhibition of complex 1 of the mitochondrial respiratory chain. *Biochem. J.* **348**(Pt 3): 607–614 (2000).
24. Xiao, B. *et al.* Structural basis of AMPK regulation by small molecule activators. *Nat. Commun.* **4,** 3017 (2013).
25. Lai, Y. C. *et al.* A small-molecule benzimidazole derivative that potently activates AMPK to increase glucose transport in skeletal muscle: comparison with effects of contraction and other AMPK activators. *Biochem. J.* **460,** 363–375 (2014).
26. Hayes, J. S. & Mayer, S. E. Regulation of guinea pig heart phosphorylase kinase by cAMP, protein kinase, and calcium. *Am. J. Physiol.* **240,** E340–E349 (1981).
27. Nichols, M. *et al.* Phosphorylation of CREB affects its binding to high and low affinity sites: implications for cAMP induced gene transcription. *EMBO J.* **11,** 3337–3346 (1992).
28. Heyworth, C. M., Wallace, A. V. & Houslay, M. D. Insulin and glucagon regulate the activation of two distinct membrane-bound cyclic AMP phosphodiesterases in hepatocytes. *Biochem. J.* **214,** 99–110 (1983).
29. Hermsdorf, T., Richter, W. & Dettmer, D. Effects of dexamethosone and glucagon after long-term exposure on cyclic AMP phosphodiesterase 4 in cultured rat hepatocytes. *Cell. Signal.* **11,** 685–690 (1999).
30. Hermsdorf, T. & Dettmer, D. Combined effects of insulin and dexamethasone on cyclic AMP phosphodiesterase 3 and glycogen metabolism in cultured rat hepatocytes. *Cell. Signal.* **10,** 629–635 (1998).
31. Abdollahi, M., Chan, T. S., Subrahmanyam, V. & O'Brien, P. J. Effects of phosphodiesterase 3,4,5 inhibitors on hepatocyte cAMP levels, glycogenolysis, gluconeogenesis and susceptibility to a mitochondrial toxin. *Mol. Cell. Biochem.* **252,** 205–211 (2003).
32. MacKenzie, S. J. *et al.* Long PDE4 cAMP specific phosphodiesterases are activated by protein kinase A-mediated phosphorylation of a single serine residue in Upstream Conserved Region 1 (UCR1). *Br. J. Pharmacol.* **136,** 421–433 (2002).
33. Richter, W., Jin, S. L. & Conti, M. Splice variants of the cyclic nucleotide phosphodiesterase PDE4D are differentially expressed and regulated in rat tissue. *Biochem. J.* **388,** 803–811 (2005).
34. Sheppard, C. L. *et al.* Mitotic activation of the DISC1-inducible cyclic AMP phosphodiesterase-4D9 (PDE4D9), through multi-site phosphorylation, influences cell cycle progression. *Cell. Signal.* **26,** 1958–1974 (2014).
35. Patel, K. *et al.* The LKB1-salt-inducible kinase pathway functions as a key gluconeogenic suppressor in the liver. *Nat. Commun.* **5,** 4535 (2014).

36. Itoh, Y. *et al.* Salt inducible kinase 3 signaling is important for the gluconeogenic programs in mouse hepatocytes. *J. Biol. Chem.* **290,** 17879–17893 (2015).
37. Kim, M. J. *et al.* Salt-inducible kinase 1 terminates cAMP signaling by an evolutionarily conserved negative-feedback loop in beta-cells. *Diabetes* **64,** 3189–3202 (2015).
38. Ducommun, S. *et al.* Motif affinity and mass spectrometry proteomic approach for the discovery of cellular AMPK targets: identification of mitochondrial fission factor as a new AMPK substrate. *Cell. Signal.* **27,** 978–988 (2015).
39. Omori, K. & Kotera, J. Overview of PDEs and their regulation. *Circ. Res.* **100,** 309–327 (2007).
40. Pilkis, S. J., Claus, T. H., Johnson, R. A. & Park, C. R. Hormonal control of cyclic 3′:5′-AMP levels and gluconeogenesis in isolated hepatocytes from fed rats. *J. Biol. Chem.* **250,** 6328–6336 (1975).
41. Tolbert, M. E., Butcher, F. R. & Fain, J. N. Lack of correlation between catecholamine effects on cyclic adenosine 3′:5′-monophosphate and gluconeogenesis in isolated rat liver cells. *J. Biol. Chem.* **248,** 5686–5692 (1973).
42. Garrison, J. C. & Haynes, Jr R. C. Hormonal control of glycogenolysis and gluconeogenesis in isolated rat liver cells. *J. Biol. Chem.* **248,** 5333–5343 (1973).
43. Robles-Flores, M., Allende, G., Pina, E. & Garcia-Sainz, J. A. Cross-talk between glucagon- and adenosine-mediated signalling systems in rat hepatocytes: effects on cyclic AMP-phosphodiesterase activity. *Biochem. J.* **312,** 763–767 (1995).
44. Jin, S. L. C. & Conti, M. Induction of the cyclic nucleotide phosphodiesterase PDE4B is essential for LPS-activated TNF- responses. *Proc. Natl Acad. Sci. USA* **99,** 7628–7633 (2002).
45. Leroy, J. *et al.* Phosphodiesterase 4B in the cardiac L-type Ca(2)(+) channel complex regulates Ca(2)(+) current and protects against ventricular arrhythmias in mice. *J. Clin. Invest.* **121,** 2651–2661 (2011).
46. Zhang, R., Maratos-Flier, E. & Flier, J. S. Reduced adiposity and high-fat diet-induced adipose inflammation in mice deficient for phosphodiesterase 4B. *Endocrinology* **150,** 3076–3082 (2009).
47. Hue, L. & Rider, M. H. The AMP-activated protein kinase: more than an energy sensor. *Essays Biochem.* **43,** 121–137 (2007).
48. Burgess, S. C. *et al.* Carbohydrate-response element-binding protein deletion alters substrate utilization producing an energy-deficient liver. *J. Biol. Chem.* **283,** 1670–1678 (2008).
49. Stoll, B., Gerok, W., Lang, F. & Haussinger, D. Liver cell volume and protein synthesis. *Biochem. J.* **287,** 217–222 (1992).
50. Cusi, K., Consoli, A. & DeFronzo, R. A. Metabolic effects of metformin on glucose and lactate metabolism in noninsulin-dependent diabetes mellitus. *J. Clin. Endocrinol. Metab.* **81,** 4059–4067 (1996).
51. van Staveren, W. C. *et al.* Gene expression in human thyrocytes and autonomous adenomas reveals suppression of negative feedbacks in tumorigenesis. *Proc. Natl Acad. Sci. USA* **103,** 413–418 (2006).
52. Bultot, L. *et al.* AMP-activated protein kinase phosphorylates and inactivates liver glycogen synthase. *Biochem. J.* **443,** 193–203 (2012).
53. Guigas, B. *et al.* 5-Aminoimidazole-4-carboxamide-1-beta-D-ribofuranoside and metformin inhibit hepatic glucose phosphorylation by an AMP-activated protein kinase-independent effect on glucokinase translocation. *Diabetes* **55,** 865–874 (2006).
54. Brooker, G., Harper, J. F., Terasaki, W. L. & Moylan, R. D. Radioimmunoassay of cyclic AMP and cyclic GMP. *Adv. Cyclic Nucleotide Res.* **10,** 1–33 (1979).
55. Glass, D. B., Masaracchia, R. A., Feramisco, J. R. & Kemp, B. E. Isolation of phosphorylated peptides and proteins on ion exchange papers. *Anal. Biochem.* **87,** 566–575 (1978).
56. Roskoski, Jr R. Assays of protein kinase. *Methods Enzymol.* **99,** 3–6 (1983).
57. Hue, L., Bontemps, F. & Hers, H. The effects of glucose and of potassium ions on the interconversion of the two forms of glycogen phosphorylase and of glycogen synthetase in isolated rat liver preparations. *Biochem. J.* **152,** 105–114 (1975).
58. Erneux, C., Couchie, D. & Dumont, J. E. Characterization of horse thyroid cyclic nucleotide phosphodiesterases. *Eur. J. Biochem.* **104,** 297–304 (1980).
59. Plaideau, C. *et al.* Effects of pharmacological AMP deaminase inhibition and Ampd1 deletion on nucleotide levels and AMPK activation in contracting skeletal muscle. *Chem. Biol.* **21,** 1497–1510 (2014).
60. Lee, J. H. *et al.* Dynamic regulation of cystic fibrosis transmembrane conductance regulator by competitive interactions of molecular adaptors. *J. Biol. Chem.* **282,** 10414–10422 (2007).
61. Vertommen, D. *et al.* Regulation of protein kinase D by multisite phosphorylation. Identification of phosphorylation sites by mass spectrometry and characterization by site-directed mutagenesis. *J. Biol. Chem.* **275,** 19567–19576 (2000).

Acknowledgements

We thank Nusrat Hussain and Gaëtan Herinckx for expert technical assistance. Y.-C.L. was supported by the Fund for Medical Scientific Research (FNRS, Belgium) and the Interuniversity Attraction Poles (IAP) Programme of the Belgian Science Policy (P7/13). M.J. was supported by the Fund for Scientific Research in Industry and Agriculture (FRIA). The work was funded by the Interuniversity Poles of Attraction Belgian Science Policy (P7/13), by the Directorate General Higher Education and Scientific Research French Community of Belgium, by the Fonds de la Recherche Scientifique (FNRS, Belgium) under Grant no. 3.4518.11, by the Région Ile-de-France (CORDDIM) and by the Société Francophone du Diabète (SFD).

Author contributions

M.J. and Y.-C.L. performed most of the experimental work; M.-F.H. and R.J. prepared and incubated mouse hepatocytes; D.V. measured nucleotide levels and identified phosphorylation sites by mass spectrometry; J.V.S. and J.E.D. measured cAMP levels in hepatocyte extracts; A.W. and D.C. generated whole-body AMPK-β1 knockout mice; M.F. and B.V. generated mice bearing a liver-specific deletion of the two AMPK catalytic subunits and M.F. prepared and incubated hepatocytes; L.H. along with M.J., Y.-C.L. and M.H.R. participated in conception and design, analysis and interpretation of the data; M.J. and M.H.R. drafted the article with contributions from Y.-C.L., M.F. and B.V.

Additional information

Supplementary Information accompanies this paper at http://www.nature.com/naturecommunications

Competing financial interests: The authors declare no competing financial interests.

Reprints and permission information is available online at http://npg.nature.com/reprintsandpermissions/

How to cite this article: Johanns, M. *et al.* AMPK antagonizes hepatic glucagon-stimulated cyclic AMP signalling via phosphorylation-induced activation of cyclic nucleotide phosphodiesterase 4B. *Nat. Commun.* 7:10856 doi: 10.1038/ncomms10856 (2016).

Supplementary Fig. 1: Submaximal doses of biguanides activate PDE in hepatocytes. Mouse hepatocytes were incubated with increasing concentrations of phenformin for 2 h or metformin for 24 h. The cells were harvested and lysed for measurement of total PDE activity in cell extracts and AMPK phosphorylation was quantified by immunoblotting (A). In (B), phosphorylated and total ACC and AMPK levels were measured by immunoblotting as indicated with GAPDH as loading control. The data are means ± S.E.M. of 3 separate experiments and in (B) representative immunoblots are shown. Statistical analysis was by a paired Student's *t*-test and * indicates a significant difference ($P<0.05$) compared to control incubations.

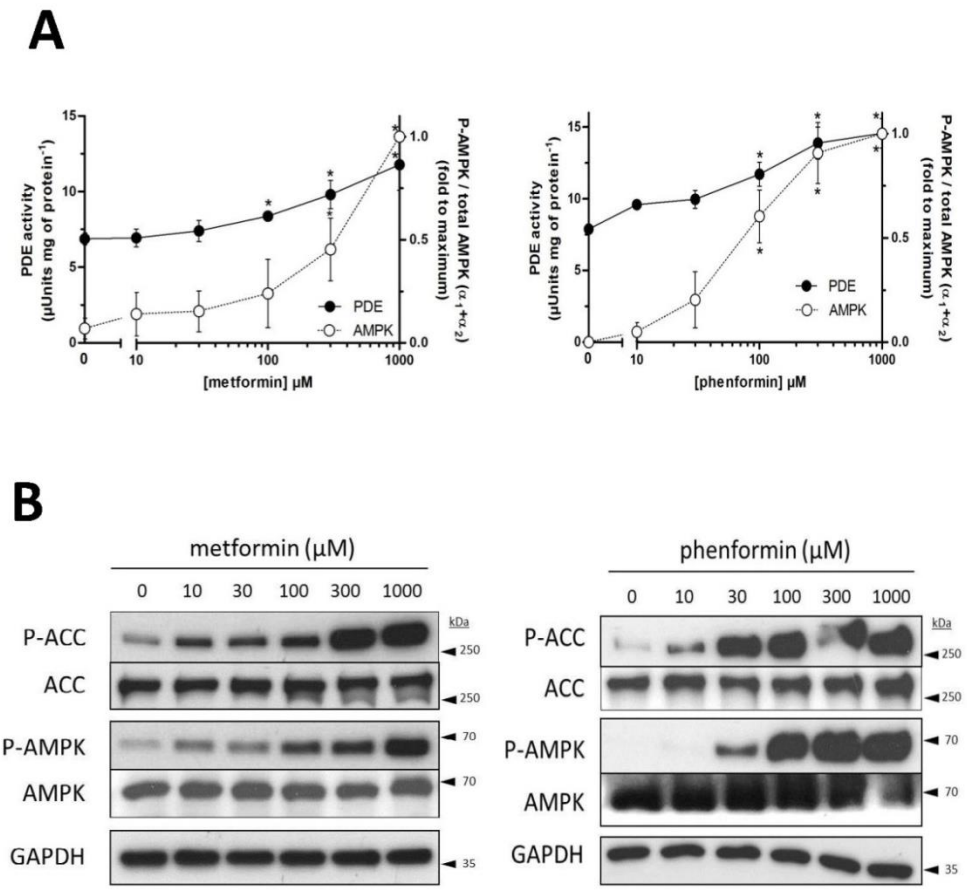

Supplementary Fig. 2: The decrease in glucagon-induced cAMP by 991 is abolished in hepatocytes from AMPK $\beta_1^{-/-}$ mice. Primary hepatocytes from wild-type mice or mice bearing a full-body deletion of the AMPK beta 1 subunit (AMPK $\beta_1^{-/-}$) were treated with 10 µM 991 (or DMSO as vehicle) prior to stimulation with 10 nM glucagon (Glg) for 15 min. The cells were harvested and lysed for the measurement of intracellular cAMP concentrations (A), and for immunoblotting levels of phosphorylated and total ACC, AMPK and Raptor (B) with GAPDH as loading control. The data are means ± S.E.M. of 3 separate experiments and in (B) representative immunoblots are shown. Statistical analysis was by a paired Student's *t*-test and * indicates a significant difference ($P<0.05$) compared to control incubations with DMSO.

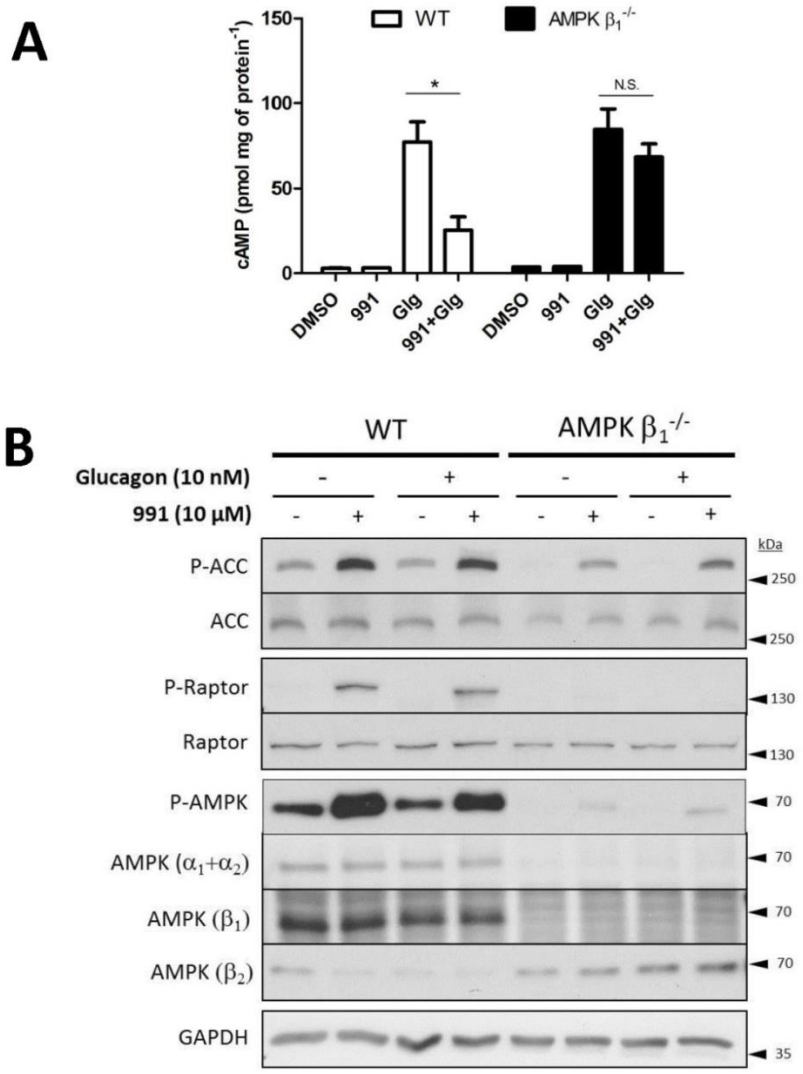

Supplementary Fig. 3: The three main AMPK phosphoryaltion sites in PDE4B are conserved and present in all PDE4 isoforms. Multiple sequence alignments were made using the Clustal W2 (EMBL-EBI) software with standard settings taking sequences from the Uniprot database for the PDE4B reference isoform from different species (A) and the mouse PDE4 A-D isoenzymes (B). The three AMPK phosphorylation sites identified (Ser118, Ser125 and Ser304) are shown in black boxes. The colors indicate different amino acid families (red: hydrophobic, green: polar uncharged, pink: positively charged, blue: negatively charged) and the symbols (*, :, .) beneath indicate the degree of conservation, in decreasing order.

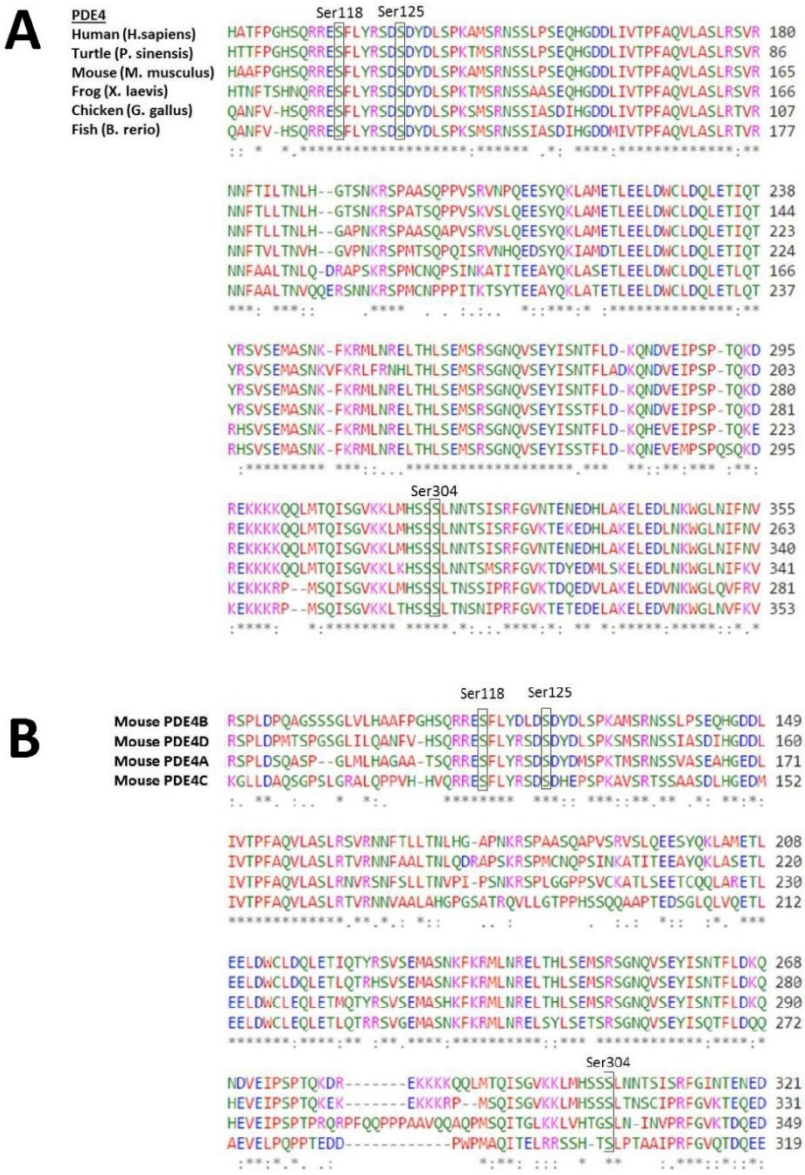

Supplementary Fig. 4: Radioactive HPLC profiles of PDE4B mutants phosphorylated by AMPK and digested with trypsin. Purified recombinant PDE4B mutant proteins were phosphorylated by activated AMPK and [γ-^{32}P] ATP as described in the legend to Fig. 5 of the main manuscript, where I, II and III indicate the three major peaks obtained for wild-type PDE4B. The arrows indicate the phosphorylation peak which disappears for each of the mutated Ser → Ala residues. The data are from one representative experiment.

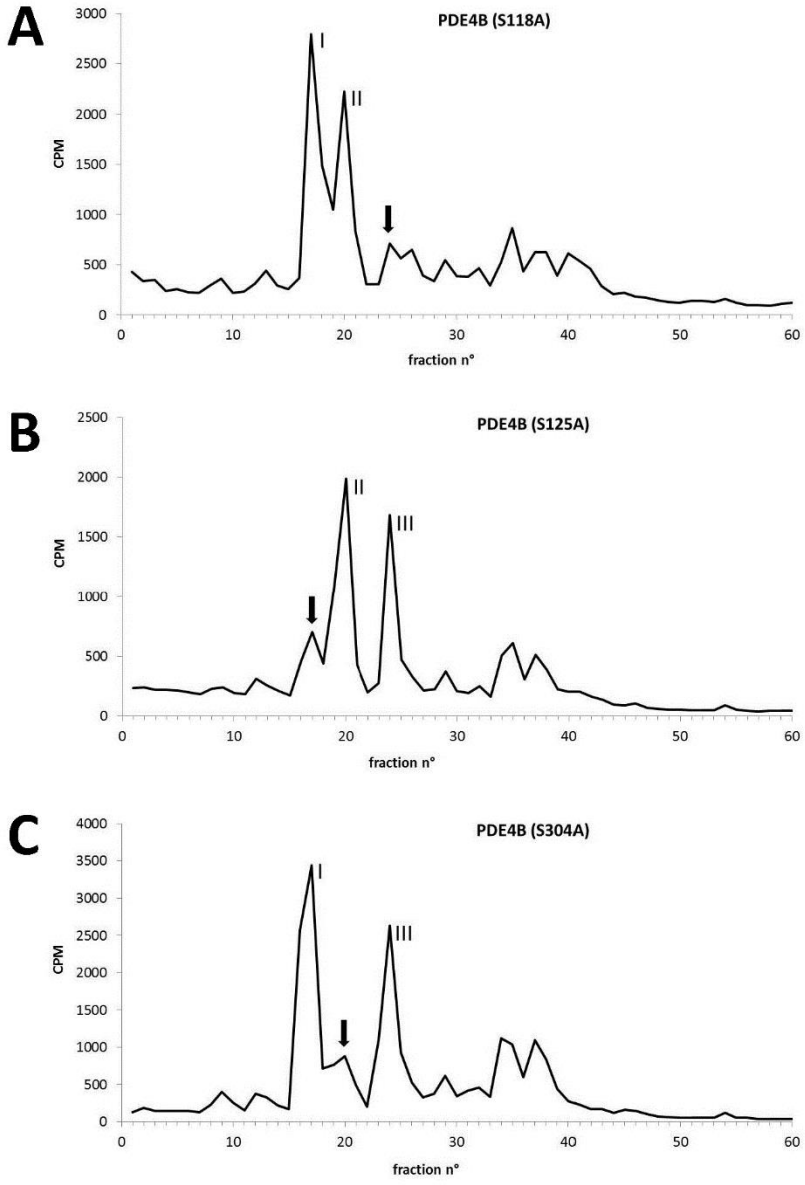

II. Regulation of protein synthesis by AMPK-induced eEF2K activation

Preface

In 2002, our laboratory found that protein synthesis in hepatocytes was rapidly inhibited by anoxia- or AICAR-induced AMPK activation, involving eEF2K activation and subsequent phosphorylation of eEF2 at T56[139]. In 2004, the group of our collaborator, Prof. C. Proud, identified S398 as the major site in eEF2K phosphorylated by AMPK[168]. However, functional evidence was lacking to confirm that this site was indeed responsible for eEF2K activation. The group of Proud also found that eEF2K was inhibited by mTORC1 signalling[169], which was known to be inhibited by AMPK activation. In 2012, our group showed that activation of eEF2K by Ca^{2+}/CaM involved multi-site autophosphorylation[170]. The aim of this part of my thesis was to study the participation of different regulatory inputs (Ca^{2+}, mTORC1 and AMPK) and to determine in more detail the molecular mechanism of eEF2K activation by AMPK.

The work is currently under revision in *Cellular Signalling*.

Protein synthesis

Protein synthesis is the biological process by which cells produce new proteins (polypeptides) from individual amino acids. Specific transfer ribonucleic acids (tRNAs) first need to be charged by aminoacylation with their corresponding amino acids. During maturation of messenger RNAs

(mRNAs), a 5’ cap and a 3’ poly-A tail are generally added to protect against degradation and improve translation efficiency. The assembly of polypeptides occurs during translation. The genetic information carried by the mRNA codons is “translated” into an amino acid sequence by ribosomes with the help of translation factors. Protein synthesis can be divided into three phases. During initiation in eukaryotes, the ribosomal translation machinery assembles around the initiator Met-tRNA bound to the AUG start codon. In the second phase of elongation, the nascent peptide chain in transferred onto the next amino acid bound via its tRNA and the ribosome translocates to the next codon. When reaching the last codon (a stop codon), termination is caused by disassembly of the translational complex and release of the newly produced polypeptide. Protein synthesis accounts for a large proportion of total energy consumption in growing cells[136]. Indeed, peptide chain elongation alone consumes at least 4 ATP equivalents per amino acid incorporated[171]. Protein synthesis is thus tightly regulated to avoid energy depletion. Translation factors are termed either initiation (eIF), elongation (eEF) or termination (eTF) factors according to their participation in protein synthesis and regulation is mainly exerted at initiation and elongation. Several signalling pathways control protein synthesis (**Scheme 11**), such as those downstream of growth factors and insulin activating the PKB pathway. An important downstream effect of PKB is to activate mTORC1 which potently stimulates protein synthesis. The mTOR kinase phosphorylates initiation factor 4E binding protein 1 (4EBP1), releasing active eIF4E to engage translation initiation of capped mRNAs. mTOR kinase also phosphorylates and activates S6K, which in turn phosphorylates rpS6 and initiation factor 4B (eIF4B), both implicated

in translation initiation. In addition, PKB activation favours initiation by inactivating GSK3, preventing phosphorylation and inhibition of eIF2B, a guanine nucleotide exchange factor (GEF) needed to generate active GTP-bound eIF2. Finally, direct phosphorylation by S6K and/or mTOR kinase inactivates eEF2K, preventing inhibitory phosphorylation of eEF2 required for peptide elongation. AMPK inhibits protein synthesis both at initiation and elongation, by a dual mechanism involving inhibition of mTORC1 signalling due to phosphorylation of TSC2 and Raptor, and by eEF2K activation.

eEF2K

eEF2K (formerly known as Ca^{2+}-calmodulin dependent kinase III, CAMKIII) is a Ser/Thr kinase of ~100 kDa belonging to the atypical family of α-kinases, members of which were proposed to be able to phosphorylate residues within alpha helixes. It is thought that α-kinases originated from bacterial histidine kinases since both families possess somewhat larger catalytic clefts[172]. In eukaryotes, eEF2K is well conserved and homologues can be found in unicellular organisms such as amoeba, but eEF2K seems to be absent from plants, fungi and some invertebrates, notably insects. Nevertheless, in these species another kinase may play an equivalent role since eEF2 homologues are present in all eukaryotes and the eEF2K phosphorylation site (T56) is remarkably well conserved. Also, eEF2 homologues in yeast and nematodes can be phosphorylated by the kinase RCK2[173]. Despite the lack of sequence homology, α-kinases share structural and catalytic features, such as functionally essential residues, with typical kinases. The only known eEF2K substrate is eEF2, suggesting it to

be a “dedicated” kinase, but this view has been challenged recently using a form of the kinase that was modified to accept thiophosphate analogs of ATP to discover other targets[174]. On the other hand, eEF2K is the only mammalian kinase capable of phosphorylating eEF2 at T56, as demonstrated using genetic deletion models[175]. Once phosphorylated, eEF2 binding to the ribosome is prevented, thereby blocking translation elongation. As a result, protein synthesis is halted but the integrity of polysomes (multiple ribosomes attached to the same mRNA) is preserved, allowing for reversal. Regulation of eEF2 by eEF2K has the advantage of being both rapid and economical, since 1) translation can resume when eEF2K returns to its inactive state and protein phosphatases (probably PP2A) dephosphorylate eEF2 and 2) there is no need to reassemble the translation initiation complex, which would consume time and energy.

The regulation of eEF2K is very complex since many cellular signalling pathways provide regulatory inputs (**Scheme 12**), as reviewed by Proud *et al*[176]. eEF2K activity is strictly dependent on its association with Ca^{2+}/CaM, leading to multi-site intramolecular cis-autophosphorylation probably to acquire an active conformation. eEF2K autophosphorylates on at least 10 different sites (S18, S61, S64, S71, S78, T348, S366, S445, S491, S500), some of which, particularly T348, are essential for activity. In addition, a decrease in pH activates the kinase, an effect that might be important in highly glycolytic and thus lactic acid-producing cells such as cancer cells. In addition, eEF2K activity can be modulated by trans-phosphorylation at multiple sites. Regulation of eEF2K has been demonstrated by 1) cAMP signalling via phosphorylation of S500 by PKA, conferring Ca^{2+}/CaM-independent activity; 2) growth factor signalling (e.g.

insulin) via phosphorylation of S78 and S359/S366 by mTORC1 (and S6K) inhibiting CaM binding and eEF2K activity, respectively; 3) activation by AMPK-mediated multi-site phosphorylation under various stress conditions.

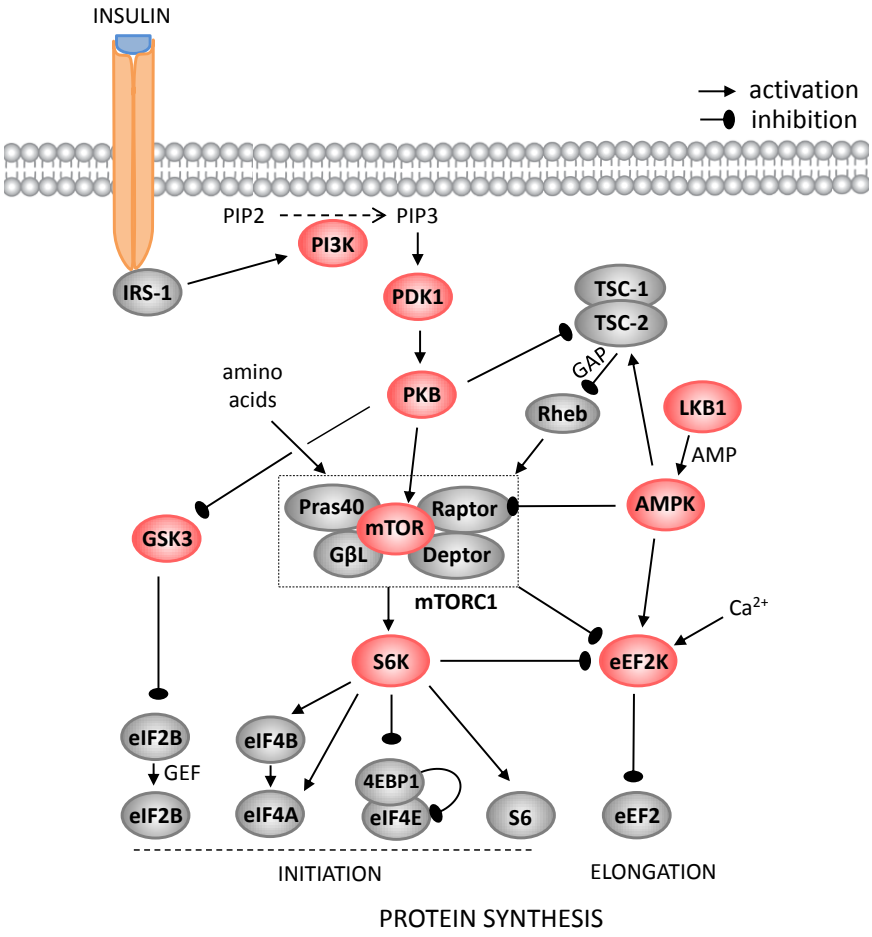

Scheme 11: **Regulation of protein synthesis by growth factors (insulin)/PKB signalling and AMPK.** Key protein translation factors are regulated positively or negatively through phosphorylation by kinases of the PKB or AMPK signalling pathways, respectively, in response to growth factors and nutrient availability.

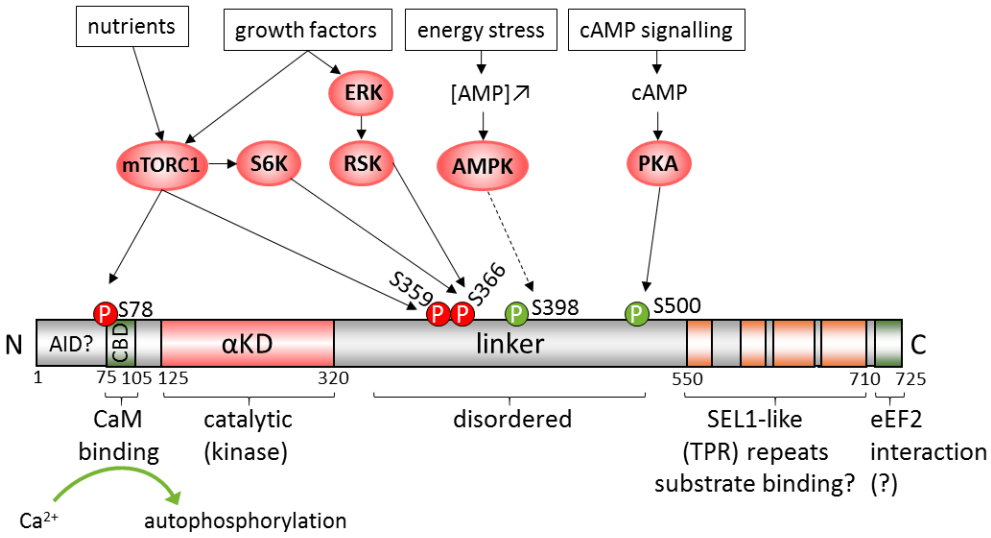

Scheme 12: **Domain structure and regulation of eEF2K.**
eEF2K activity is regulated by Ca^{2+}/calmodulin(CaM) leading to activating autophosphorylation at numerous sites and via multi-site phosphorylation by other kinases such as mTOR, S6K, RSK, AMPK and PKA. (Source: adapted from Kenney *et al*, 2014[173]). Abbreviations: AID = auto-inhibitory domain; CBD = calmodulin binding domain; αKD = α-kinase domain; TPR = tetratricopeptide repeat; SEL1 = Suppressor Of Lin 12 (*C.elegans*). Color code for effects of phosphorylation: red = inhibition, green = activation. Approximate residue numbers refer to the human sequence.

Direct and indirect activation of eukaryotic elongation factor 2 kinase by AMP-activated protein kinase

M. Johanns[1*], S. Pyr dit Ruys[1*], A. Houddane[1], D. Vertommen[1], G. Herinckx[1], L. Hue[1], C.G. Proud[2] & M.H. Rider[1§]

[1] : Université catholique de Louvain (UCL) and de Duve Institute, Avenue Hippocrate 75 bte 74.02, 1200-Brussels, Belgium

[2] : South Australian Health and Medical Research Institute (SAHMRI), and School of Biological Sciences, University of Adelaide, North Terrace, Adelaide SA 5000, Australia

§: Corresponding author. email: mark.rider@uclouvain.be; phone: +32(0)27647485; postal address: de Duve Institute, Avenue Hippocrate 75,1200-Brussels, Belgium

*: These authors contributed equally to this work.

1. INTRODUCTION

eEF2K is a highly conserved Ser/Thr kinase and member of the atypical alpha kinase family[1-3]. eEF2K is a highly regulated protein kinase and its activity is almost entirely dependent on Ca^{2+}-calmodulin (CaM), which binds to an amino-terminal regulatory region[4,5]. eEF2K activity is also controlled by multi-site phosphorylation, which modulates CaM-binding, kinetic properties and proteasomal degradation[6-9]. Besides control by protein kinases from various signaling pathways, such as inactivation by p70 ribosomal S6 kinase (S6K) downstream of mammalian target of rapamycin complex-1 (mTORC1)[10,11] and activation by AMPK[12] or cAMP-dependent protein kinase (PKA)[13,14], eEF2K extensively autophosphorylates at several sites in the presence of Ca^{2+}/CaM [15,16] to acquire maximal activity. Once activated, eEF2K phosphorylates eEF2 on Thr56[17,18], preventing its binding to the ribosome, which leads to ribosomal stalling and reversibly halts protein synthesis elongation. It is noteworthy that eEF2K is the only protein kinase known to phosphorylate eEF2 at Thr56.

AMPK is a key regulator of cellular energy homeostasis becoming activated during metabolic stress via a rise in AMP:ATP ratio. AMPK phosphorylates eEF2K *in vitro* and phosphorylation at Ser398 was proposed to cause eEF2K activation[12]. The inhibition of protein synthesis by AMPK at peptide elongation is crucial for survival under energy-depleting conditions and logical, since this step of protein synthesis is the most costly in terms of ATP equivalents consumed[19]. It is therefore not surprising that AMPK activation leads to the phosphorylation of eEF2[20], thereby decreasing the rate of protein synthesis. AMPK activation also inhibits protein synthesis initiation by decreasing PKB/mTORC1 signaling at different levels[21-23].

Several cellular stresses, most of which activate AMPK, have been shown to increase eEF2 Thr56 phosphorylation, namely skeletal muscle contraction[24-26], ischemia[27], hypoxia[28], increasing cell density[29], nutrient deprivation[30], growth factor retrieval[31], genotoxic agents[32], endoplasmic reticulum stress[33,34], ribosomal stress[35], oxidative stress[29,36], osmotic stress[37], chemical stress[29], alcohol[38], changes in pH[39,40] or temperature[41]. Also, treatment of cells with AMPK activators such as 5-aminoimidazole-4-carboxamide ribonucleoside (AICAR)[12], 2-deoxy-D-glucose (2DG)[12], the "Abbott compound" A-769662[42], metformin/phenformin[43] or oligomycin[20] leads to increased eEF2

phosphorylation. Most of these chemical treatments activate AMPK indirectly by causing ATP depletion (2DG[44], metformin[45], oligomycin[46]) and thus lack specificity. On the other hand, A-769622 and a small-molecule benzimidazole derivative called "991" activate AMPK by binding directly to the AMPKβ subunit[47]. Compound 991 is the more potent of the two direct AMPK activators and A-769622 seems only to target AMPKβ1. Incubation of skeletal muscles with 991 led to activation of both AMPKβ1- and AMPKβ2-containing complexes to increase glucose-uptake[48,49] and 991 treatment of hepatocytes antagonized glucagon signalling [50], both in an AMPK-dependent manner.

In the present study, we used 991 to activate AMPK in genetically modified mouse embryonic fibroblast (MEF) cell lines deficient for either the two AMPK catalytic subunits, tuberin of the tuberous sclerosis complex (TSC2), a negative regulator of mTORC1 signaling, or eEF2K to monitor eEF2 phosphorylation. In parallel, we identified Ser491 as a new key *in vitro* phosphorylation site for AMPK in eEF2K and studied eEF2 phosphorylation by 991 treatment and effects on protein synthesis in eEF2K-*null* MEFs in which wild-type eEF2K or a S491A/S492A mutant had been re-introduced by viral transfection. Our data provide new insights into the mechanisms by which AMPK activation leads to increased eEF2 phosphorylation with implications for protein synthesis inhibition in response to cellular stresses.

2. MATERIAL AND METHODS

2.1. Reagents and materials.

Compound 991 (previously referred to as ex229[47] from patent application WO2010036613, Merck Sharp & Dohme Corp., Metabasis Therapeutics, Inc. Novel cyclic benzimidazole derivatives useful anti-diabetic agents, 2010) was kindly provided by AstraZeneca, Mölndal, Sweden. All other reagents were from Sigma Aldrich. Cell culture reagents were from Life Technologies. Oligonucleotides were from Integrated DNA Technologies (IDT). [γ-^{32}P] ATP was from Perkin Elmer. Anti-total ACC (Merck Millipore, Catalogue No. 04-322), anti-P-Ser79-ACC (Merck-Millipore, Catalogue No. 07-303), anti-glyceraldehyde-3-phosphate dehydrogenase (GAPDH; Merck-Millipore, Catalogue No. MAB374), anti-total eEF2 (Santa Cruz Biotechnology, Catalogue No. 13003), anti-P-Thr56-eEF2 (Cell Signaling Technologies, Catalogue No. 2331), anti-total p70S6K (Cell Signaling Technologies, Catalogue No. 9202), anti-P-Thr389-p70S6K (Cell Signaling Technologies, Catalogue No. 9234), anti-P-Thr172-AMPKα (Cell Signaling Technologies, Catalogue No. 2535) and anti-total eEF2K (Cell Signaling Technologies, Catalogue No. 3692) antibodies were from the sources cited. Sheep polyclonal anti-total AMPKα1/2 antibodies were kindly provided by Prof. G. Hardie (Dundee, UK). HRP-conjugated secondary antibodies were from Santa Cruz Biotechnology. A peptide surrounding Ser491 of eEF2K (CKWNLLNSSRLHLPI) was synthesized with or without Ser491 phosphorylated and with a N-terminal Cys for coupling to keyhole limpet haemocyanin (KLH) or bovine serum albumin (BSA) (Imject maleimide-activated KLH/BSA kit, Thermo Fisher Scientific). The KLH-coupled phosphopeptide was injected in rabbits (Thermo Fisher Scientific) and the serum was affinity purified on both BSA-coupled phosphopeptide and non-phosphopeptide linked to CH-activated Sepharose 4B (GE Healthcare). Catalytic subunits of PKA from bovine heart and recombinant bacterially expressed AMPK (AMPKα2β1γ1 or AMPKα2β1γ1 complexes) activated by recombinant bacterially expressed LKB1-MO25-STRAD complex were prepared as described[51]. Peptides were synthesized by Vincent Stroobant (LICR, Brussels, BE). The pMSCV-neo vector was provided by Jean-Bernard Beaudry (de Duve Institute, Brussels).

2.2. Cell culture & immortalization

MEFs were maintained in classic culture medium (DMEM containing 4.5 $g.l^{-1}$ glucose, 4 mM glutamine, 1 mM pyruvate, penicillin/streptomycin and 10% (v/v) FBS) under a humid atmosphere containing 5% CO_2. Typically, cells were seeded in 6-well-plates (2 ml per well) and grown overnight to subconfluence. Prior to stimulation, the cells were washed in warm PBS and the medium was changed to 1 ml of stimulation medium (DMEM with or without $CaCl_2$ containing 4.5 $g.l^{-1}$ glucose, 4 mM glutamine, 1 mM pyruvate). All calcium-free media were supplemented with 0.5 mM EGTA. Primary MEF cells from $eEF2K^{-/-}$ mice and MEF cells deleted for TSC2 were generated as described[52]. Primary $eEF2K^{-/-}$ MEFs were immortalized using a retrovirus coding for BMI1 as described[53]. Wild-type or S491A/S492A mutant Nt-FLAG-eEF2K was retrovirally introduced into the genome of $eEF2K^{-/-}$ MEFs using the murine stem cell virus (MSCV) approach (Clontech) and neomycin resistance carried by the viral genome was selected. SV40-T-transformed MEF cells deficient for both AMPK catalytic α subunits or for LKB1 were kindly provided by Benoit Viollet (INSERM and Cochin Institute, Paris).

2.3. Cell lysis & immunoblotting

Following cell incubation, media were removed and the cells were washed in cold PBS before lysis in buffer containing 50 mM HEPES, pH 7.5, 1 mM EDTA, 1 mM EGTA, 0.5% (v/v) 2-mercaptoethanol, 50 mM NaF, 5 mM $Na_4P_2O_7$, 5 mM sodium β-glycerophosphate, 1 mM $NaVO_3$, 1 mM dithiothreitol, 0.1% (w/v) Triton X-100 and Complete™ protease inhibitor cocktail (150 µl of lysis buffer per well). Extracts were centrifuged (20000g x 5 min at 4 °C) and protein concentrations were measured using the Bio-Rad Protein Assay with BSA as a standard. For immunoblotting, extracts (10 µg of sample protein) were first boiled in Laemmli buffer (60 mM TRIS-HCl pH 6.8, 2% (w/v) SDS, 10% (v/v) glycerol, 5% (v/v) beta-mercaptoethanol, 0.01% (w/v) bromophenol blue) and loaded on 7.5% or 10% (w/v) polyacrylamide gels. Following SDS-PAGE, proteins were transferred onto PVDF membranes, which were then blocked in TRIS-buffered saline (TBS) containing 0.1% (v/v) TWEEN and 5% (w/v) BSA. Membranes were incubated overnight at 4 °C with the indicated primary antibodies diluted in blocking buffer, then washed extensively with TBS containing 0.1% (v/v) TWEEN before and after incubation for 1 h with HRP-conjugated secondary antibodies. All antibodies were used at a dilution of 1:1000,

except anti-total eEF2, anti-total AMPK, anti-P-eEF2 and anti-GAPDH antibodies were used at dilutions of 1:5000, 1:10000, 1:20000 and 1:40000, respectively. Secondary antibodies were used at a dilution of 1:20000. Immunodetection was by ECL Classico substrate (Merck Millipore). Immunoblots were quantified by scanning densitometry using ImageJ software.

2.4. Protein kinase assays

Purified recombinant activated AMPK and purified PKA were assayed for 10 min at 30 °C in phosphorylation buffer (10 mM MOPS, pH 7.0, 0.5 mM EDTA, 10 mM magnesium acetate, 5 mM DTT, 100 µM [γ-^{32}P] ATP (specific radioactivity 1000 cpm/pmol) by measuring ^{32}P incorporation into 200 µM AMARA peptide (AMARAASAAALRRR) for AMPK and 200 µM PFK-2 peptide (PVRMRRNSFT) for PKA as described[54]. Recombinant eEF2K was assayed in phosphorylation buffer without EDTA containing 10 µg/ml calmodulin and the indicated concentrations of free Ca^{2+} obtained with 2 mM EGTA and up to 2 mM of $CaCl_2$ calculated with Maxchelator (Stanford University). Assays were for 4 min at 30 °C using 0.5 mM MHC1 peptide (RKKFGESEKTKTKEFL) as substrate. One unit of protein kinase activity catalyzes the incorporation of 1 nmol min^{-1} of ^{32}P into the substrate peptide under the assay conditions.

2.5. Expression and purification of recombinant eEF2K

The pGEX6p1 vector containing wild-type human eEF2K cDNA was generated as described[55]. Site-directed mutagenesis was carried out using the Herculase II Fusion DNA polymerase (Stratagen) with the QuikChange (Agilent) protocol. GST-tagged eEF2K expressed in BL21 *E. coli* cells was purified as described[15]. Briefly, centrifuged cell lysate was subjected to chromatography first on DEAE-Sepharose and then on GSH-Sepharose. Fractions containing eEF2K activity were pooled and concentrated using a 100 kD ultra-filtration unit (Amicon) while changing the buffer to enzyme storage buffer (50 mM TRIS-HCl, pH 7.5, 150 mM NaCl, 0.1% (v/v) 2-mercaptoethanol, 10% (v/v) glycerol).

2.6. *In vitro* phosphorylation

Recombinant eEF2K (1 µg) was phosphorylated with 0.4 units of purified activated recombinant bacterially expressed AMPK or purified PKA catalytic subunits in 20 µl

of kinase assay buffer containing 200 µM AMP (for AMPK only) and 100 µM [γ-^{32}P] ATP (specific radioactivity 1000 cpm/pmol). For kinetic studies, incubations contained non-radioactive ATP at the same concentration. After 1 h at 30 °C, reactions were stopped on ice and 10 µl of mixture was taken for further analysis. For kinetic studies, samples were diluted 5-fold in enzyme storage buffer prior to eEF2K assay. For measurements of the stoichiometry of phosphorylation, proteins were separated by SDS-PAGE in 7.5% (w/v) polyacrylamide gels. Gels were stained using PageBlueTM (Thermo Fisher Scientific) for protein band quantification by OdysseyTM infrared imaging. Bands were then excised from the gels for measurement of ^{32}P-incorporation by liquid scintillation as described previously[51].

2.7. Phosphorylation site identification

Recombinant GST-eEF2K (3 µg) was phosphorylated as described above with 1 U of activated AMPK in a final volume of 60 µl at 30 °C. After 1 h, the reaction was stopped on ice, 20 µg of BSA was added as carrier and proteins were precipitated with a final concentration of 10% (w/v) trichloroacetic acid for 45 min on ice. Precipitated proteins were collected by centrifugation (20000 g x 10 min at 4 °C), washed in acetone, vacuum-dried and resuspended in 50 µl of 50 mM NH_4HCO_3 pH 8.0 for overnight digestion with trypsin at 30 °C. Peptides were separated by reverse-phase narrow-bore HPLC and radioactive peaks were analyzed by LC-MS/MS as described[56]. Multi Stage Activation (MSA) was enabled for phosphate neutral loss of 98, 49 or 32.66 with respect to the precursor m/z. Peak lists were generated and searched using SequestHT and PhosphoRS 3.1 within Proteome Discoverer 1.4 software package (Thermo Fisher Scientific) against a home-made protein database containing the human eEF2K sequences obtained from Uniprot and the different mutants used in this study. Phosphorylation site identification was performed as described[56] and validated manually.

2.8. Measurement of protein synthesis

Protein synthesis rates were determined by [2,3,4,5,6-^{3}H]-Phe incorporation into tricholoroacetic acid-precipitated material as described[57]. Cells grown to ~50% confluence were incubated for 30 min with AMPK activators and/or Torin prior to incubation for 4 hours with [2,3,4,5,6-^{3}H]-Phe at 2 µCi/ml with 0.4 mM of cold Phe coming from the medium.

2.9. Statistical analysis

The results are expressed as means ± S.E.M. of at least three separate experiments. Multiple comparisons were tested for statistically significant differences by 2-way ANOVA followed by Bonferroni's *post-hoc* test using the GraphPad Prism software and $P<0.05$ was considered significant. Otherwise, a paired 2-sided Student's t-test was used.

3. RESULTS

3.1. Increased eEF2 phosphorylation by AMPK activators requires Ca^{2+} and is partly dependent on AMPK.

Several studies have reported that both physiological and pharmacological AMPK activation leads to increased eEF2 phosphorylation, most likely via eEF2K activation. Accordingly, in immortalized MEF cells lacking eEF2K, no eEF2 (Thr56) phosphorylation was seen under conditions that led to AMPK activation monitored by AMPKα (Thr172) phosphorylation (Supplemental Fig. S1). We therefore investigated whether eEF2 phosphorylation was also strictly dependent on AMPK. In wild-type MEF cells incubated under normal conditions with Ca^{2+} present, eEF2 phosphorylation was seen in the basal condition, and increased in response to treatment of the cells with AMPK activators phenformin, AICAR, A769662 and compound 991 (Fig. 1A,B). To our surprise, when MEFs deleted for both AMPK catalytic subunits were incubated under the same conditions, eEF2 phosphorylation persisted in basal conditions as well as upon treatment with AMPK activators, albeit mostly at reduced levels (Fig. 1A). An increase in intracellular Ca^{2+} concentration ($[Ca^{2+}]_i$) can activate eEF2K, as proposed in exercise/contracting skeletal muscle before AMPK becomes activated[24,26], and off-target effects of the AMPK-activating compounds might increase ($[Ca^{2+}]_i$. Therefore, we performed the same incubations in Ca^{2+}-free media. In wild-type MEFs incubated without Ca^{2+}, eEF2 phosphorylation still increased upon treatment with AMPK activators, however the effect was totally abolished in cells lacking AMPKα1/α2 (Fig. 1A). Interestingly, the 991-mediated increase in eEF2 phosphorylation was also strongly reduced in cells lacking the major AMPK activating kinase LKB1 (Supplemental Fig. S2). Taken together, the results suggest that AMPK activation is partly responsible for increased eEF2 phosphorylation under these conditions and that Ca^{2+} is needed for full eEF2 phosphorylation in cells treated with AMPK activators. In the series of experiments that follow, incubations were carried out in Ca^{2+}-free media to reduce high levels of basal eEF2 phosphorylation, thereby focusing on AMPK-dependent eEF2 phosphorylation.

3.2. eEF2 phosphorylation due to AMPK activation is mainly mTORC1-independent.

In intact cells, AMPK activation could lead to increased eEF2 phosphorylation by at least two distinct mechanisms: direct activation of eEF2K by AMPK or indirect inhibition of mTOR signaling as a result of AMPK-induced phosphorylation of TSC2 and Raptor, leading to reduced S6K activity which phosphorylates and inactivates eEF2K. In growing cells with sufficient nutrients, mTORC1 signalling is active and continuously inhibits eEF2K via multiple inputs, allowing high rates of protein synthesis[58]. To distinguish between mTOR-dependent and mTOR-independent effects of AMPK activation on eEF2 phosphorylation, we used a potent specific inhibitor of mTOR kinase, Torin, which inhibits mTORC1 and mTORC2, in MEFs deleted for TSC2. As a consequence, these cells display elevated mTORC1 signalling, as reflected by high S6K phosphorylation (Fig. 2A,B), which was resistant to AMPK activation by 991. Basal eEF2 phosphorylation was undetectable in these cells, but treatment with 991 was able to cause an increase in eEF2 phosphorylation regardless of the lack of effect on mTORC1 signalling. Furthermore, pre-treatment of cells with Torin completely abolished S6K phosphorylation and increased eEF2 phosphorylation, which could be further increased on incubation with 991 (Fig. 2A,B). Taken together, the data suggest that the effect of AMPK activation by 991 to increase eEF2 phosphorylation was mainly independent of mTORC1 inhibition.

3.3. Phosphorylation-induced eEF2K activation by AMPK.

Since purified recombinant wild-type eEF2K undergoes multi-site autophosphorylation in the presence of Ca^{2+}/CaM[15,16], masking phosphorylation by other protein kinases such as AMPK (Fig. 3A), we investigated whether purified recombinant kinase-inactive (K170M) eEF2K[15] was phosphorylated by purified recombinant activated AMPK *in vitro*. However, phosphorylation of this eEF2K mutant by AMPK was barely detectable, even though the kinase-inactive mutant could be phosphorylated by PKA on previously identified sites[14] (Ser366, Ser500) and a novel site, Ser71 (Fig. 3B). We therefore turned to the use of purified recombinant wild-type eEF2K as a substrate, but incubated in the absence of Ca^{2+}/CaM to largely reduce autophosphorylation. Under these conditions, significant AMPK-dependent ^{32}P-incorporation from [γ-^{32}P]ATP into purified recombinant eEF2K was seen (Fig. 3A), suggesting that some eEF2K activity/autophosphorylation is

required for eEF2K phosphorylation by AMPK. Indeed, five sites (Ser18, Ser61, Ser64, Ser66 and Thr348) were identified in peaks whose labelling was unaffected by AMPK (Fig. 3C), suggesting Ca^{2+}/CaM-independent autophosphorylation at these residues. Following trypsin digestion and peptide separation by HPLC, LC-MS/MS analysis allowed the identification of 7 phosphorylation sites in the major peaks whose radioactive labelling was increased by AMPK (Ser18, Ser71, Ser78, Ser366, Ser398, Ser491, Ser500) (Fig. 3C), three of which (Ser18, Ser491, Ser500) had not been identified in a previous study[12]. Interestingly, Ser71, Ser366 and Ser500 were identified when wild-type eEF2K was phosphorylated from [γ-^{32}P]ATP by PKA under identical conditions (Supplemental Fig. S4). In fact, Ser500 phosphorylation has previously been implicated in Ca^{2+}-independent eEF2K activation by PKA[14]. When purified recombinant wild-type eEF2K was phosphorylated by AMPK without Ca^{2+}/CaM in the presence of protein kinase inhibitors, AMPK-dependent radiolabelling of the HPLC peaks was substantially reduced by Compound C (selective AMPK inhibitor *in vitro*) but labeling of the peaks seen with AMPK was largely preserved in the presence of A484954 (a selective inhibitor of eEF2K *in vitro* and in intact cells) (Fig. 3D). When identical incubations were carried out with AMPK and nonradioactive ATP, eEF2K activity increased by ~50% and AMPK-induced eEF2K activation was still seen in the presence of A484954 (to inhibit autophosphorylation of eEF2K), but not in the presence of Compound C (Fig. 3E), suggesting that autophosphorylation is not crucially involved in the mechanism of eEF2K activation by AMPK. To further investigate AMPK-induced eEF2K activation, purified recombinant wild-type eEF2K was assayed by ^{32}P-incorporation into MHC1 peptide[4] from [γ-^{32}P]ATP with increasing free Ca^{2+} concentrations. Treatment with AMPK led to an increase in V_{max} of eEF2K at saturating Ca^{2+} concentrations with no change in Ca^{2+} affinity (K_a = ~98 nM and ~95 nM with or without AMPK, respectively) (Fig. 3F). Interestingly, the effect of AMPK to increase the V_{max} of eEF2K was somewhat less when recombinant AMPKα1-containing trimers rather than AMPKα2-containing trimers were used (Supplemental Fig. S3). Furthermore, eEF2K activation by PKA was seen only at low free Ca^{2+} concentrations, whereas a decrease in V_{max} was seen at high (μM) free Ca^{2+} (Supplemental Figure S4). Both effects were largely abolished in the S500A eEF2K mutant treated with ATP and PKA, while this mutant was still activated after phosphorylation by AMPK (Supplemental Figure S4).

3.4. Ser491/Ser492 phosphorylation is essential for eEF2K activation by AMPK

In a previous study, phosphorylation of Ser398 was implicated in mediating eEF2K activation by partially purified AMPK[12]. However, the profile of eEF2K activation of purified recombinant eEF2K S398A mutant by AMPK with increasing free Ca^{2+} concentrations was not different from that seen with purified recombinant wild-type eEF2K (compare Fig. 4A and Fig. 3F). AMPK-induced activation of purified recombinant eEF2K mutants with non-phosphorylatable Ala residues at each of the AMPK-dependent Ser phosphorylation sites identified by MS was thus investigated. Most of the mutations did not drastically affect basal eEF2K activity, except the Ser366 to Ala mutation, as reported previously[15] (Fig. 4B and legend). For the Ser to Ala eEF2K phosphorylation site mutants, incubation with AMPK led to significant increases in eEF2K activity compared with the wild-type, except for the eEF2K S491A/S492A mutant (Fig. 4B). In fact, incubation of the single mutant eEF2K S491A with [γ-^{32}P]ATP and AMPK followed by trypsin digestion and MS analysis of a radiolabelled peak purified by HPLC indicated phosphorylation of the adjacent Ser492 residue (Supplemental Fig. S6). We therefore continued using an eEF2K S491A/S492A double mutant for which V_{max} was not increased after incubation with AMPK when eEF2K was assayed at saturating free Ca^{2+} concentrations (Fig. 4C).

To extend our study to intact cells, immortalized MEF cells obtained from mice bearing a global deletion of eEF2K[59] were used (Supplemental Fig. S1). The wild-type or S491A/S492A eEF2K coding sequence was introduced into these cells by retroviral (MSCV) infection in order to achieve equal and stable expression of both wild-type and mutant eEF2K, albeit at low levels. In cells expressing wild-type eEF2K incubated with 991, a dose-dependent increase in eEF2 phosphorylation was observed, indicative of eEF2K activation as a result of AMPK activation as reflected by dose-dependent increases in AMPKα-Thr172 and ACC-Ser79 phosphorylation (Fig. 4D). However, in cells expressing S491A/S492A eEF2K, 991-induced eEF2 phosphorylation was markedly reduced while dose-dependent AMPK and ACC phosphorylation were still evident (Fig. 4D). Furthermore, in cells expressing wild-type eEF2K, inhibition of mTOR by Torin led to an increase in basal eEF2 phosphorylation, which was further increased upon incubation with 991 (Fig. 4D,E), whereas AMPK and ACC phosphorylation in response to 991 treatment was unaffected (Fig. 4D). In cells expressing eEF2K S491A/S492A and incubated with

Torin, only a slight dose-dependent increase in eEF2 phosphorylation was apparent with 991 (Fig. 4D,E) and again 991-induced AMPK and ACC phosphorylation was seen in the presence of Torin. A dose-dependent decrease in p70S6K-Thr389 phosphorylation was seen in both wild-type and eEF2K S491A/S492A expressing cells incubated with 991 that was completely lost on incubation with Torin (Fig. 4D). We did try to produce an anti-phospho Ser491 peptide eEF2K antibody (see Methods) but the reagent was not phosphospecific enough to be used to monitor eEF2K Ser491 phosphorylation in cell lysates by immunoblotting, even after immunoprecipitation of eEF2K (data not shown). Taken together though, the results suggest that the increase in eEF2 phosphorylation following AMPK activation by 991 is mainly due to eEF2K activation via phosphorylation at Ser491/Ser492, but that reduced mTORC1 activity by AMPK also plays a minor role, at least in this cell type.

3.5. eEF2K Ser491/Ser492 phosphorylation is required for mTORC1-independent regulation of protein synthesis by AMPK

Protein synthesis rates were compared in eEF2K-*null* cells rescued with either wild-type or S491A/S492A eEF2K (Fig. 4F). Protein synthesis was decreased to the same extent in both cell lines by ~25% following AMPK activation by 991 and by ~40% when AICAR was used to activate AMPK as positive control. Complete inhibition of mTORC1 with Torin (as confirmed by undetectable p70S6K phosphorylation in Fig. 4D) reduced protein synthesis by over 60% in both cell lines, which could be further decreased by treatment with 991 or AICAR, but only in cells expressing wild-type but not S491A/S492A eEF2K. These results were consistent with eEF2 phosphorylation observed in these cells (Fig. 4D,E), although it should be pointed out that inhibition of mTORC1 affects both translation elongation and initiation, explaining the pronounced effect of Torin treatment on protein synthesis. Taken together, the results indicate that eEF2K Ser491/Ser492 phosphorylation mediates the mTORC1-independent inhibition of protein synthesis by AMPK.

4. DISCUSSION

eEF2K is a complicated multi-modulated protein kinase and the control of its activity integrates inputs from many cellular signaling pathways. In addition, eEF2K activity is controlled by $[Ca^{2+}]_i$ and pH, such that an increase in $[Ca^{2+}]_i$ via CaM leads to increased eEF2K autophosphorylation/activity and eEF2K displays optimal activity at pH 6.4. Multi-site phosphorylation by protein kinases of different signaling pathways can lead to eEF2K activation or inactivation, change CaM affinity/Ca^{2+}-dependence or affect stability towards proteasomal degradation. Increased eEF2K activity caused by increases in $[Ca^{2+}]_i$ leading to increased eEF2 phosphorylation is probably important during skeletal muscle contraction and neuronal signalling, while eEF2K activation by a fall in intracellular pH might be important during anoxia and hypoxia to slow down protein synthesis [7,60]. Growth factors that induce cell proliferation tend to decrease eEF2K affinity for CaM and eEF2K activity via phosphorylation of Ser78 and Ser359/Ser366 mediated by mitogen-activated protein kinases (MAPKs) and various inputs from mTORC1 signaling (directly or via S6K)[58]. On the other hand, cAMP signaling through phosphorylation of Ser500 by PKA increases Ca^{2+}-independent eEF2K activity. Together, these multiple inputs would allow fine-tuning of eEF2K activity to control protein synthesis via downstream eEF2 phosphorylation, in both a quantitative and qualitative way via translational rewiring towards specific mRNA subsets through unexplained mechanisms. Phosphorylation of eEF2 at Thr56 impairs ribosome binding and arrests protein synthesis elongation. This residue is extremely highly conserved in all eukaryotes including protists, yeast, plants and insects although in fungi plants and arthropods, eEF2K orthologues are absent, suggesting that eEF2 Thr56 might be phosphorylated by alternative kinase(s) in these organisms[7,60,61]. Also surprising is the fact that eEF2K deletion is not lethal, either in mice or *C. elegans*, although oocyte quality and embryonic viability were compromised in both species[62].

In the present study using AMPK-*null* and TSC2-*null* MEFs combined with TOR inhibition by Torin, we show that pharmacological AMPK activation by 991 led to eEF2 phosphorylation (Figs 1,2), which was mainly mTORC1-independent, but dependent on the presence of both AMPK and eEF2K as shown by using the two kinase gene-deficient MEF cell lines (Figs. 1,S1). It is noteworthy that treatment of

MEFs with commonly used pharmacological AMPK activators, whether acting directly (991, A769662) or indirectly (AICAR, phenformin), led to an increase in eEF2 phosphorylation that was, to some extent, independent of AMPK as shown in cells lacking both AMPK catalytic subunits (Fig. 1). However, these effects were observed only in presence of Ca^{2+} in the medium, suggesting that eEF2K activation might have been partly due to a rise in $[Ca^{2+}]_i$ by these AMPK activators[63,64]. Indeed, using the fluorescent probe FURA-2, we were able to detect a significant rise in $[Ca^{2+}]_i$ in MEFs, but only in cells treated with A769662 and not with the other AMPK activators at the doses used in this study (data not shown). When MEF incubations were carried out in Ca^{2+}-free media to solely focus on AMPK-dependent effects, direct activation of eEF2K by AMPK was more important than indirect eEF2K activation via AMPK-induced reduction in mTORC1/p70S6K activity. However the contributions of direct versus indirect eEF2K activation might well differ across different cell types.

In the absence of Ca^{2+}/CaM, recombinant AMPK phosphorylated recombinant wild-type eEF2K on at least 7 different sites (Fig. 3C) and *in vitro* phosphorylation of eEF2K by AMPK led to an increase in the V_{max} of the kinase without affecting Ca^{2+} sensitivity in the presence of CaM (Fig. 3F). By site-directed mutagenesis, Ser491/Ser492 was shown to be required for AMPK-induced eEF2K activation (Fig. 4B). Some of the phosphorylation sites identified are also autophosphorylation sites, which could become phosphorylated as a consequence of increased kinase activity due to eEF2K phosphorylation by AMPK at Ser491/Ser492. Indeed, Ser491 was found to be crucial for eEF2K autophosphorylation at other sites[15]. Kinase-inactive eEF2K was a very poor substrate for AMPK *in vitro* (Fig. 3B), probably because some (Ca^{2+}-independent) autophosphorylation would be required to induce structural changes in eEF2K[40] allowing phosphorylation by AMPK. Comparison of the sequences surrounding the identified AMPK phosphorylation sites revealed that none perfectly fits the AMPK consensus[65] (Supplemental Fig. S5), but recent evidence suggests that there might be flexibility in this regard[66]. Phosphorylation at Ser491/492 was found to be essential for eEF2K activation by AMPK *in vitro* (Fig. 4C) and in MEFs there was a major requirement for eEF2K Ser491/492 phosphorylation for increased eEF2 phosphorylation in response to 991 treatment (Fig. 4D). *In vitro* phosphorylation of eEF2K by AMPK and rescue in eEF2K-*null* MEFs was based on the use of human eEF2K. However, since mutation of Ser491 to Ala resulted in Ser492 phosphorylation of human eEF2K by AMPK *in vitro*

(Supplemental Fig. S6), we resorted to the use of the S491A/S492A double mutant when human eEF2K was stably reintroduced in eEF2K-*null* cells to be sure of abolishing AMPK-induced eEF2K activation (Fig. 4C). Supplemental Fig. S7 shows that in mouse and rat, the Ser491 site is not present but the equivalent of the adjacent Ser492 in human eEF2K is conserved (Ser491 in the mouse and rat sequence). Thus in normal MEFs, it is likely that effects of AMPK activation are mediated by phosphorylation at the endogenous eEF2K Ser491 site.

An important role of eEF2K is to protect cells against nutrient deprivation and hypoxia with implications for cancer cell survival[30]. eEF2K as well as its substrate eEF2 appear to be highly expressed in various malignant tissues and cancer cell lines, including breast carcinoma and glioblastoma[7,60]. eEF2K has been implicated in other physiological processes such as autophagy, cell cycle control, cell migration and invasion, angiogenesis, vascular inflammation, glycolysis and cognitive learning/depression[7,60]. Although eEF2K is considered as a dedicated protein kinase, an *in vitro* phosphoproteomics study identified some other targets and AMPKα1 was also proposed[67]. Whether any of these are bona fide *in vivo* eEF2K substrates remains to be confirmed. Both AMPK and eEF2K seem to have dual and probably contextual roles towards tumor establishment and persistence: on the one hand by decreasing cancer cell proliferation through inhibition of protein synthesis and regulation of cell cycle progression, and on the other hand by favoring cancer cell survival during nutrient deprivation and anti-cancer treatments. Specific eEF2K inhibitors therefore have therapeutic potential for cancer treatment.

5. CONCLUSIONS

Activation of AMPK using pharmacological activators leads to increased phosphorylation of eEF2 through different mechanisms, including increased cytosolic Ca^{2+}, inhibition of mTORC1 by AMPK and direct activation of eEF2K by AMPK-mediated multi-site phosphorylation. Direct activation of eEF2K is the major mechanism, increasing the V_{max} of the kinase and requiring phosphorylation of the newly identified Ser491/Ser492 in human eEF2K.

6. FIGURE LEGENDS

Figure 1: Role of AMPK and Ca^{2+} in increasing eEF2 phosphorylation in MEFs treated with AMPK activators.

Immortalized wild-type MEFs or MEFs lacking both catalytic subunits of AMPK ($\alpha_1^{-/-}$ $\alpha_2^{-/-}$) were incubated for 1 h in serum-free medium with (+) or without (-) $CaCl_2$ (the latter containing 0.5 mM EGTA) and DMSO (vehicle) or AMPK activators at the indicated concentrations. Cell extracts were prepared for immunoblotting with the indicated antibodies. Panel (A) shows one representative experiment in which incubations of wild-type and AMPK $\alpha_1^{-/-}$ $\alpha_2^{-/-}$ MEFs were performed in parallel. In (B), for wild-type MEFs incubated without $CaCl_2$, band intensities relative to GAPDH as loading control were determined by densitometric scanning and normalized to the maximal value. Data are means ± s.e.m. of 3 separate experiments and * indicates a significant difference (P<0.05) between the indicated conditions.

Figure 2: Role of mTOR-inhibition in the AMPK-induced increase in eEF2 phosphorylation by 991 treatment. Immortalized MEFs lacking TSC2 ($TSC2^{-/-}$) were incubated for 30 min in serum-free medium without $CaCl_2$ (with 0.5 mM EGTA) containing 0.25 μM Torin (or DMSO as vehicle) prior to incubation with the indicated concentrations of 991 (or DMSO as vehicle). Cell extracts were prepared for immunoblotting with the indicated antibodies. Panel (A) shows one representative experiment. In (B), band intensities relative to GAPDH as loading control were determined by densitometric scanning and normalized to the maximal value. Data are means ± s.e.m. of 3 separate experiments and significant differences (P<0.05) are indicated compared to control conditions in the absence (*) or presence ($) of Torin.

Figure 3: Phosphorylation-induced eEF2K activation by AMPK *in vitro*.

In (A, C, D), purified recombinant eEF2K (wild-type (WT)) was incubated for 1 h with purified recombinant activated AMPKα2β1γ1 (211) in the presence of [γ-^{32}P]ATP for analysis of ^{32}P-incorporation by SDS-PAGE and phosphorimaging (A) or for trypsin digestion and phosphopeptide separation by HPLC (C, D) and phosphosite identification by LC-MS (C). In (B) kinase-inactive (K170M) eEF2K was incubated for 1 h with purified recombinant activated AMPK or purified PKA in the presence of [γ-

^{32}P]ATP for trypsin digestion and phosphopeptide separation by HPLC. In E-F, eEF2K was incubated as above but with non-radioactive ATP prior to eEF2K assay with MHC1 peptide as substrate and with saturating Ca^{2+} (E) or with increasing free Ca^{2+} concentrations using a $CaCl_2$-EGTA buffer system (F). In D, E, 100 µM eEF2K inhibitor A484954 or 10 µM AMPK inhibitor compound C (or DMSO as vehicle) were included for labelling. Data are from one representative experiment (A-D) or the means ± s.e.m. of at least 3 separate experiments (E-F) and * indicates a significant difference (P<0.05) compared to control conditions.

Figure 4: Ser491 phosphorylation is crucial for eEF2K activation by AMPK.
Purified recombinant eEF2K, wild-type (WT) or the indicated non-phosphorylatable Ser to Ala mutants, were incubated for 1 h with purified recombinant activated AMPK and ATP for eEF2K assay using MHC1 peptide as substrate and with increasing concentrations of free Ca^{2+} using a $CaCl_2$-EGTA buffer system (A, C) or with saturating Ca^{2+} (B). Basal activities were 492 ± 20 U/mg of protein (WT), 481 ± 20 U/mg of protein (S18A), 528 ± 47 U/mg of protein (S78A), 13 ± 1 U/mg of protein (S366A), 371 ± 21 U/mg of protein (S398A), 357 ± 28 U/mg of protein (S491A/S492A) and 266 ± 28 U/mg of protein (S500A) and * indicates a significant difference compared to control incubations without AMPK, $ compared to activation of the wild-type by AMPK. In D and E, immortalized MEFs from eEF2K$^{-/-}$ mice were retrovirally (MSCV) transfected to reintroduce either wild-type or S491A/S492A eEF2K. The cells were cultured overnight and then incubated for 30 min in serum-free medium without $CaCl_2$ (with 0.5 mM EGTA) containing 0.25 µM Torin (or DMSO as vehicle) prior to incubation with the indicated concentrations of 991 (or DMSO as vehicle). Cell extracts were prepared for immunoblotting with the indicated antibodies. Panel D shows one representative experiment. In E, band intensities relative to GAPDH as loading control were determined by densitometric scanning and normalized to the maximal value. In F, MEFs were incubated for 30 min with 0.25 µM Torin, 10 µM 991 or 0.5 mM AICAR (or with DMSO as vehicle control) in $CaCl_2$-containing medium, prior to addition of [^{3}H]-Phe and further incubation of 4 h. Incorporation of [^{3}H]-Phe into TCA-precipitable material was measured as described in the Methods section. Control values of protein synthesis rates in cells rescued with wild-type or S491A/S492A eEF2K were not significantly different and corresponded to roughly 7000 cpm (~1.3 pmol of Phe) per hour per mg of total cell proteins. Data

are means ± s.e.m. of 3 separate experiments and significant differences (P<0.05) are indicated compared to control conditions in absence (*) or presence ($) of Torin.

7. ACKNOLEDGEMENTS

We thank Benoît Viollet (INSERM and Cochin Institute, Paris) for kindly providing AMPK- and LKB1-deficient MEFs. M.J. was supported by the Fund for Scientific Research in Industry and Agriculture (FRIA). Funding was from the Interuniversity Poles of Attraction Belgian Science Policy (P7/13), the Directorate General Higher Education and Scientific Research, French Community of Belgium, the Fund for Medical Scientific Research (FNRS, Belgium) grant numbers 3.4518.11 and T.0008.15 and a Programme Grant to C.G.P. from the Wellcome Trust (reference 086688).

8. REFERENCES

[1] Nairn, A.C., Bhagat, B., Palfrey, H.C., 1985. Identification of calmodulin-dependent protein kinase III and its major Mr 100,000 substrate in mammalian tissues. Proc Natl Acad Sci U S A 82(23):7939-7943.

[2] Redpath, N.T., Price, N.T., Proud, C.G., 1996. Cloning and expression of cDNA encoding protein synthesis elongation factor-2 kinase. J Biol Chem 271(29):17547-17554.

[3] Ryazanov, A.G., Ward, M.D., Mendola, C.E., Pavur, K.S., Dorovkov, M.V., Wiedmann, M., et al., 1997. Identification of a new class of protein kinases represented by eukaryotic elongation factor-2 kinase. Proc Natl Acad Sci U S A 94(10):4884-4889.

[4] Pavur, K.S., Petrov, A.N., Ryazanov, A.G., 2000. Mapping the functional domains of elongation factor-2 kinase. Biochemistry 39(40):12216-12224.

[5] Diggle, T.A., Seehra, C.K., Hase, S., Redpath, N.T., 1999. Analysis of the domain structure of elongation factor-2 kinase by mutagenesis. FEBS Lett 457(2):189-192.

[6] Tavares, C.D., Ferguson, S.B., Giles, D.H., Wang, Q., Wellmann, R.M., O'Brien, J.P., et al., 2014. The molecular mechanism of eukaryotic elongation factor 2 kinase activation. J Biol Chem 289(34):23901-23916.

[7] Proud, C.G., 2015. Regulation and roles of elongation factor 2 kinase. Biochem Soc Trans 43(3):328-332.

[8] Huber-Keener, K.J., Evans, B.R., Ren, X., Cheng, Y., Zhang, Y., Hait, W.N., et al., 2012. Phosphorylation of elongation factor-2 kinase differentially regulates the enzyme's stability under stress conditions. Biochem Biophys Res Commun 424(2):308-314.

[9] Arora, S., Yang, J.M., Hait, W.N., 2005. Identification of the ubiquitin-proteasome pathway in the regulation of the stability of eukaryotic elongation factor-2 kinase. Cancer Res 65(9):3806-3810.

[10] Wang, X., Li, W., Williams, M., Terada, N., Alessi, D.R., Proud, C.G., 2001. Regulation of elongation factor 2 kinase by p90(RSK1) and p70 S6 kinase. EMBO J 20(16):4370-4379.

[11] Browne, G.J., Proud, C.G., 2004. A novel mTOR-regulated phosphorylation site in elongation factor 2 kinase modulates the activity of the kinase and its binding to calmodulin. Mol Cell Biol 24(7):2986-2997.

[12] Browne, G.J., Finn, S.G., Proud, C.G., 2004. Stimulation of the AMP-activated protein kinase leads to activation of eukaryotic elongation factor 2 kinase and to its phosphorylation at a novel site, serine 398. J Biol Chem 279(13):12220-12231.

[13] Diggle, T.A., Redpath, N.T., Heesom, K.J., Denton, R.M., 1998. Regulation of protein-synthesis elongation-factor-2 kinase by cAMP in adipocytes. Biochem J 336 (Pt 3):525-529.

[14] Diggle, T.A., Subkhankulova, T., Lilley, K.S., Shikotra, N., Willis, A.E., Redpath, N.T., 2001. Phosphorylation of elongation factor-2 kinase on serine 499 by cAMP-dependent protein kinase induces Ca2+/calmodulin-independent activity. Biochem J 353(Pt 3):621-626.

[15] Pyr Dit Ruys, S., Wang, X., Smith, E.M., Herinckx, G., Hussain, N., Rider, M.H., et al., 2012. Identification of autophosphorylation sites in eukaryotic elongation factor-2 kinase. Biochem J 442(3):681-692.

[16] Tavares, C.D., O'Brien, J.P., Abramczyk, O., Devkota, A.K., Shores, K.S., Ferguson, S.B., et al., 2012. Calcium/calmodulin stimulates the autophosphorylation of elongation factor 2 kinase on Thr-348 and Ser-500 to regulate its activity and calcium dependence. Biochemistry 51(11):2232-2245.

[17] Redpath, N.T., Foulstone, E.J., Proud, C.G., 1996. Regulation of translation elongation factor-2 by insulin via a rapamycin-sensitive signalling pathway. EMBO J 15(9):2291-2297.

[18] Redpath, N.T., Price, N.T., Severinov, K.V., Proud, C.G., 1993. Regulation of elongation factor-2 by multisite phosphorylation. Eur J Biochem 213(2):689-699.

[19] Browne, G.J., Proud, C.G., 2002. Regulation of peptide-chain elongation in mammalian cells. Eur J Biochem 269(22):5360-5368.

[20] Horman, S., et al., 2002. Activation of AMP-Activated Protein Kinase Leads to the Phosphorylation of Elongation Factor 2 and an Inhibition of Protein Synthesis. Curr Biol 12:1419–1423.
[21] Bolster, D.R., Crozier, S.J., Kimball, S.R., Jefferson, L.S., 2002. AMP-activated protein kinase suppresses protein synthesis in rat skeletal muscle through down-regulated mammalian target of rapamycin (mTOR) signaling. J Biol Chem 277(27):23977-23980.
[22] Gwinn, D.M., Shackelford, D.B., Egan, D.F., Mihaylova, M.M., Mery, A., Vasquez, D.S., et al., 2008. AMPK phosphorylation of raptor mediates a metabolic checkpoint. Mol Cell 30(2):214-226.
[23] Inoki, K., Zhu, T., Guan, K.L., 2003. TSC2 mediates cellular energy response to control cell growth and survival. Cell 115(5):577-590.
[24] Rose, A.J., Broholm, C., Kiillerich, K., Finn, S.G., Proud, C.G., Rider, M.H., et al., 2005. Exercise rapidly increases eukaryotic elongation factor 2 phosphorylation in skeletal muscle of men. J Physiol 569(Pt 1):223-228.
[25] Miranda, L., Horman, S., De Potter, I., Hue, L., Jensen, J., Rider, M.H., 2008. Effects of contraction and insulin on protein synthesis, AMP-activated protein kinase and phosphorylation state of translation factors in rat skeletal muscle. Pflugers Arch 455(6):1129-1140.
[26] Rose, A.J., Alsted, T.J., Jensen, T.E., Kobbero, J.B., Maarbjerg, S.J., Jensen, J., et al., 2009. A Ca(2+)-calmodulin-eEF2K-eEF2 signalling cascade, but not AMPK, contributes to the suppression of skeletal muscle protein synthesis during contractions. J Physiol 587(Pt 7):1547-1563.
[27] Horman, S., Beauloye, C., Vertommen, D., Vanoverschelde, J.L., Hue, L., Rider, M.H., 2003. Myocardial ischemia and increased heart work modulate the phosphorylation state of eukaryotic elongation factor-2. J Biol Chem 278(43):41970-41976.
[28] Connolly, E., Braunstein, S., Formenti, S., Schneider, R.J., 2006. Hypoxia inhibits protein synthesis through a 4E-BP1 and elongation factor 2 kinase pathway controlled by mTOR and uncoupled in breast cancer cells. Mol Cell Biol 26(10):3955-3965.
[29] Patel, J., McLeod, L.E., Vries, R.G.J., Flynn, A., Wang, X., Proud, C.G., 2002. Cellular stresses profoundly inhibit protein synthesis and modulate the states of phosphorylation of multiple translation factors. Eur J Biochem 269(12):3076-3085.
[30] Leprivier, G., Remke, M., Rotblat, B., Dubuc, A., Mateo, A.R., Kool, M., et al., 2013. The eEF2 kinase confers resistance to nutrient deprivation by blocking translation elongation. Cell 153(5):1064-1079.
[31] Cheng, Y., Li, H., Ren, X., Niu, T., Hait, W.N., Yang, J., 2010. Cytoprotective effect of the elongation factor-2 kinase-mediated autophagy in breast cancer cells subjected to growth factor inhibition. PLoS One 5(3):e9715.
[32] Kruiswijk, F., Yuniati, L., Magliozzi, R., Low, T.Y., Lim, R., Bolder, R., et al., 2012. Coupled activation and degradation of eEF2K regulates protein synthesis in response to genotoxic stress. Sci Signal 5(227):ra40.
[33] Boyce, M., Py, B.F., Ryazanov, A.G., Minden, J.S., Long, K., Ma, D., et al., 2008. A pharmacoproteomic approach implicates eukaryotic elongation factor 2 kinase in ER stress-induced cell death. Cell Death Differ 15(3):589-599.
[34] Cheng, Y., Ren, X., Zhang, Y., Shan, Y., Huber-Keener, K.J., Zhang, L., et al., 2013. Integrated regulation of autophagy and apoptosis by EEF2K controls cellular fate and modulates the efficacy of curcumin and velcade against tumor cells. Autophagy 9(2):208-219.
[35] Gismondi, A., Caldarola, S., Lisi, G., Juli, G., Chellini, L., Iadevaia, V., et al., 2014. Ribosomal stress activates eEF2K-eEF2 pathway causing translation elongation inhibition and recruitment of terminal oligopyrimidine (TOP) mRNAs on polysomes. Nucleic Acids Res 42(20):12668-12680.
[36] Usui, T., Okada, M., Hara, Y., Yamawaki, H., 2013. Eukaryotic elongation factor 2 kinase regulates the development of hypertension through oxidative stress-dependent vascular inflammation. Am J Physiol Heart Circ Physiol 305(5):H756-768.
[37] Bevilacqua, E., Wang, X., Majumder, M., Gaccioli, F., Yuan, C.L., Wang, C., et al., 2010. eIF2alpha phosphorylation tips the balance to apoptosis during osmotic stress. J Biol Chem 285(22):17098-17111.

[38] Hong-Brown, L.Q., Brown, C.R., Huber, D.S., Lang, C.H., 2007. Alcohol regulates eukaryotic elongation factor 2 phosphorylation via an AMP-activated protein kinase-dependent mechanism in C2C12 skeletal myocytes. J Biol Chem 282(6):3702-3712.
[39] Dorovkov, M.V., Pavur, K.S., Petrov, A.N., Ryazanov, A.G., 2002. Regulation of elongation factor-2 kinase by pH. Biochemistry 41(45):13444-13450.
[40] Pigott, C.R., Mikolajek, H., Moore, C.E., Finn, S.J., Phippen, C.W., Werner, J.M., et al., 2012. Insights into the regulation of eukaryotic elongation factor 2 kinase and the interplay between its domains. Biochem J 442(1):105-118.
[41] Knight, J.R., Bastide, A., Roobol, A., Roobol, J., Jackson, T.J., Utami, W., et al., 2015. Eukaryotic elongation factor 2 kinase regulates the cold stress response by slowing translation elongation. Biochem J 465(2):227-238.
[42] de Meester, C., Timmermans, A.D., Balteau, M., Ginion, A., Roelants, V., Noppe, G., et al., 2014. Role of AMP-activated protein kinase in regulating hypoxic survival and proliferation of mesenchymal stem cells. Cardiovasc Res 101(1):20-29.
[43] Chan, A.Y., Soltys, C.L., Young, M.E., Proud, C.G., Dyck, J.R., 2004. Activation of AMP-activated protein kinase inhibits protein synthesis associated with hypertrophy in the cardiac myocyte. J Biol Chem 279(31):32771-32779.
[44] Sato, R., Goldstein, J.L., Brown, M.S., 1993. Replacement of serine-871 of hamster 3-hydroxy-3-methylglutaryl-CoA reductase prevents phosphorylation by AMP-activated kinase and blocks inhibition of sterol synthesis induced by ATP depletion. Proc Natl Acad Sci U S A 90(20):9261-9265.
[45] Zhou, G., Myers, R., Li, Y., Chen, Y., Shen, X., Fenyk-Melody, J., et al., 2001. Role of AMP-activated protein kinase in mechanism of metformin action. J Clin Invest 108(8):1167-1174.
[46] Stefanelli, C., Stanic, I., Bonavita, F., Flamigni, F., Pignatti, C., Guarnieri, C., et al., 1998. Inhibition of glucocorticoid-induced apoptosis with 5-aminoimidazole-4-carboxamide ribonucleoside, a cell-permeable activator of AMP-activated protein kinase. Biochem Biophys Res Commun 243(3):821-826.
[47] Xiao, B., Sanders, M.J., Carmena, D., Bright, N.J., Haire, L.F., Underwood, E., et al., 2013. Structural basis of AMPK regulation by small molecule activators. Nat Commun 4:3017.
[48] Lai, Y.C., Kviklyte, S., Vertommen, D., Lantier, L., Foretz, M., Viollet, B., et al., 2014. A small-molecule benzimidazole derivative that potently activates AMPK to increase glucose transport in skeletal muscle: comparison with effects of contraction and other AMPK activators. Biochem J 460(3):363-375.
[49] Bultot, L., Jensen, T.E., Lai, Y.C., Madsen, A.L., Collodet, C., Kviklyte, S., et al., 2016. Benzimidazole derivative small-molecule 991 enhances AMPK activity and glucose uptake induced by AICAR or contraction in skeletal muscle. Am J Physiol Endocrinol Metab 311(4):E706-e719.
[50] Johanns, M., Lai, Y.C., Hsu, M.F., Jacobs, R., Vertommen, D., Van Sande, J., et al., 2016. AMPK antagonizes hepatic glucagon-stimulated cyclic AMP signalling via phosphorylation-induced activation of cyclic nucleotide phosphodiesterase 4B. Nat Commun 7:10856.
[51] Bultot, L., Guigas, B., Von Wilamowitz-Moellendorff, A., Maisin, L., Vertommen, D., Hussain, N., et al., 2012. AMP-activated protein kinase phosphorylates and inactivates liver glycogen synthase. Biochem J 443(1):193-203.
[52] Smith, E.M., Finn, S.G., Tee, A.R., Browne, G.J., Proud, C.G., 2005. The tuberous sclerosis protein TSC2 is not required for the regulation of the mammalian target of rapamycin by amino acids and certain cellular stresses. J Biol Chem 280(19):18717-18727.
[53] Nacerddine, K., Beaudry, J.B., Ginjala, V., Westerman, B., Mattiroli, F., Song, J.Y., et al., 2012. Akt-mediated phosphorylation of Bmi1 modulates its oncogenic potential, E3 ligase activity, and DNA damage repair activity in mouse prostate cancer. J Clin Invest 122(5):1920-1932.
[54] Bultot, L., Horman, S., Neumann, D., Walsh, M.P., Hue, L., Rider, M.H., 2009. Myosin light chains are not a physiological substrate of AMPK in the control of cell structure changes. FEBS Lett 583(1):25-28.
[55] Smith, E.M., Proud, C.G., 2008. cdc2-cyclin B regulates eEF2 kinase activity in a cell cycle- and amino acid-dependent manner. EMBO J 27(7):1005-1016.

[56] Vertommen, D., Rider, M., Ni, Y., Waelkens, E., Merlevede, W., Vandenheede, J.R., et al., 2000. Regulation of protein kinase D by multisite phosphorylation. Identification of phosphorylation sites by mass spectrometry and characterization by site-directed mutagenesis. J Biol Chem 275(26):19567-19576.
[57] Houddane, A., Bultot, L., Novellasdemunt, L., Johanns, M., Gueuning, M.A., Vertommen, D., et al., 2017. Role of Akt/PKB and PFKFB isoenzymes in the control of glycolysis, cell proliferation and protein synthesis in mitogen-stimulated thymocytes. Cell Signal 34:23-37.
[58] Wang, X., Regufe da Mota, S., Liu, R., Moore, C.E., Xie, J., Lanucara, F., et al., 2014. Eukaryotic elongation factor 2 kinase activity is controlled by multiple inputs from oncogenic signaling. Mol Cell Biol 34(22):4088-4103.
[59] Moore, C.E., Mikolajek, H., Regufe da Mota, S., Wang, X., Kenney, J.W., Werner, J.M., et al., 2015. Elongation Factor 2 Kinase Is Regulated by Proline Hydroxylation and Protects Cells during Hypoxia. Mol Cell Biol 35(10):1788-1804.
[60] Kenney, J.W., Moore, C.E., Wang, X., Proud, C.G., 2014. Eukaryotic elongation factor 2 kinase, an unusual enzyme with multiple roles. Adv Biol Regul 55:15-27.
[61] Rider, M.H., 2016. Role of AMP-activated protein kinase in metabolic depression in animals. J Comp Physiol B 186(1):1-16.
[62] Chu, H.P., Liao, Y., Novak, J.S., Hu, Z., Merkin, J.J., Shymkiv, Y., et al., 2014. Germline quality control: eEF2K stands guard to eliminate defective oocytes. Dev Cell 28(5):561-572.
[63] Evans, A.M., Lewis, S.A., Ogunbayo, O.A., Moral-Sanz, J., 2015. Modulation of the LKB1-AMPK Signalling Pathway Underpins Hypoxic Pulmonary Vasoconstriction and Pulmonary Hypertension. Adv Exp Med Biol 860:89-99.
[64] Vlachaki Walker, J.M., Robb, J.L., Cruz, A.M., Malhi, A., Weightman Potter, P.G., Ashford, M.L., et al., 2017. AMP-activated protein kinase activator A-769662 increases intracellular calcium and ATP release from astrocytes in an AMPK-independent manner. Diabetes Obes Metab.
[65] Hardie, D.G., Schaffer, B.E., Brunet, A., 2016. AMPK: An Energy-Sensing Pathway with Multiple Inputs and Outputs. Trends Cell Biol 26(3):190-201.
[66] Schaffer, B.E., Levin, R.S., Hertz, N.T., Maures, T.J., Schoof, M.L., Hollstein, P.E., et al., 2015. Identification of AMPK Phosphorylation Sites Reveals a Network of Proteins Involved in Cell Invasion and Facilitates Large-Scale Substrate Prediction. Cell Metab 22(5):907-921.
[67] Lazarus, M.B., Levin, R.S., Shokat, K.M., 2016. Discovery of new substrates of the elongation factor-2 kinase suggests a broader role in the cellular nutrient response. Cell Signal 29:78-83.

FIGURE 1

A

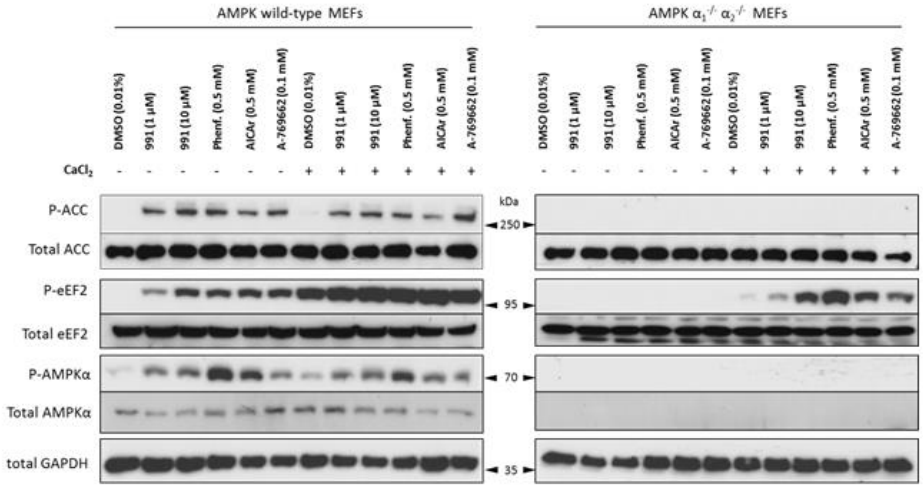
AMPK wild-type MEFs
AMPK α1-/- α2-/- MEFs
DMSO (0.01%)
991 (1 µM)
991 (10 µM)
Phenf. (0.5 mM)
AICAr (0.5 mM)
A-769662 (0.1 mM)
CaCl2
P-ACC
Total ACC
P-eEF2
Total eEF2
P-AMPKα
Total AMPKα
total GAPDH
kDa
250
95
70
35

B

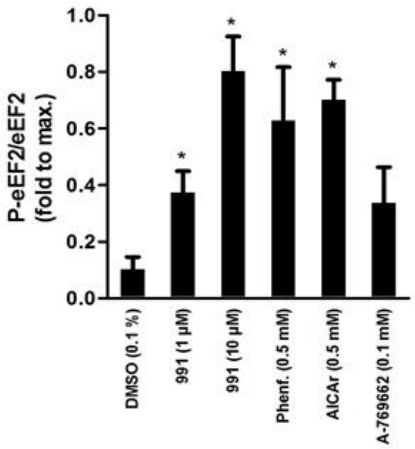
P-eEF2/eEF2 (fold to max.)
1.0
0.8
0.6
0.4
0.2
0.0
DMSO (0.1 %)
991 (1 µM)
991 (10 µM)
Phenf. (0.5 mM)
AICAr (0.5 mM)
A-769662 (0.1 mM)

FIGURE 2

A

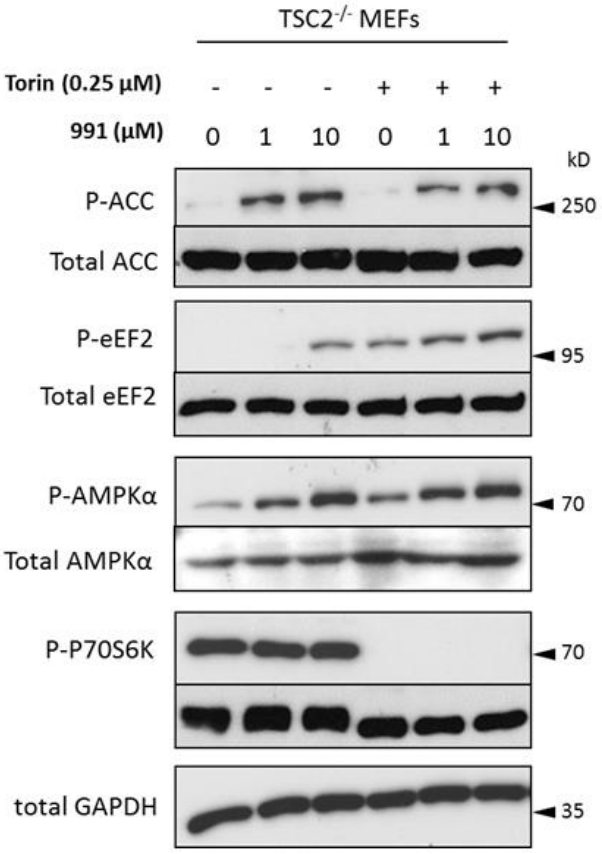
TSC2-/- MEFs
Torin (0.25 μM) - - - + + +
991 (μM) 0 1 10 0 1 10
kD
P-ACC
Total ACC
250
P-eEF2
Total eEF2
95
P-AMPKα
Total AMPKα
70
P-P70S6K
70
total GAPDH
35

B

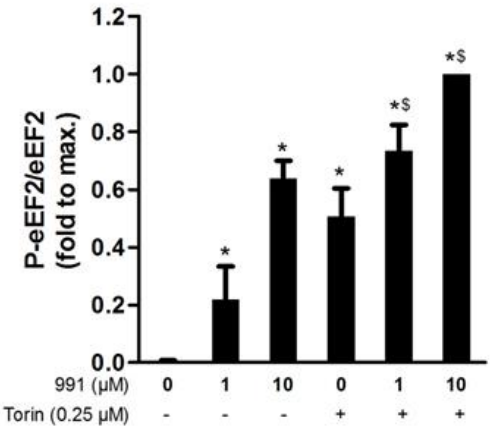
P-eEF2/eEF2 (fold to max.)
1.2
1.0
0.8
0.6
0.4
0.2
0.0
*
*
*
*$
*$
991 (μM) 0 1 10 0 1 10
Torin (0.25 μM) - - - + + +

FIGURE 3

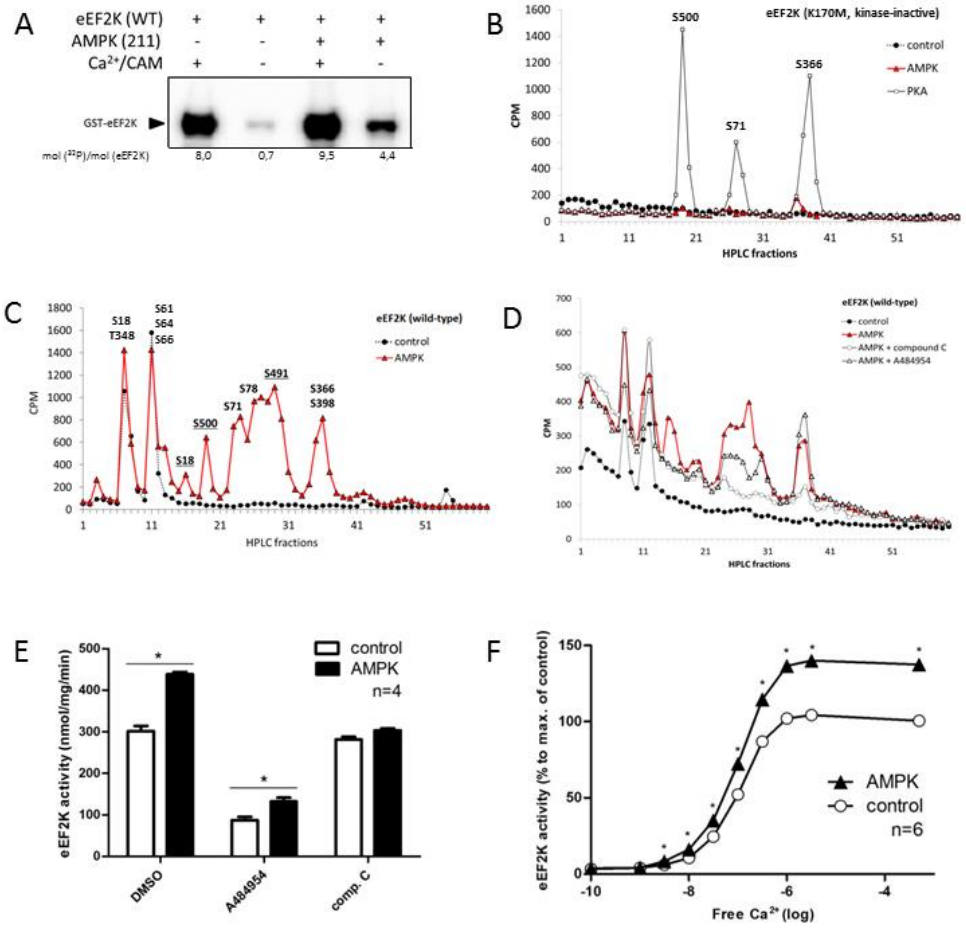
A
eEF2K (WT)
AMPK (211)
Ca2+/CAM
GST-eEF2K
mol (32P)/mol (eEF2K)
8,0
0,7
9,5
4,4
B
eEF2K (K170M, kinase-inactive)
control
AMPK
PKA
S500
S71
S366
CPM
HPLC fractions
C
eEF2K (wild-type)
control
AMPK
S18
T348
S61
S64
S66
S500
S18
S71
S78
S491
S366
S398
CPM
HPLC fractions
D
eEF2K (wild-type)
control
AMPK
AMPK + compound C
AMPK + A484954
CPM
HPLC fractions
E
control
AMPK
n=4
eEF2K activity (nmol/mg/min)
DMSO
A484954
comp. C
F
eEF2K activity (% to max. of control)
AMPK
control
n=6
Free Ca2+ (log)

FIGURE 4

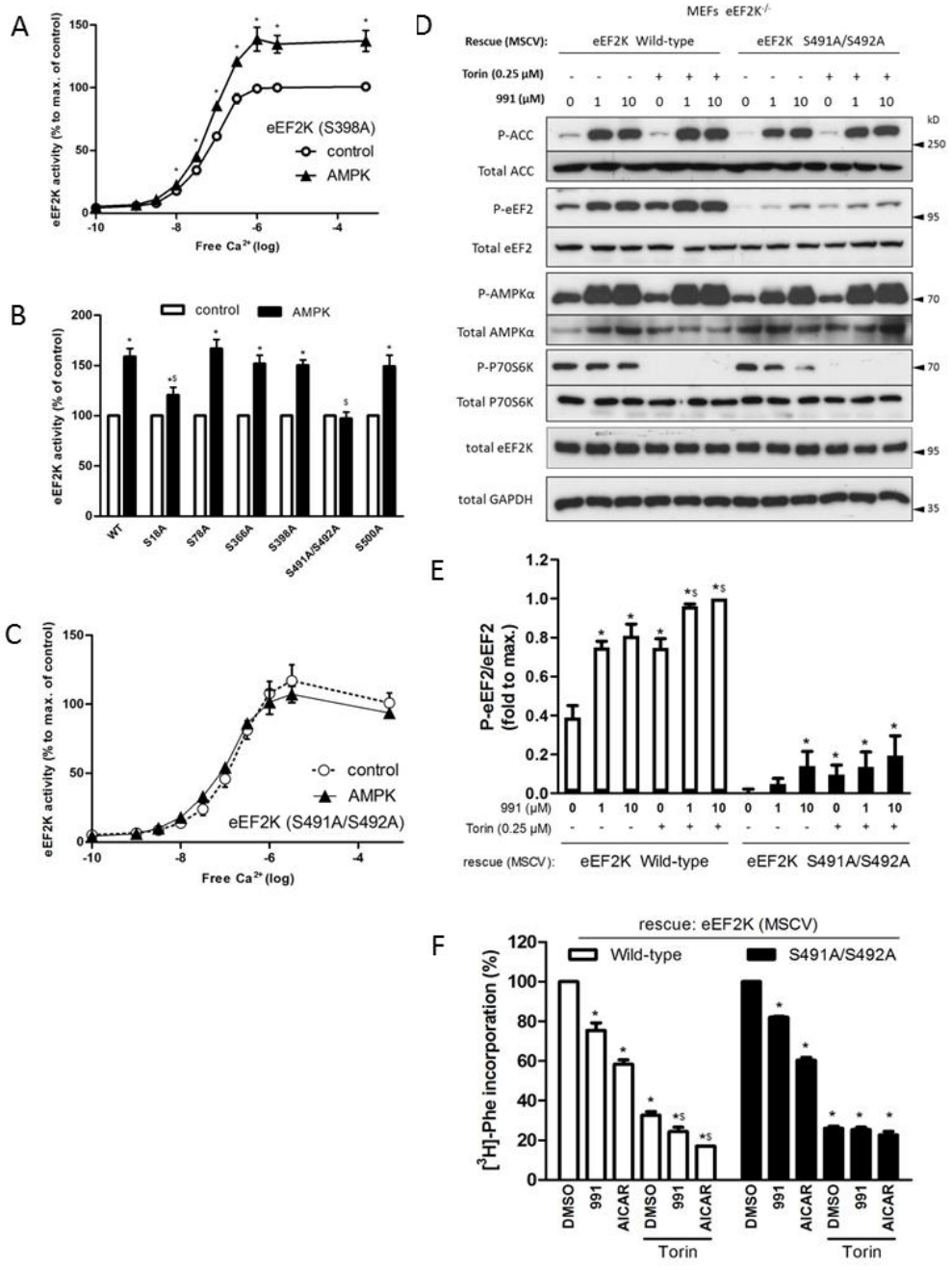
A
eEF2K activity (% to max. of control)
Free Ca2+ (log)
eEF2K (S398A)
control
AMPK
B
control
AMPK
eEF2K activity (% of control)
WT
S16A
S78A
S366A
S398A
S491A/S492A
S500A
C
eEF2K activity (% to max. of control)
Free Ca2+ (log)
control
AMPK
eEF2K (S491A/S492A)
D
MEFs eEF2K-/-
Rescue (MSCV):
eEF2K Wild-type
eEF2K S491A/S492A
Torin (0.25 μM)
991 (μM)
P-ACC
Total ACC
P-eEF2
Total eEF2
P-AMPKα
Total AMPKα
P-P70S6K
Total P70S6K
total eEF2K
total GAPDH
kD
250
95
70
70
95
35
E
P-eEF2/eEF2 (fold to max.)
991 (μM)
Torin (0.25 μM)
rescue (MSCV):
eEF2K Wild-type
eEF2K S491A/S492A
F
rescue: eEF2K (MSCV)
Wild-type
S491A/S492A
[3H]-Phe incorporation (%)
DMSO
991
AICAR
Torin

SUPPLEMENTAL FIGURES

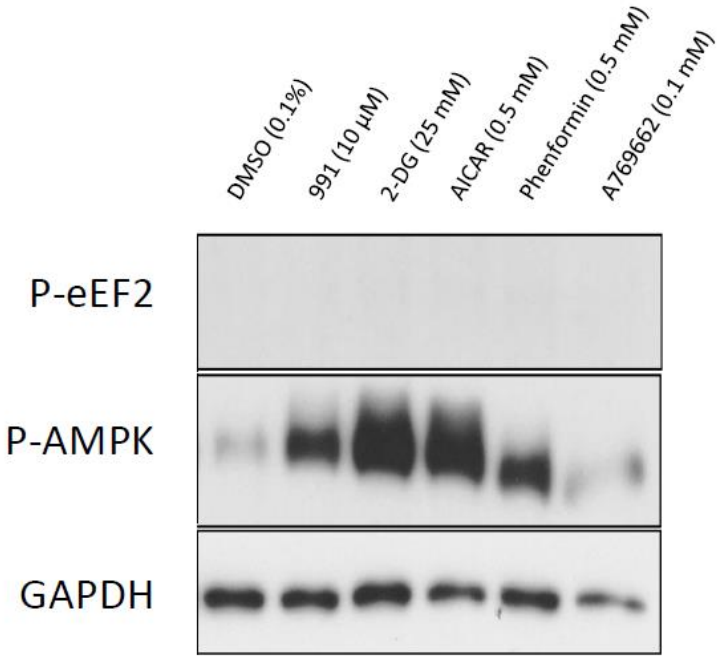

Supplemental Figure S1: eEF2 phosphorylation requires eEF2K. Immortalized MEFs lacking eEF2K ($eEF2K^{-/-}$) were incubated for 1 h with the indicated concentrations of AMPK activators in serum-free medium containing $CaCl_2$. Cells were lysed for immunoblotting with the indicated antibodies and a representative blot is shown.

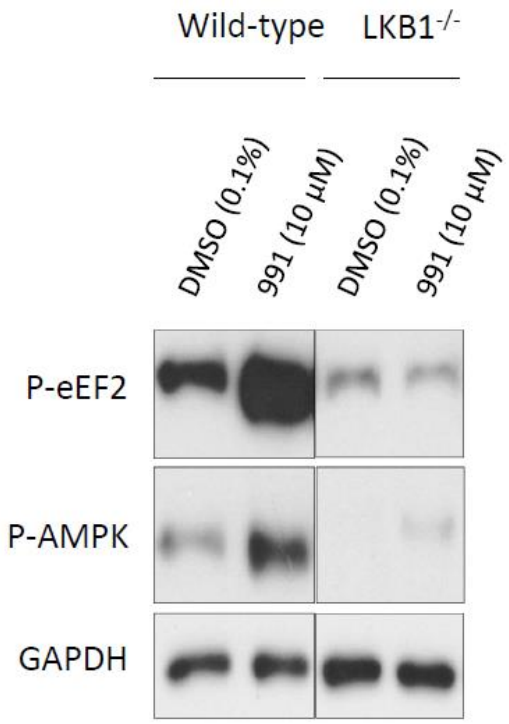

Supplemental Figure S2: AMPK-dependent eEF2 phosphorylation by 991 requires LKB1. Immortalized wild-type MEFs or MEFs lacking LKB1 (LKB1$^{-/-}$) were incubated for 1 h with DMSO (vehicle) or 991 at the indicated concentration in serum-free medium containing $CaCl_2$. Cells were lysed for immunoblotting with the indicated antibodies and representative blots are shown. Data are from the same experiment.

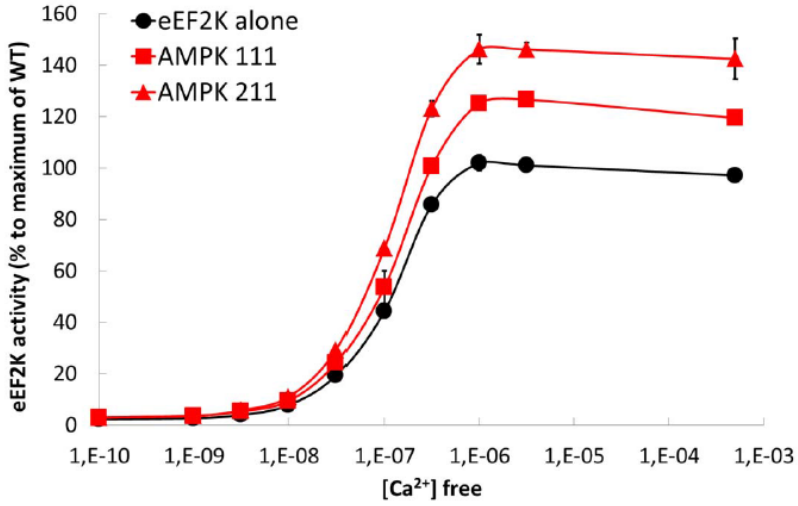

Supplemental Figure S3*:* Phosphorylation-induced eEF2K activation by AMPKα1- versus AMPKα2-containing complexes. Purified recombinant wild-type eEF2K was incubated for 1 h with purified activated AMPKα1β1γ1 (111) or AMPKα2β1γ1 (211) and ATP for eEF2K assay with MHC1 peptide as substrate and with increasing free Ca^{2+} concentrations using a $CaCl_2$-EGTA buffer system. Data are the means ± s.e.m. of at least 3 separate experiments.

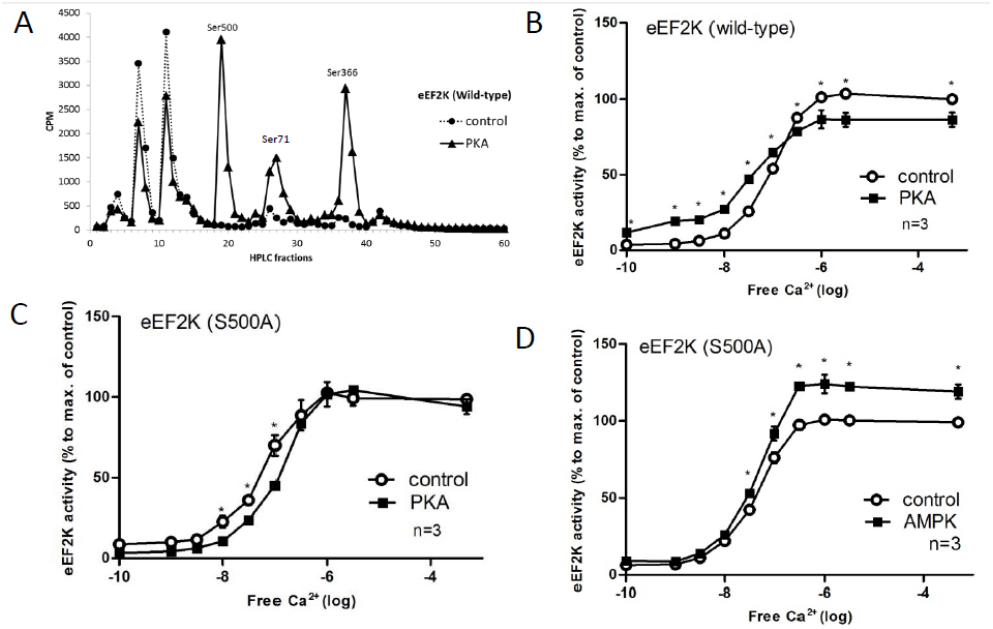

Supplemental Figure S4*: In vitro* phosphorylation of eEF2K by PKA and effects of PKA and AMPK on wild-type and S500A eEF2K activity. In (A) purified recombinant wild-type eEF2K was incubated for 1 h with purified PKA and [γ-^{32}P]ATP for trypsin digestion and phosphopeptide separation by HPLC to establish a labelling profile. Wild-type (B) or S500A (C,D) eEF2K was incubated as above with either purified PKA (B,C) or purified recombinant activated AMPK (D) but with non-radioactive ATP prior to eEF2K assay with MHC1 peptide as substrate and with increasing free Ca^{2+} concentrations using a $CaCl_2$-EGTA buffer system. Data are from one representative experiment (A) or the means ± s.e.m. of at least 3 separate experiments (B-D) and * indicates a significant difference (P<0.05) between the indicated conditions.

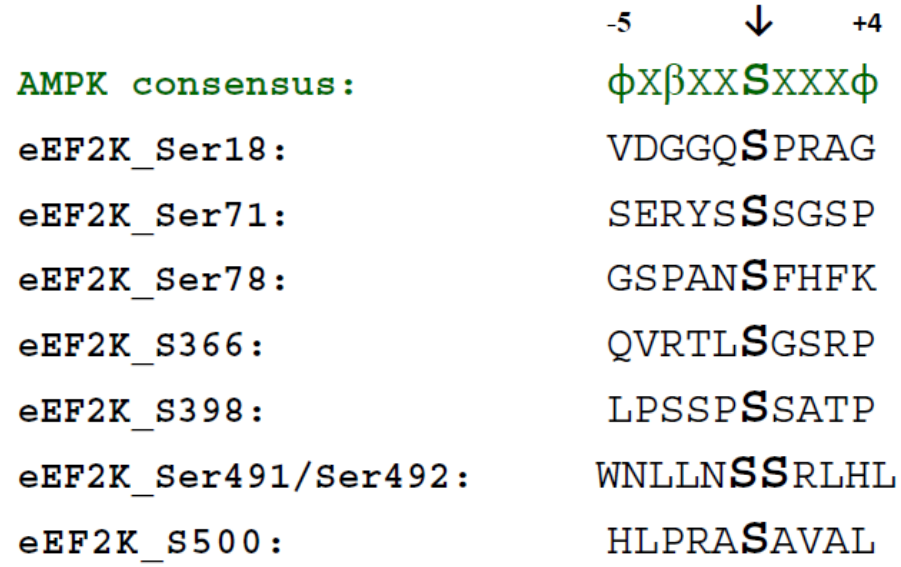

Supplemental Figure S5: Sequence alignment of AMPK phosphorylation sites in human eEF2K compared with the AMPK consensus. The amino acid sequences surrounding the Ser residues phosphorylated by AMPK (bold) were compared with the AMPK consensus target motif represented in green (Φ=hydrophobic residues, preferentially Leu; β=basic residues, preferentially Arg).

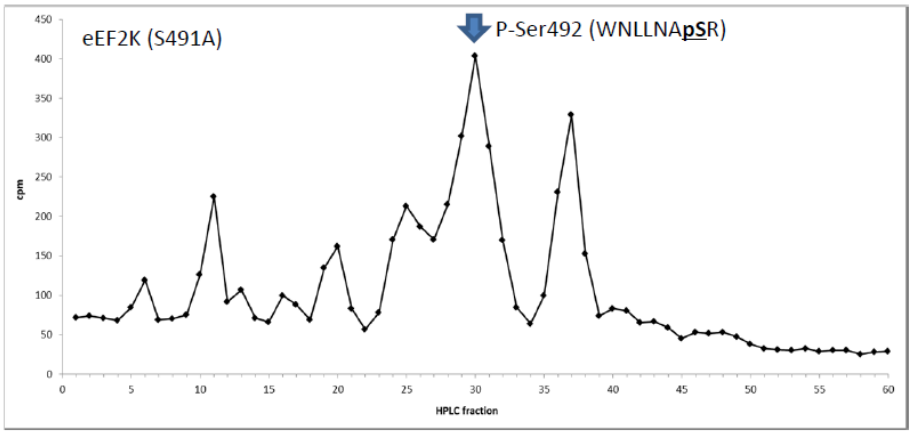

Supplemental Figure S6*: In vitro* phosphorylation of eEF2K S491A mutant by AMPK. Purified recombinant eEF2K S491A mutant was incubated for 1 h with purified activated AMPK and [γ-^{32}P]ATP for trypsin digestion and phosphopeptide separation by HPLC to establish a labelling profile. The arrow indicates the radiolabelled peak in which S492 was identified as being phosphorylated in a phosphopeptide by LC-MS/MS.

Supplemental Figure S7: Alignment of sequences surrounding AMPK sites in eEF2K from vertebrates. eEF2K amino acid sequences (Uniprot database) from the indicated species were aligned using Clustal Omega (EBI). Ser residues identified to be phosphorylated by AMPK (shown by arrows) and residue conservation is indicated (*>:>.>).

GRAPHICAL ABSTRACT

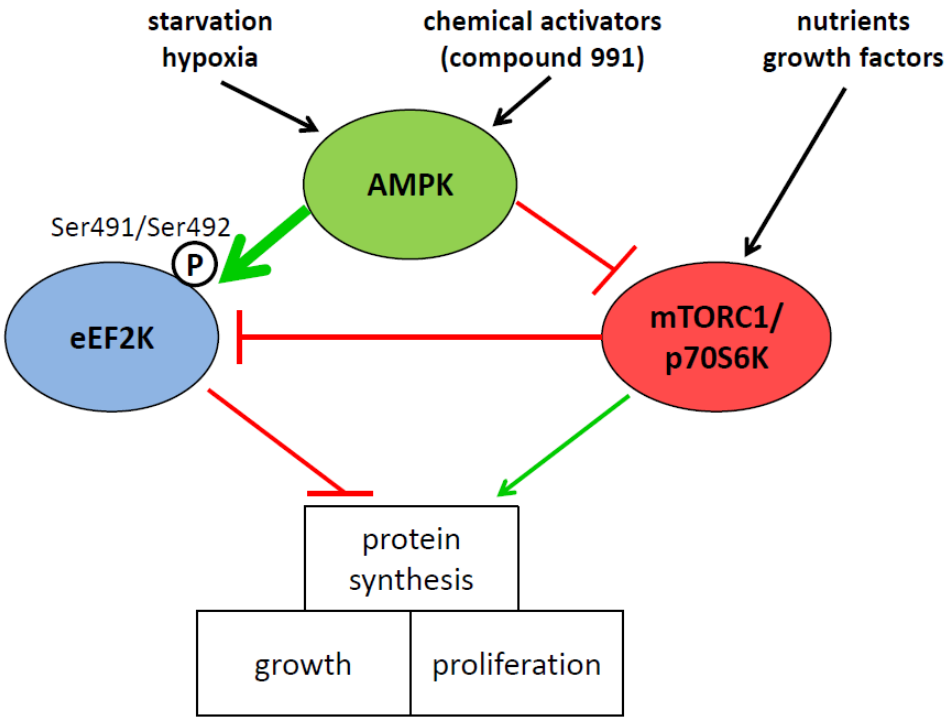

DISCUSSION

AMPK in the control of protein synthesis

It is well accepted that AMPK activation, both physiologically and pharmacologically achieved, leads to the inhibition of protein synthesis. This is due to a dual mechanism involving inhibition of mTORC1 signalling on the one hand and activation of eEF2K on the other hand, thereby decreasing both translational initiation and elongation. This work helped to clarify one piece of the very complex puzzle which is the regulation of eEF2K. We confirmed that the main activator of eEF2K is Ca^{2+}/CaM, probably through autophosphorylation of critical residues needed to obtain an active form of the kinase. Further, eEF2K activity can be fine-tuned via trans-phosphorylation by various kinases. Amongst these, multi-site phosphorylation by AMPK led to an increase in the V_{max} of eEF2K and phosphorylation of S491 was essential for activation both *in vitro* and in intact cells.

Surprisingly, full-body $eEF2K^{-/-}$ mice are perfectly viable and do not present any obvious phenotype regarding growth and morphology[175]. However, fertility and cognitive learning capacities of these mice seem to be impaired (C. Proud, personal communication). Several cell lines lacking eEF2K have been created that also present normal growth and proliferation rates under optimal conditions, such as the MEFs used in our study. However, deletion of eEF2K in cells resulted in much greater sensitivity to a series of cellular stress conditions and activation of eEF2K by AMPK has been shown to be

essential for cell survival under nutrient depletion[177]. Despite the dogma that global protein synthesis is shut down when eEF2 is phosphorylated, the result might rather be a reprogramming towards the specific translation of particular mRNA subsets ("translational rewiring")[176], particularly in the long-term. This would explain how many cancer cell lines are able to conserve high rates of growth and proliferation and thus also, protein synthesis, despite sustained high eEF2 phosphorylation observed even under optimal culture conditions. It is also imaginable that in certain circumstances, a part of the (very abundant) eEF2 pool is "protected" from eEF2K, e.g. by compartmentation or by protein complex formation. An alternative explanation would be the existence of eEF2-independent translation, where ribosomal translocation could be catalyzed by a yet unknown elongation factor or a different eEF2 isoform that would not be subjected to regulation by eEF2K. In any case, further investigation is required for clarification.

eEF2K is overexpressed/upregulated in many cancers[178-180] and genetic downregulation or pharmacological inhibition rendered cells and tumors more susceptible to growth inhibition by nutrient depletion[177] and several anti-cancer treatments[181-186]. eEF2K has thus emerged as a potential target for cancer therapy over the last years. AMPK activation can also have anti-proliferative effects but also has a cytoprotective role on the other hand. Since AMPK activates eEF2K it is tempting to speculate that it increases cellular resistance to avoid apoptosis in part by eEF2K activation and one could imagine combined treatment of AMPK activators with eEF2K inhibitors to be more effective against cancer cells than either of them alone. One mechanism to increase cellular resistance and to avoid apoptosis in

these conditions is to turn on autophagy and eEF2K has been shown to be essential for the onset of autophagy in several cancer cell lines[182,183,186,187]. The fact that eEF2K is implicated in the control of several biological processes beyond translation elongation[173] and recent evidence from a modified form of the kinase accepting bulky ATP-analogs[174], suggest the existence of eEF2K substrates other than eEF2. Further investigation is needed to determine by what mechanisms eEF2K exerts these non-canonical functions and whether this opens new doors to previously unidentified biological effects of AMPK/eEF2K activation.

cAMP phosphodiesterase activation by AMPK

This work provides the important finding that in hepatocytes, pharmacological AMPK activation can antagonize glucagon signalling, by direct phosphorylation and activation of the major liver isoform PDE4B, thereby decreasing cAMP levels and downstream PKA signalling. Interestingly, the three AMPK phosphorylation sites identified in mouse PDE4B (S118, S125, S304) are not only perfectly conserved in vertebrates but are also present in the other isoforms (PDEA/C/D) of the PDE4 family. Given their ubiquitous expression pattern, a similar mechanism might apply for antagonism of cAMP signalling by AMPK in other tissues and induced by other stimuli such as catecholamines. Interestingly, PDE4 family members are highly expressed in the cardiovascular system and have been shown to control heart contractility, hypertrophy and apoptosis of cardiomyocytes as well as contraction, movement, proliferation and stress response of vascular smooth muscle cells[166,188]. It is thus tempting to

imagine that AMPK activation could influence functional parameters in these cells, through a mechanism similar to the one we identified in hepatocytes.

Studying the regulation of biological processes by individual PDE isoforms is extremely complex due to the existence of an incredibly large number of isoforms. Indeed, 11 distinct PDE families (designated by numbers from 1 to 11) have been identified so far, each of which contain up to 4 isoforms coded by different genes (designated by letters from A to D)[167]. The use of different promoters and alternative mRNA splicing exponentially increases the number of distinct PDE enzymes differing in length and with unique N-terminal regulatory sequences. For example, the 4 genes of the PDE4 family encode more than 20 different isoforms (PDE4B1-4 *etc*.). However, the use of selective tools such as family-specific inhibitors or antibodies and genetic tools allowed to show that particular PDE isoforms control specific cellular functions.

AMPK and metformin in the control of hepatic glucose production

Historically, AMPK activation gained major interest in the field of T2D research. Firstly, the fact that AMPK became activated in skeletal muscle upon contraction[189] or exercise[190] and that AMPK activation by AICAR increased skeletal muscle glucose uptake independently of PI3K[111], led to the idea that pharmacological AMPK activation in muscle could be used as a treatment against hyperglycaemia due to insulin resistance. Even though skeletal muscle is the predominant site of insulin-mediated glucose uptake in the postprandial state[65], it became clear that modulating muscle glucose

uptake alone might not be sufficient to control glycaemia during starvation, which is mainly controlled by hepatic glucose production[50]. Of note, recent evidence suggests that even suppression of GNG in liver is compensated by upregulation of GNG in the renal cortex mainly from glutamine (driven by glucagon, glucocorticoids and acidosis)[191] that normally occurs in substantial amounts during long-term starvation, thus hepatic glucose production is not the only contributor of plasma glucose levels in the starved state. Secondly, it was shown that the most prescribed anti-diabetic drug, metformin, activates AMPK and that its anti-hyperglycaemic effects are mainly due to decreased hepatic GNG[192], an effect that is abolished when LKB1 is deleted in liver[122]. However, later reports using genetically deleted mouse models pointed out that some of these effects might be independent of AMPK, at least in the long-term (> 24 hours), through downregulation of GNG gene expression[125]. Genetic deletion models have shown that metformin action in the long-term is mainly independent of AMPK[125]. However, there might well be short-term effects of metformin that are mediated by AMPK, as our study[126] (see Results section) and others[130,192,193] suggests. It is important to point out that metformin concentrations used in such studies might be a major determinant for its mechanism of action and could lead to misinterpretation of results[194]. It was shown that plasma concentrations of metformin after oral administration of a therapeutic dose are highest but below 100 µM in the portal vein of mice and peaks at less than 50 µM in blood samples from patients[195]. Clearly, all beneficial effects of metformin cannot be attributed to AMPK activation by the drug. Nevertheless, our study revealed that in the short-term (<1 hour), pharmacological AMPK activation specifically

antagonizes hepatic glucagon signalling, by activating a phosphodiesterase and thereby decreasing cAMP levels and subsequent PKA activation. The main function of glucagon in liver is to increase glucose production (both through glycogenolysis and GNG). Interestingly, metformin has blood-glucose lowering effects only on diabetic individuals[48] whose plasma glucagon levels are elevated. One could thus speculate that the main action mechanism of the drug is to antagonize excessive glucagon signalling via AMPK.

In the follow-up of our study, we found that treatment of hepatocytes with the AMPK activator 991 reduced both glucagon induced and basal glucose production. This suggests an additional, glucagon-independent mechanism for suppression of GNG by 991 and the implication of AMPK in this effect remains to be confirmed. Even though the final proof and underlying mechanisms are still to be established, there are strong indications in the literature that AMPK indeed controls hepatic GNG. On the one hand, mice deleted for AMPKα2[94] (or both AMPKα1/2[162]) in liver showed elevated hepatic glucose production and are hyperglycaemic. On the other hand, adenoviral tail-vein injection (targeting mainly the liver) of constitutively active AMPK markedly decreased hepatic glucose output, resulting in mild hypoglycaemia[196], while dominant-negative AMPK ablated the effect of metformin to decrease hepatic GNG[193]. Also, effects of metformin were shown to be AMPK-dependent when AMPK expression in hepatocytes was transiently knocked down by adenoviral shRNA transfer[195]. Of note, AMPK-related kinases such as SIK also appear to be implicated in the control of hepatic GNG (see references below). This is supported by the fact that liver-specific deletion of their common activating upstream kinase,

LKB1, resulted in mice with much more severe hyperglycaemia[122] than the one of mice lacking only AMPKα1 or both AMPKα1/2 in liver. Several features make SIK kinases, particularly SIK1, good candidates for (AMPK-independent) regulation of hepatic GNG. As such, they downregulate cAMP signalling both through direct activation of phosphodiesterases (e.g. PDE4D)[197] and inhibition of the GNG gene transcriptional coactivator CRTC2[198], under the effect of insulin/PKB or as part of a negative feedback loop of cAMP/PKA signalling. In addition, the SIK inhibitor HG-9-91-01 promotes hepatic glucose production[199] and metformin might favour SIK activation by LKB1[200]. Hence, there seems to be some redundancy in the physiological functions of AMPK and related kinases. This should not be neglected when interpreting results obtained with long-term and complete gene knockout models, where compensatory changes might also occur. Studies with pharmacological AMPK activators have the disadvantage of potential off-target effects, perhaps on AMPK-related kinases. Redundancy in activation and effects among members of this kinase family could lead to misinterpretation of effects that seem to persist in AMPK knockout models, namely the conclusion that the deleted kinase is not implicated in the control of the physiological process studied (*e.g.* GNG). This is one of the reasons why future studies should not only use tissue-specific but also inducible (short-term) gene deletion models.

Pharmacological AMPK activation: drawbacks and perspectives

Over the last years, it has become clear that AMPK cannot be considered as a single kinase but rather a family of (at least) 12 kinases, all of which seem to display distinct tissue expression profiles, probably subcellular localizations and perhaps substrate specificities. This and the fact that AMPK activation in certain situations might not be beneficial[201], underlines the requirement for isoform-selective activators (and/or inhibitors) both for the study of AMPK function in research but also for their potential use as therapeutic agents with limited side-effects. This raises the question of how to activate AMPK optimally, by what type of direct activator and what subunit to target best? With regard to isoform-specific functions, it remains to be seen which heterotrimers target certain substrates and through what mechanism. The most widely used AMPK activator in the past was AICAR which is transformed into the AMP mimetic ZMP. AMP mimetics target the AMPKγ subunit to activate AMPK in a way more similar to physiological conditions but potentially have more off-target effects. However, the fact that AMPKγ subunits seem to react differently to changes in cellular AMP levels[84] might offer the possibility of selective activation by this type of activators. The most promising class of activators are perhaps new-generation compounds targeting the ADAM pocket between the α and β subunits. Some of these (namely A-769662[202]) display preferences for one AMPKβ isoform over the other. There is evidence for differences in AMPKα1/2 sensitivity to Thr172 dephosphorylation by PP2C[203] and most activators protect AMPK against dephosphorylation. However, no direct activator specifically binding to only one of the AMPKα isoforms (via the ADAM pocket) has yet been identified, which would be

extremely useful for selective AMPK activation *in vivo*. So far, only the AMP mimetic C2 selectively activated AMPKα1-containing complexes[153]. With this in mind, it is debatable whether it would be best to target "specialized" AMPKα2 rather than "housekeeping" AMPKα1. For example, the major skeletal muscle isoform activated by contraction was shown to be AMPKα2β2γ3[204] whereas in liver, our data and those of others suggest a predominant role for AMPKα2β1γ1/2 heterotrimers[94,126,158] and in adipose tissue and heart muscle, AMPKα1 or AMPKα2 containing complexes are almost exclusively expressed, respectively. Another challenge for the therapeutic use of AMPK activators is the duration of treatment. Although AMPK activators can be found for online purchase as "all beneficial life expanding drugs", it has been shown that chronic AMPK activation (both genetically-based[205] or AICAR-induced[206]) leads to increased glycogen content in heart and skeletal muscle, which ultimately can have deleterious effects on contractile function due to hypertrophy caused by excessive glycogen storage. In hepatocytes, prolonged AMPK activation by treatment with AICAR or by adenoviral transfection of a constitutively active form of the kinase caused apoptosis[207]. Thus, it is probably wiser to target AMPK only for a limited period when using non-selective activators acting in a broad range of tissues. However, this might be dependent on the degree of activation, since unwanted side-effect do not seem to occur upon mild AMPK activation by long-term treatment with metformin. Interestingly, long-term metformin treatment was shown to decrease cancer incidence, but the role of AMPK in this effect (as in cancer in general) remains controversial[208,209]. Also, when targeting AMPK in the liver for the treatment of non-diabetic (non-hyperglycaemic) patients, it

should be considered that hypoglycaemia during starvation could possibly occur due to decreased hepatic glucose output. In any case, tissue-specific or isoform-selective AMPK activation will have to be the future strategy to avoid negative side-effects. However, as mentioned in the Introduction, the first step required for tissue-specific AMPK activation should be to establish a full-body protein expression profile of AMPK subunits in humans and rodents.

BIBLIOGRAPHY

[1] R Sender, *et al*. Revised Estimates for the Number of Human and Bacteria Cells in the Body. *PLoS Biol* 14(8):e1002533 (2016).

[2] R Curi, *et al*. Regulatory principles in metabolism-then and now. *Biochem J* 473(13):1845-1857 (2016).

[3] HV Westerhoff, *et al*. Modern theories of metabolic control and their applications (review). *Biosci Rep* 4(1):1-22 (1984).

[4] HA Krebs & T Yoshida. RENAL GLUCONEOGENESIS. 2. THE GLUCONEOGENIC CAPACITY OF THE KIDNEY CORTEX OF VARIOUS SPECIES. *Biochem J* 89:398-400 (1963).

[5] VN Popov, *et al*. Comparative Analysis of Glyoxylate Cycle Key Enzyme Isocitrate Lyase from Organisms of Different Systematic Groups. *J Evol Biochem Physiol* 41(6):631-639 (2005).

[6] RC Nordlie & HA Lardy. Mammalian liver phosphoneolpyruvate carboxykinase activities. *J Biol Chem* 238:2259-2263 (1963).

[7] AK Groen, *et al*. Control of gluconeogenesis in rat liver cells. Flux control coefficients of the enzymes in the gluconeogenic pathway in the absence and presence of glucagon. *Biochem J* 237(2):379-389 (1986).

[8] HG Hers & L Hue. Gluconeogenesis and related aspects of glycolysis. *Annu Rev Biochem* 52:617-653 (1983).

[9] SJ Pilkis, *et al*. Hormonal regulation of hepatic gluconeogenesis and glycolysis. *Annu Rev Biochem* 57:755-783 (1988).

[10] L Hue, *Regulation of Gluconeogenesis in Liver*, in *Comprehensive Physiology*. 2010, John Wiley & Sons, Inc.

[11] ML Massa, *et al*. Liver glucokinase: An overview on the regulatory mechanisms of its activity. *IUBMB Life* 63(1):1-6 (2011).

[12] E van Schaftingen. A protein from rat liver confers to glucokinase the property of being antagonistically regulated by fructose 6-phosphate and fructose 1-phosphate. *Eur J Biochem* 179(1):179-184 (1989).

[13] E Van Schaftingen & HG Hers. Phosphofructokinase 2: the enzyme that forms fructose 2,6-bisphosphate from fructose 6-phosphate and ATP. *Biochem Biophys Res Commun* 101(3):1078-1084 (1981).

[14] IJ Kurland, *et al*. Rat liver 6-phosphofructo-2-kinase/fructose-2,6-bisphosphatase. Properties of phospho- and dephospho- forms and of two mutants in which Ser32 has been changed by site-directed mutagenesis. *J Biol Chem* 267(7):4416-4423 (1992).

[15] E Van Schaftingen, *et al*. Inactivation of phosphofructokinase 2 by cyclic AMP - dependent protein kinase. *Biochem Biophys Res Commun* 103(1):362-368 (1981).

[16] E Van Schaftingen, *et al*. Fructose 2,6-bisphosphate, the probably structure of the glucose- and glucagon-sensitive stimulator of phosphofructokinase. *Biochem J* 192(3):897-901 (1980).

[17] E Van Schaftingen & HG Hers. Inhibition of fructose-1,6-bisphosphatase by fructose 2,6-biphosphate. *Proc Natl Acad Sci U S A* 78(5):2861-2863 (1981).
[18] SJ Pilkis, *et al*. Regulation by glucagon of hepatic pyruvate kinase, 6-phosphofructo 1-kinase, and fructose-1,6-bisphosphatase. *Fed Proc* 41(10):2623-2628 (1982).
[19] JE Feliu, *et al*. Hormonal control of pyruvate kinase activity and of gluconeogenesis in isolated hepatocytes. *Proc Natl Acad Sci U S A* 73(8):2762-2766 (1976).
[20] L Engstrom. The regulation of liver pyruvate kinase by phosphorylation--dephosphorylation. *Curr Top Cell Regul* 13:28-51 (1978).
[21] Diabetes.co.uk © 2017 Diabetes Digital Media Ltd - the global diabetes community. Retrieved 15.02.2017 from: http://www.diabetes.co.uk/.
[22] S Melmed, *et al*, *Williams Textbook of Endocrinology E-Book*. 2011: Elsevier Health Sciences.
[23] B Desbuquois, *et al*. [Regulation of insulin receptor expression and its gene]. *Ann Endocrinol (Paris)* 54(6):373-384 (1993).
[24] J Terrettaz, *et al*. Inhibition of hepatic glucose production by insulin in vivo in rats: contribution of glycolysis. *Am J Physiol* 250(4 Pt 1):E346-351 (1986).
[25] EG Loten, *et al*. Stimulation of a low Km phosphodiesterase from liver by insulin and glucagon. *J Biol Chem* 253(3):746-757 (1978).
[26] T Hermsdorf, *et al*. Effects of dexamethosone and glucagon after long-term exposure on cyclic AMP phosphodiesterase 4 in cultured rat hepatocytes. *Cell Signal* 11(9):685-690 (1999).
[27] T Kitamura, *et al*. Insulin-induced phosphorylation and activation of cyclic nucleotide phosphodiesterase 3B by the serine-threonine kinase Akt. *Mol Cell Biol* 19(9):6286-6296 (1999).
[28] ME Krahl. Insulin and protein synthesis in isolated tissues. *Diabetes* 11:144-146 (1962).
[29] RE Hulse, *et al*. Structure, function, and regulation of insulin-degrading enzyme. *Vitam Horm* 80:635-648 (2009).
[30] H Yoo-Warren, *et al*. Regulation of rat glucagon receptor expression. *Biochem Biophys Res Commun* 205(1):347-353 (1994).
[31] L Hue, *et al*. Control of gluconeogenesis and of enzymes of glycogen metabolism in isolated rat hepatocytes. A parallel study of the effect of phenylephrine and of glucagon. *Biochem J* 176(3):791-797 (1978).
[32] P De Meyts, *The Insulin Receptor and Its Signal Transduction Network*, in *Endotext*, L.J. De Groot, et al., Editors. 2000, MDText.com, Inc.: South Dartmouth (MA).
[33] RW Mackenzie & BT Elliott. Akt/PKB activation and insulin signaling: a novel insulin signaling pathway in the treatment of type 2 diabetes. *Diabetes Metab Syndr Obes* 7:55-64 (2014).
[34] SW Cushman & LJ Wardzala. Potential mechanism of insulin action on glucose transport in the isolated rat adipose cell. Apparent translocation of intracellular transport systems to the plasma membrane. *J Biol Chem* 255(10):4758-4762 (1980).
[35] H Sano, *et al*. Insulin-stimulated phosphorylation of a Rab GTPase-activating protein regulates GLUT4 translocation. *J Biol Chem* 278(17):14599-14602 (2003).

[36] DA Cross, *et al*. Inhibition of glycogen synthase kinase-3 by insulin mediated by protein kinase B. *Nature* 378(6559):785-789 (1995).
[37] G Tzivion, *et al*. FoxO transcription factors; Regulation by AKT and 14-3-3 proteins. *Biochim Biophys Acta* 1813(11):1938-1945 (2011).
[38] X Li, *et al*. Akt/PKB regulates hepatic metabolism by directly inhibiting PGC-1alpha transcription coactivator. *Nature* 447(7147):1012-1016 (2007).
[39] JS Hayes & SE Mayer. Regulation of guinea pig heart phosphorylase kinase by cAMP, protein kinase, and calcium. *Am J Physiol* 240(3):E340-349 (1981).
[40] CG Proud, *et al*. Amino acid sequences at the two sites on glycogen synthetase phosphorylated by cyclic AMP-dependent protein kinase and their dephosphorylation by protein phosphatase-III. *FEBS Lett* 80(2):435-442 (1977).
[41] PG Quinn. Inhibition by insulin of protein kinase A-induced transcription of the phosphoenolpyruvate carboxykinase gene. Mediation by the activation domain of cAMP response element-binding protein (CREB) and factors bound to the TATA box. *J Biol Chem* 269(20):14375-14378 (1994).
[42] MW Anthonsen, *et al*. Identification of novel phosphorylation sites in hormone-sensitive lipase that are phosphorylated in response to isoproterenol and govern activation properties in vitro. *J Biol Chem* 273(1):215-221 (1998).
[43] World Health Organization (WHO). Retrieved 15.02.2017 from: http://www.who.int/diabetes/en/.
[44] C Herder & M Roden. Genetics of type 2 diabetes: pathophysiologic and clinical relevance. *Eur J Clin Invest* 41(6):679-692 (2011).
[45] Healthline Media© 2005 - 2017. Retrieved 15.02.2017 from: http://www.healthline.com/health/type-2-diabetes.
[46] RS Hundal, *et al*. Mechanism by which metformin reduces glucose production in type 2 diabetes. *Diabetes* 49(12):2063-2069 (2000).
[47] N Wollen & CJ Bailey. Inhibition of hepatic gluconeogenesis by metformin. Synergism with insulin. *Biochem Pharmacol* 37(22):4353-4358 (1988).
[48] K Cusi, *et al*. Metabolic effects of metformin on glucose and lactate metabolism in noninsulin-dependent diabetes mellitus. *J Clin Endocrinol Metab* 81(11):4059-4067 (1996).
[49] FP Alford, *et al*. Glucagon levels in normal and diabetic subjects: use of a specific immunoabsorbent for glucagon radioimmunoassay. *Diabetologia* 13(1):1-6 (1977).
[50] PJ Campbell, *et al*. Quantification of the relative impairment in actions of insulin on hepatic glucose production and peripheral glucose uptake in non-insulin-dependent diabetes mellitus. *Metabolism* 37(1):15-21 (1988).
[51] MK Cavaghan, *et al*. Interactions between insulin resistance and insulin secretion in the development of glucose intolerance. *J Clin Invest* 106(3):329-333 (2000).
[52] J Boucher, *et al*. Insulin receptor signaling in normal and insulin-resistant states. *Cold Spring Harb Perspect Biol* 6(1) (2014).
[53] G Sabio, *et al*. A stress signaling pathway in adipose tissue regulates hepatic insulin resistance. *Science* 322(5907):1539-1543 (2008).
[54] G Sabio, *et al*. Role of muscle c-Jun NH2-terminal kinase 1 in obesity-induced insulin resistance. *Mol Cell Biol* 30(1):106-115 (2010).

[55] V Aguirre, *et al*. The c-Jun NH(2)-terminal kinase promotes insulin resistance during association with insulin receptor substrate-1 and phosphorylation of Ser(307). *J Biol Chem* 275(12):9047-9054 (2000).
[56] G Solinas & B Becattini. JNK at the crossroad of obesity, insulin resistance, and cell stress response. *Mol Metab* 6(2):174-184 (2017).
[57] DM Tsukumo, *et al*. Loss-of-function mutation in Toll-like receptor 4 prevents diet-induced obesity and insulin resistance. *Diabetes* 56(8):1986-1998 (2007).
[58] S Ikemoto, *et al*. Expression of an insulin-responsive glucose transporter (GLUT4) minigene in transgenic mice: effect of exercise and role in glucose homeostasis. *Proc Natl Acad Sci U S A* 92(3):865-869 (1995).
[59] PS MacLean, *et al*. Exercise-induced transcription of the muscle glucose transporter (GLUT 4) gene. *Biochem Biophys Res Commun* 292(2):409-414 (2002).
[60] KL Hoehn, *et al*. Insulin resistance is a cellular antioxidant defense mechanism. *Proc Natl Acad Sci U S A* 106(42):17787-17792 (2009).
[61] R Cui, *et al*. Overexpression of superoxide dismutase 3 gene blocks high-fat diet-induced obesity, fatty liver and insulin resistance. *Gene Ther* 21(9):840-848 (2014).
[62] KM Pires, *et al*. Treatment with a SOD mimetic reduces visceral adiposity, adipocyte death and adipose tissue inflammation in high fat fed mice. *Obesity (Silver Spring)* 22(1):178-187 (2014).
[63] R Ragheb, *et al*. Free fatty acid-induced muscle insulin resistance and glucose uptake dysfunction: evidence for PKC activation and oxidative stress-activated signaling pathways. *Biochem Biophys Res Commun* 389(2):211-216 (2009).
[64] SB Haugaard, *et al*. Dietary intervention increases n-3 long-chain polyunsaturated fatty acids in skeletal muscle membrane phospholipids of obese subjects. Implications for insulin sensitivity. *Clin Endocrinol (Oxf)* 64(2):169-178 (2006).
[65] RA DeFronzo & D Tripathy. Skeletal Muscle Insulin Resistance Is the Primary Defect in Type 2 Diabetes. *Diabetes Care* 32(Suppl 2):S157-163 (2009).
[66] EU Alejandro, *et al*. Natural history of beta-cell adaptation and failure in type 2 diabetes. *Mol Aspects Med* 42:19-41 (2015).
[67] HH Ponssen, *et al*. Combined metformin and insulin therapy for patients with type 2 diabetes mellitus. *Clin Ther* 22(6):709-718 (2000).
[68] H Taegtmeyer, *et al*. Insulin resistance protects the heart from fuel overload in dysregulated metabolic states. *Am J Physiol Heart Circ Physiol* 305(12):H1693-1697 (2013).
[69] DG Hardie. AMP-activated protein kinase: an energy sensor that regulates all aspects of cell function. *Genes Dev* 25(18):1895-1908 (2011).
[70] PP Dzeja, *et al*. Adenylate kinase: kinetic behavior in intact cells indicates it is integral to multiple cellular processes. *Mol Cell Biochem* 184(1-2):169-182 (1998).
[71] B Xiao, *et al*. Structural basis for AMP binding to mammalian AMP-activated protein kinase. *Nature* 449(7161):496-500 (2007).
[72] DG Hardie, *et al*. AMP-activated protein kinase: an ultrasensitive system for monitoring cellular energy charge. *Biochem J* 338 (Pt 3):717-722 (1999).

[73] R Bergeron, *et al*. Chronic activation of AMP kinase results in NRF-1 activation and mitochondrial biogenesis. *Am J Physiol Endocrinol Metab* 281(6):E1340-1346 (2001).
[74] GR Steinberg & BE Kemp. AMPK in Health and Disease. *Physiol Rev* 89(3):1025-1078 (2009).
[75] D Carling, *et al*. Purification and characterization of the AMP-activated protein kinase. Copurification of acetyl-CoA carboxylase kinase and 3-hydroxy-3-methylglutaryl-CoA reductase kinase activities. *Eur J Biochem* 186(1-2):129-136 (1989).
[76] DE Atkinson. The energy charge of the adenylate pool as a regulatory parameter. Interaction with feedback modifiers. *Biochemistry* 7(11):4030-4034 (1968).
[77] NJ Bright, *et al*. The regulation and function of mammalian AMPK-related kinases. *Acta Physiol (Oxf)* 196(1):15-26 (2009).
[78] T Monteverde, *et al*. Evidence of cancer-promoting roles for AMPK and related kinases. *FEBS J* 282(24):4658-4671 (2015).
[79] SM Warden, *et al*. Post-translational modifications of the beta-1 subunit of AMP-activated protein kinase affect enzyme activity and cellular localization. *Biochem J* 354(Pt 2):275-283 (2001).
[80] SL McGee, *et al*. Exercise increases nuclear AMPK alpha2 in human skeletal muscle. *Diabetes* 52(4):926-928 (2003).
[81] FA Ross, *et al*. AMP-activated protein kinase: a cellular energy sensor that comes in 12 flavours. *Febs j* 283(16):2987-3001 (2016).
[82] SA Hawley, *et al*. Characterization of the AMP-activated protein kinase kinase from rat liver and identification of threonine 172 as the major site at which it phosphorylates AMP-activated protein kinase. *J Biol Chem* 271(44):27879-27887 (1996).
[83] L Zhu, *et al*. Structural insights into the architecture and allostery of full-length AMP-activated protein kinase. *Structure* 19(4):515-522 (2011).
[84] FA Ross, *et al*. Differential regulation by AMP and ADP of AMPK complexes containing different gamma subunit isoforms. *Biochem J* 473(2):189-199 (2016).
[85] KI Mitchelhill, *et al*. Posttranslational modifications of the 5'-AMP-activated protein kinase beta1 subunit. *J Biol Chem* 272(39):24475-24479 (1997).
[86] N Ali, *et al*. beta-subunit myristoylation functions as an energy sensor by modulating the dynamics of AMP-activated Protein Kinase. *Sci Rep* 6:39417 (2016).
[87] JS Oakhill, *et al*. beta-Subunit myristoylation is the gatekeeper for initiating metabolic stress sensing by AMP-activated protein kinase (AMPK). *Proc Natl Acad Sci U S A* 107(45):19237-19241 (2010).
[88] ER Hudson, *et al*. A novel domain in AMP-activated protein kinase causes glycogen storage bodies similar to those seen in hereditary cardiac arrhythmias. *Curr Biol* 13(10):861-866 (2003).
[89] A McBride, *et al*. The glycogen-binding domain on the AMPK beta subunit allows the kinase to act as a glycogen sensor. *Cell Metab* 9(1):23-34 (2009).
[90] M Bendayan, *et al*. Association of AMP-activated Protein Kinase Subunits With Glycogen Particles as Revealed In Situ by Immunoelectron Microscopy. *J Histochem Cytochem* 57(10):963-971 (2009).

[91] JF Wojtaszewski, *et al*. Glycogen-dependent effects of 5-aminoimidazole-4-carboxamide (AICA)-riboside on AMP-activated protein kinase and glycogen synthase activities in rat skeletal muscle. *Diabetes* 51(2):284-292 (2002).
[92] A Woods, *et al*. The alpha1 and alpha2 isoforms of the AMP-activated protein kinase have similar activities in rat liver but exhibit differences in substrate specificity in vitro. *FEBS Lett* 397(2-3):347-351 (1996).
[93] SB Jorgensen, *et al*. Knockout of the alpha2 but not alpha1 5'-AMP-activated protein kinase isoform abolishes 5-aminoimidazole-4-carboxamide-1-beta-4-ribofuranosidebut not contraction-induced glucose uptake in skeletal muscle. *J Biol Chem* 279(2):1070-1079 (2004).
[94] F Andreelli, *et al*. Liver adenosine monophosphate-activated kinase-alpha2 catalytic subunit is a key target for the control of hepatic glucose production by adiponectin and leptin but not insulin. *Endocrinology* 147(5):2432-2441 (2006).
[95] DG Hardie. AMPK: positive and negative regulation, and its role in whole-body energy homeostasis. *Curr Opin Cell Biol* 33:1-7 (2015).
[96] S Ducommun, *et al*. Motif affinity and mass spectrometry proteomic approach for the discovery of cellular AMPK targets: Identification of mitochondrial fission factor as a new AMPK substrate. *Cell Signal* 27(5):978-988 (2015).
[97] DG Hardie, *et al*. AMPK: An Energy-Sensing Pathway with Multiple Inputs and Outputs. *Trends Cell Biol* 26(3):190-201 (2016).
[98] SA Hawley, *et al*. Complexes between the LKB1 tumor suppressor, STRAD alpha/beta and MO25 alpha/beta are upstream kinases in the AMP-activated protein kinase cascade. *J Biol* 2(4):28 (2003).
[99] SA Hawley, *et al*. Calmodulin-dependent protein kinase kinase-beta is an alternative upstream kinase for AMP-activated protein kinase. *Cell Metab* 2(1):9-19 (2005).
[100] HJ Koh, *et al*. Skeletal muscle-selective knockout of LKB1 increases insulin sensitivity, improves glucose homeostasis, and decreases TRB3. *Mol Cell Biol* 26(22):8217-8227 (2006).
[101] K Sakamoto, *et al*. Deficiency of LKB1 in heart prevents ischemia-mediated activation of AMPKalpha2 but not AMPKalpha1. *Am J Physiol Endocrinol Metab* 290(5):E780-788 (2006).
[102] M Xie, *et al*. A pivotal role for endogenous TGF-beta-activated kinase-1 in the LKB1/AMP-activated protein kinase energy-sensor pathway. *Proc Natl Acad Sci U S A* 103(46):17378-17383 (2006).
[103] RJ Valentine, *et al*. Insulin inhibits AMPK activity and phosphorylates AMPK Ser(4)(8)(5)/(4)(9)(1) through Akt in hepatocytes, myotubes and incubated rat skeletal muscle. *Arch Biochem Biophys* 562:62-69 (2014).
[104] HR Heathcote, *et al*. Protein kinase C phosphorylates AMP-activated protein kinase α1 Ser487. *Biochem J* 473(24):4681-4697 (2016).
[105] KA Coughlan, *et al*. PKD1 Inhibits AMPKalpha2 through Phosphorylation of Serine 491 and Impairs Insulin Signaling in Skeletal Muscle Cells. *J Biol Chem* 291(11):5664-5675 (2016).
[106] L He, *et al*. Activation of the cAMP-PKA pathway Antagonizes Metformin Suppression of Hepatic Glucose Production. *J Biol Chem* 291(20):10562-10570 (2016).

[107] D Carling, *et al*. AMP-activated protein kinase: new regulation, new roles? *Biochem J* 445(1):11-27 (2012).
[108] KM Geraghty, *et al*. Regulation of multisite phosphorylation and 14-3-3 binding of AS160 in response to IGF-1, EGF, PMA and AICAR. *Biochem J* 407(2):231-241 (2007).
[109] S Chen, *et al*. Complementary regulation of TBC1D1 and AS160 by growth factors, insulin and AMPK activators. *Biochem J* 409(2):449-459 (2008).
[110] Y Liu, *et al*. Phosphatidylinositol 3-phosphate 5-kinase (PIKfyve) is an AMPK target participating in contraction-stimulated glucose uptake in skeletal muscle. *Biochem J* 455(2):195-206 (2013).
[111] GF Merrill, *et al*. AICA riboside increases AMP-activated protein kinase, fatty acid oxidation, and glucose uptake in rat muscle. *Am J Physiol* 273(6 Pt 1):E1107-1112 (1997).
[112] SN Jakobsen, *et al*. 5'-AMP-activated protein kinase phosphorylates IRS-1 on Ser-789 in mouse C2C12 myotubes in response to 5-aminoimidazole-4-carboxamide riboside. *J Biol Chem* 276(50):46912-46916 (2001).
[113] GS Hotamisligil. Inflammation and metabolic disorders. *Nature* 444(7121):860-867 (2006).
[114] A Ginion, *et al*. Inhibition of the mTOR/p70S6K pathway is not involved in the insulin-sensitizing effect of AMPK on cardiac glucose uptake. *Am J Physiol Heart Circ Physiol* 301(2):H469-477 (2011).
[115] D Zheng, *et al*. Regulation of muscle GLUT-4 transcription by AMP-activated protein kinase. *J Appl Physiol (1985)* 91(3):1073-1083 (2001).
[116] S Jager, *et al*. AMP-activated protein kinase (AMPK) action in skeletal muscle via direct phosphorylation of PGC-1alpha. *Proc Natl Acad Sci U S A* 104(29):12017-12022 (2007).
[117] D Carling & DG Hardie. The substrate and sequence specificity of the AMP-activated protein kinase. Phosphorylation of glycogen synthase and phosphorylase kinase. *Biochim Biophys Acta* 1012(1):81-86 (1989).
[118] WG Aschenbach, *et al*. Effect of AICAR treatment on glycogen metabolism in skeletal muscle. *Diabetes* 51(3):567-573 (2002).
[119] SL Longnus, *et al*. 5-Aminoimidazole-4-carboxamide 1-beta -D-ribofuranoside (AICAR) stimulates myocardial glycogenolysis by allosteric mechanisms. *Am J Physiol Regul Integr Comp Physiol* 284(4):R936-944 (2003).
[120] AS Marsin, *et al*. Phosphorylation and activation of heart PFK-2 by AMPK has a role in the stimulation of glycolysis during ischaemia. *Curr Biol* 10(20):1247-1255 (2000).
[121] AS Marsin, *et al*. The stimulation of glycolysis by hypoxia in activated monocytes is mediated by AMP-activated protein kinase and inducible 6-phosphofructo-2-kinase. *J Biol Chem* 277(34):30778-30783 (2002).
[122] RJ Shaw, *et al*. The kinase LKB1 mediates glucose homeostasis in liver and therapeutic effects of metformin. *Science* 310(5754):1642-1646 (2005).
[123] YH Hong, *et al*. AMP-activated protein kinase regulates HNF4alpha transcriptional activity by inhibiting dimer formation and decreasing protein stability. *J Biol Chem* 278(30):27495-27501 (2003).

[124] M Abdollahi, *et al*. Effects of phosphodiesterase 3,4,5 inhibitors on hepatocyte cAMP levels, glycogenolysis, gluconeogenesis and susceptibility to a mitochondrial toxin. *Mol Cell Biochem* 252(1-2):205-211 (2003).
[125] M Foretz, *et al*. Metformin inhibits hepatic gluconeogenesis in mice independently of the LKB1/AMPK pathway via a decrease in hepatic energy state. *J Clin Invest* 120(7):2355-2369 (2010).
[126] M Johanns, *et al*. AMPK antagonizes hepatic glucagon-stimulated cyclic AMP signalling via phosphorylation-induced activation of cyclic nucleotide phosphodiesterase 4B. *Nat Commun* 7:10856 (2016).
[127] JJ Luiken, *et al*. Contraction-induced fatty acid translocase/CD36 translocation in rat cardiac myocytes is mediated through AMP-activated protein kinase signaling. *Diabetes* 52(7):1627-1634 (2003).
[128] MR Munday, *et al*. Identification by amino acid sequencing of three major regulatory phosphorylation sites on rat acetyl-CoA carboxylase. *Eur J Biochem* 175(2):331-338 (1988).
[129] HM O'Neill, *et al*. AMPK phosphorylation of ACC2 is required for skeletal muscle fatty acid oxidation and insulin sensitivity in mice. *Diabetologia* 57(8):1693-1702 (2014).
[130] MD Fullerton, *et al*. Single phosphorylation sites in Acc1 and Acc2 regulate lipid homeostasis and the insulin-sensitizing effects of metformin. *Nat Med* 19(12):1649-1654 (2013).
[131] M Foretz, *et al*. AMP-activated protein kinase inhibits the glucose-activated expression of fatty acid synthase gene in rat hepatocytes. *J Biol Chem* 273(24):14767-14771 (1998).
[132] VT Samuel, *et al*. Lipid-induced insulin resistance: unravelling the mechanism. *Lancet* 375(9733):2267-2277 (2010).
[133] DM Muoio, *et al*. AMP-activated kinase reciprocally regulates triacylglycerol synthesis and fatty acid oxidation in liver and muscle: evidence that sn-glycerol-3-phosphate acyltransferase is a novel target. *Biochem J* 338 (Pt 3):783-791 (1999).
[134] M Daval, *et al*. Anti-lipolytic action of AMP-activated protein kinase in rodent adipocytes. *J Biol Chem* 280(26):25250-25257 (2005).
[135] ZH Beg, *et al*. Modulation of 3-hydroxy-3-methylglutaryl coenzyme A reductase activity with cAMP and wth protein fractions of rat liver cytosol. *Biochem Biophys Res Commun* 54(4):1362-1369 (1973).
[136] F Buttgereit & MD Brand. A hierarchy of ATP-consuming processes in mammalian cells. *Biochem J* 312 (Pt 1):163-167 (1995).
[137] K Inoki, *et al*. TSC2 mediates cellular energy response to control cell growth and survival. *Cell* 115(5):577-590 (2003).
[138] DM Gwinn, *et al*. AMPK phosphorylation of raptor mediates a metabolic checkpoint. *Mol Cell* 30(2):214-226 (2008).
[139] S Horman, et al. Activation of AMP-Activated Protein Kinase Leads to the Phosphorylation of Elongation Factor 2 and an Inhibition of Protein Synthesis. *Curr Biol* 12:1419–1423 (2002).
[140] X Wang, *et al*. Eukaryotic elongation factor 2 kinase activity is controlled by multiple inputs from oncogenic signaling. *Mol Cell Biol* 34(22):4088-4103 (2014).
[141] KF Petersen, *et al*. Impaired mitochondrial activity in the insulin-resistant offspring of patients with type 2 diabetes. *N Engl J Med* 350(7):664-671 (2004).

[142] A Fu, *et al*. Role of AMPK in pancreatic beta cell function. *Mol Cell Endocrinol* 366(2):127-134 (2013).
[143] L Miranda, *et al*. AMP-activated protein kinase induces actin cytoskeleton reorganization in epithelial cells. *Biochem Biophys Res Commun* 396(3):656-661 (2010).
[144] K Imamura, *et al*. Cell cycle regulation via p53 phosphorylation by a 5'-AMP activated protein kinase activator, 5-aminoimidazole- 4-carboxamide-1-beta-D-ribofuranoside, in a human hepatocellular carcinoma cell line. *Biochem Biophys Res Commun* 287(2):562-567 (2001).
[145] M Zhao & DJ Klionsky. AMPK-dependent phosphorylation of ULK1 induces autophagy. *Cell Metab* 13(2):119-120 (2011).
[146] KO Cameron & RG Kurumbail. Recent progress in the identification of adenosine monophosphate-activated protein kinase (AMPK) activators. *Bioorg Med Chem Lett* 26(21):5139-5148 (2016).
[147] B Guigas & B Viollet. Targeting AMPK: From Ancient Drugs to New Small-Molecule Activators. *EXS* 107:327-350 (2016).
[148] J Kim, *et al*. AMPK activators: mechanisms of action and physiological activities. *Exp Mol Med* 48:e224 (2016).
[149] S Meng, *et al*. Metformin Activates AMP-activated Protein Kinase by Promoting Formation of the alphabetagamma Heterotrimeric Complex. *J Biol Chem* 290(6):3793-3802 (2015).
[150] MR Owen, *et al*. Evidence that metformin exerts its anti-diabetic effects through inhibition of complex 1 of the mitochondrial respiratory chain. *Biochem J* 348 Pt 3:607-614 (2000).
[151] R Giannarelli, *et al*. Reducing insulin resistance with metformin: the evidence today. *Diabetes Metab* 29(4 Pt 2):6s28-35 (2003).
[152] B Viollet, *et al*. AMPK: Lessons from transgenic and knockout animals. *Front Biosci (Landmark Ed)* 14:19-44 (2009).
[153] RW Hunter, *et al*. Mechanism of action of compound-13: an alpha1-selective small molecule activator of AMPK. *Chem Biol* 21(7):866-879 (2014).
[154] B Xiao, *et al*. Structural basis of AMPK regulation by small molecule activators. *Nat Commun* 4:3017 (2013).
[155] YC Lai, *et al*. A small-molecule benzimidazole derivative that potently activates AMPK to increase glucose transport in skeletal muscle: comparison with effects of contraction and other AMPK activators. *Biochem J* 460(3):363-375 (2014).
[156] A Woods, *et al*. Characterization of the role of AMP-activated protein kinase in the regulation of glucose-activated gene expression using constitutively active and dominant negative forms of the kinase. *Mol Cell Biol* 20(18):6704-6711 (2000).
[157] B Viollet, *et al*. The AMP-activated protein kinase alpha2 catalytic subunit controls whole-body insulin sensitivity. *J Clin Invest* 111(1):91-98 (2003).
[158] N Dzamko, *et al*. AMPK beta1 deletion reduces appetite, preventing obesity and hepatic insulin resistance. *J Biol Chem* 285(1):115-122 (2010).
[159] GR Steinberg, *et al*. Whole body deletion of AMP-activated protein kinase {beta}2 reduces muscle AMPK activity and exercise capacity. *J Biol Chem* 285(48):37198-37209 (2010).
[160] HM O'Neill, *et al*. AMP-activated protein kinase (AMPK) beta1beta2 muscle null mice reveal an essential role for AMPK in maintaining mitochondrial content and

glucose uptake during exercise. *Proc Natl Acad Sci U S A* 108(38):16092-16097 (2011).
[161] BR Barnes, *et al*. The 5'-AMP-activated protein kinase gamma3 isoform has a key role in carbohydrate and lipid metabolism in glycolytic skeletal muscle. *J Biol Chem* 279(37):38441-38447 (2004).
[162] B Guigas, *et al*. 5-Aminoimidazole-4-carboxamide-1-beta-D-ribofuranoside and metformin inhibit hepatic glucose phosphorylation by an AMP-activated protein kinase-independent effect on glucokinase translocation. *Diabetes* 55(4):865-874 (2006).
[163] M Claret, *et al*. AMPK is essential for energy homeostasis regulation and glucose sensing by POMC and AgRP neurons. *J Clin Invest* 117(8):2325-2336 (2007).
[164] K Sakamoto, *et al*. Deficiency of LKB1 in skeletal muscle prevents AMPK activation and glucose uptake during contraction. *EMBO J* 24(10):1810-1820 (2005).
[165] A Woods, *et al*. LKB1 is required for hepatic bile acid transport and canalicular membrane integrity in mice. *Biochem J* 434(1):49-60 (2011).
[166] MD Houslay, *et al*. cAMP-Specific phosphodiesterase-4 enzymes in the cardiovascular system: a molecular toolbox for generating compartmentalized cAMP signaling. *Circ Res* 100(7):950-966 (2007).
[167] K Omori & J Kotera. Overview of PDEs and their regulation. *Circ Res* 100(3):309-327 (2007).
[168] GJ Browne, *et al*. Stimulation of the AMP-activated protein kinase leads to activation of eukaryotic elongation factor 2 kinase and to its phosphorylation at a novel site, serine 398. *J Biol Chem* 279(13):12220-12231 (2004).
[169] GJ Browne & CG Proud. A novel mTOR-regulated phosphorylation site in elongation factor 2 kinase modulates the activity of the kinase and its binding to calmodulin. *Mol Cell Biol* 24(7):2986-2997 (2004).
[170] S Pyr Dit Ruys, *et al*. Identification of autophosphorylation sites in eukaryotic elongation factor-2 kinase. *Biochem J* 442(3):681-692 (2012).
[171] P Schimmel. GTP hydrolysis in protein synthesis: two for Tu? *Science* 259(5099):1264-1265 (1993).
[172] D Drennan & AG Ryazanov. Alpha-kinases: analysis of the family and comparison with conventional protein kinases. *Prog Biophys Mol Biol* 85(1):1-32 (2004).
[173] JW Kenney, *et al*. Eukaryotic elongation factor 2 kinase, an unusual enzyme with multiple roles. *Adv Biol Regul* 55:15-27 (2014).
[174] MB Lazarus, *et al*. Discovery of new substrates of the elongation factor-2 kinase suggests a broader role in the cellular nutrient response. *Cell Signal* 29:78-83 (2016).
[175] HP Chu, *et al*. Germline quality control: eEF2K stands guard to eliminate defective oocytes. *Dev Cell* 28(5):561-572 (2014).
[176] CG Proud. Regulation and roles of elongation factor 2 kinase. *Biochem Soc Trans* 43(3):328-332 (2015).
[177] G Leprivier, *et al*. The eEF2 kinase confers resistance to nutrient deprivation by blocking translation elongation. *Cell* 153(5):1064-1079 (2013).

[178] TG Parmer, *et al*. Activity and regulation by growth factors of calmodulin-dependent protein kinase III (elongation factor 2-kinase) in human breast cancer. *Br J Cancer* 79(1):59-64 (1999).
[179] DM Bagaglio, *et al*. Phosphorylation of elongation factor 2 in normal and malignant rat glial cells. *Cancer Res* 53(10 Suppl):2260-2264 (1993).
[180] H Wu, *et al*. Elongation factor-2 kinase regulates autophagy in human glioblastoma cells. *Cancer Res* 66(6):3015-3023 (2006).
[181] AA Ashour, *et al*. Targeting elongation factor-2 kinase (eEF-2K) induces apoptosis in human pancreatic cancer cells. *Apoptosis* 19(1):241-258 (2014).
[182] Y Cheng, *et al*. eEF-2 kinase dictates cross-talk between autophagy and apoptosis induced by Akt Inhibition, thereby modulating cytotoxicity of novel Akt inhibitor MK-2206. *Cancer Res* 71(7):2654-2663 (2011).
[183] Y Cheng, *et al*. Integrated regulation of autophagy and apoptosis by EEF2K controls cellular fate and modulates the efficacy of curcumin and velcade against tumor cells. *Autophagy* 9(2):208-219 (2013).
[184] XY Liu, *et al*. Inhibition of elongation factor-2 kinase augments the antitumor activity of Temozolomide against glioma. *PLoS One* 8(11):e81345 (2013).
[185] HG Russnes & C Caldas. eEF2K--a new target in breast cancers with combined inactivation of p53 and PTEN. *EMBO Mol Med* 6(12):1512-1514 (2014).
[186] H Zhu, *et al*. Eukaryotic elongation factor 2 kinase confers tolerance to stress conditions in cancer cells. *Cell Stress Chaperones* 20(2):217-220 (2015).
[187] C-M Xie, *et al*. Silencing of EEF2K (eukaryotic elongation factor-2 kinase) reveals AMPK-ULK1-dependent autophagy in colon cancer cells. *Autophagy* 10(9):0-13 (2014).
[188] W Richter, *et al*. Conserved expression and functions of PDE4 in rodent and human heart. *Basic Res Cardiol* 106(2):249-262 (2011).
[189] CA Hutber, *et al*. Electrical stimulation inactivates muscle acetyl-CoA carboxylase and increases AMP-activated protein kinase. *Am J Physiol* 272(2 Pt 1):E262-266 (1997).
[190] WW Winder & DG Hardie. Inactivation of acetyl-CoA carboxylase and activation of AMP-activated protein kinase in muscle during exercise. *Am J Physiol* 270(2 Pt 1):E299-304 (1996).
[191] E Mutel, *et al*. Control of blood glucose in the absence of hepatic glucose production during prolonged fasting in mice: induction of renal and intestinal gluconeogenesis by glucagon. *Diabetes* 60(12):3121-3131 (2011).
[192] G Zhou, *et al*. Role of AMP-activated protein kinase in mechanism of metformin action. *J Clin Invest* 108(8):1167-1174 (2001).
[193] YD Kim, *et al*. Metformin inhibits hepatic gluconeogenesis through AMP-activated protein kinase-dependent regulation of the orphan nuclear receptor SHP. *Diabetes* 57(2):306-314 (2008).
[194] L He & FE Wondisford. Metformin action: concentrations matter. *Cell Metab* 21(2):159-162 (2015).
[195] J Cao, *et al*. Low concentrations of metformin suppress glucose production in hepatocytes through AMP-activated protein kinase (AMPK). *J Biol Chem* 289(30):20435-20446 (2014).

[196] M Foretz, *et al*. Short-term overexpression of a constitutively active form of AMP-activated protein kinase in the liver leads to mild hypoglycemia and fatty liver. *Diabetes* 54(5):1331-1339 (2005).
[197] MJ Kim, *et al*. Salt-Inducible Kinase 1 Terminates cAMP Signaling by an Evolutionarily Conserved Negative-Feedback Loop in beta-Cells. *Diabetes* 64(9):3189-3202 (2015).
[198] R Dentin, *et al*. Insulin modulates gluconeogenesis by inhibition of the coactivator TORC2. *Nature* 449(7160):366-369 (2007).
[199] K Patel, *et al*. The LKB1-salt-inducible kinase pathway functions as a key gluconeogenic suppressor in the liver. *Nat Commun* 5:4535 (2014).
[200] HM Tang, *et al*. LKB1 tumor suppressor and salt-inducible kinases negatively regulate human T-cell leukemia virus type 1 transcription. *Retrovirology* 10:40 (2013).
[201] B Viollet, *et al*. AMPK inhibition in health and disease. *Crit Rev Biochem Mol Biol* 45(4):276-295 (2010).
[202] JW Scott, *et al*. Thienopyridone drugs are selective activators of AMP-activated protein kinase beta1-containing complexes. *Chem Biol* 15(11):1220-1230 (2008).
[203] F Rajamohan, *et al*. Probing the enzyme kinetics, allosteric modulation and activation of alpha1- and alpha2-subunit-containing AMP-activated protein kinase (AMPK) heterotrimeric complexes by pharmacological and physiological activators. *Biochem J* 473(5):581-592 (2016).
[204] JB Birk & JF Wojtaszewski. Predominant alpha2/beta2/gamma3 AMPK activation during exercise in human skeletal muscle. *J Physiol* 577(Pt 3):1021-1032 (2006).
[205] L Barre, *et al*. Genetic model for the chronic activation of skeletal muscle AMP-activated protein kinase leads to glycogen accumulation. *Am J Physiol Endocrinol Metab* 292(3):E802-811 (2007).
[206] BF Holmes, *et al*. Chronic activation of 5'-AMP-activated protein kinase increases GLUT-4, hexokinase, and glycogen in muscle. *J Appl Physiol (1985)* 87(5):1990-1995 (1999).
[207] D Meisse, *et al*. Sustained activation of AMP-activated protein kinase induces c-Jun N-terminal kinase activation and apoptosis in liver cells. *FEBS Lett* 526(1-3):38-42 (2002).
[208] W Li, *et al*. Targeting AMPK for cancer prevention and treatment. *Oncotarget* 6(10):7365-7378 (2015).
[209] J Kasznicki, *et al*. Metformin in cancer prevention and therapy. *Ann Transl Med* 2(6) (2014).